Chapter 2

Fourier Series and Integrals with Applications to Signal Analysis

Perhaps the most important orthogonal functions in engineering applications are trigonometric functions. These were briefly discussed in 1.5.2 as one example of LMS approximation by finite orthogonal function sets. In this chapter we reexamine the LMS approximation problem in terms of infinite trigonometric function sets. When the approximating sum converges to the given function we obtain a Fourier Series; in case of a continuous summation index (i.e., an integral as in (1.92) the converging approximating integral is referred to as a Fourier Integral.

2.1 Fourier Series

2.1.1 Pointwise Convergence at Interior Points for Smooth Functions

We return to 1.5.2 and the LMS approximation of $f(t)$ within the interval $-T/2 < t < T/2$ by $2N+1$ using complex exponentials as given by (1.211). The approximating sum reads

$$f^N(t) = \sum_{n=-N}^{N} \hat{f}_n e^{i2\pi nt/T}, \tag{2.1}$$

while for the expansion coefficients we find from (1.214)

$$\hat{f}_n = \frac{1}{T}\int_{-T/2}^{T/2} f(t)\, e^{-i2\pi nt/T} dt. \tag{2.2}$$

W. Wasylkiwskyj, *Signals and Transforms in Linear Systems Analysis*,
DOI 10.1007/978-1-4614-3287-6_2, © Springer Science+Business Media, LLC 2013

Upon substituting (2.2) in (2.1) and interchanging summation and integration we obtain

$$f^N(t) = \int_{-T/2}^{T/2} f(t') K_N(t-t')\, dt', \tag{2.3}$$

where

$$K_N(t-t') = \frac{1}{T}\sum_{n=-N}^{N} e^{i2\pi n(t-t')/T} = \sum_{n=-N}^{N}\left(\frac{1}{\sqrt{T}}e^{i2\pi nt/T}\right)\left(\frac{1}{\sqrt{T}}e^{i2\pi nt'/T}\right)^*, \tag{2.4}$$

and as shown in the following, approaches a delta function at points of continuity as N approaches infinity. The last form highlights the fact that this kernel can be represented as a sum of symmetric products of expansion functions in conformance with the general result in (1.301) and (1.302). Using the geometrical series sum formula we readily obtain

$$K_N(t-t') = \frac{\sin\left[2\pi\left(N+1/2\right)\left(t-t'\right)/T\right]}{T\sin\left[\pi\left(t-t'\right)/T\right]}, \tag{2.5}$$

which is known as the Fourier series kernel. As is evident from (2.4) this kernel is periodic with period T and is comprised of an infinite series of regularly spaced peaks each similar to the a-periodic sinc function kernel encountered in (1.254). A plot of $T\ K_N(\tau)$ for $N = 5$ as a function of $(t-t')/T \equiv \tau/T$ is shown in Fig. 2.1. The peak value attained by $T\ K_N(\tau)$ at $\tau/T = 0, \pm 1, \pm 2,$

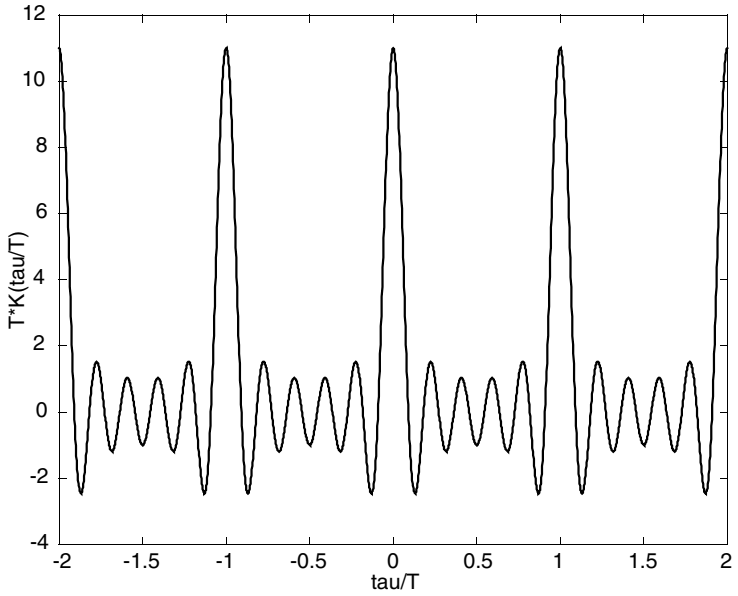

Figure 2.1: Fourier series kernel (N=5)

is in general $2N+1$, as may be verified directly with the aid of (2.4) or (2.5). As the peaks of these principal lobes grow in proportion with N their widths diminish with increasing N. In fact we readily find directly from (2.5) that the peak-to-first null lobe width is $\Delta\tau = T/(2N+1)$. We note that $\Delta\tau K_N(\pm kT) = 1$, so that the areas under the principal lobes should be on the order of unity for sufficiently large N. This suggests that the infinite series of peaks in Fig. 2.1 should tend to an infinite series of delta functions as the number N increases without bound. This is in fact the case. To prove this we must show that for any piecewise differentiable function defined in any of the intervals $(k-1/2)T < t < (k+1/2)\,T$, $k = 0, \pm 1, \ldots$ the limit

$$\lim_{N\longrightarrow\infty}\int_{(k-1/2)T}^{(k+1/2)T} f(t')\,K_N(t-t')\,dt' = \frac{1}{2}\left[f\left(t^+\right)+f\left(t^-\right)\right] \tag{2.6}$$

holds. Of course, because of the periodicity of the Fourier Series kernel it suffices if we prove (2.6) for $k = 0$ only. The proof employs steps very similar to those following (1.263) except that the constraint on the behavior of $f(t)$ at infinity, (1.266), presently becomes superfluous since the integration interval is finite. Consequently the simpler form of the RLL given by (1.262) applies. As in (1.267) we designate the limit by $I(t)$ and write

$$I(t) = \lim_{N\longrightarrow\infty}\int_{-T/2}^{T/2} g(t,t')\sin\left[2\pi\left(N+1/2\right)\left(t-t'\right)/T\right]dt', \tag{2.7}$$

where by analogy with (1.264) we have defined the function

$$g(t,t') = \frac{f(t')}{T\sin\left[\pi\left(t-t'\right)/T\right]}. \tag{2.8}$$

In (2.7) we may identify the large parameter $2\pi\left(N+1/2\right)/T$ with ω in (1.262) and apply the RLL provided we again exclude the point $t = t'$where $g(t,t')$ becomes infinite. We then proceed as in (1.265) to obtain

$$\begin{aligned} I(t) \;=\; & \lim_{N\longrightarrow\infty}\int_{-T/2}^{t-\epsilon/2} g(t,t')\sin\left[2\pi\left(N+1/2\right)\left(t-t'\right)/T\right]dt' \\ & + \lim_{N\longrightarrow\infty}\int_{t-\epsilon/2}^{t+\epsilon/2} g(t,t')\sin\left[2\pi\left(N+1/2\right)\left(t-t'\right)/T\right]dt' \\ & + \lim_{N\longrightarrow\infty}\int_{t+\epsilon/2}^{T/2} g(t,t')\sin\left[2\pi\left(N+1/2\right)\left(t-t'\right)/T\right]dt', \end{aligned} \tag{2.9}$$

where ϵ is an arbitrarily small positive number. Let us first assume that $f(t')$ is smooth, i.e., piecewise differentiable and continuous. In that case then $g(t,t')$ has the same properties provided $t \neq t'$. This is true for the function in the integrand of the first and third integral in (2.9). Hence by the RLL these vanish so that $I(t)$ is determined solely by the middle integral

$$I(t) = \lim_{N\longrightarrow\infty}\int_{t-\epsilon/2}^{t+\epsilon/2} f(t')\,\frac{\sin\left[2\pi\left(N+1/2\right)\left(t-t'\right)/T\right]}{T\sin\left[\pi\left(t-t'\right)/T\right]}dt'. \tag{2.10}$$

Since ϵ is arbitrarily small, $f(t')$ can be approximated as closely as desired by $f(t)$ and therefore factored out of the integrand. Also for small ϵ the $\sin[\pi(t-t')/T]$ in the denominator can be replaced by its argument. With these changes (2.10) becomes

$$I(t) = f(t) \lim_{N\longrightarrow\infty} \int_{t-\epsilon/2}^{t+\epsilon/2} \frac{\sin[2\pi(N+1/2)(t-t')/T]}{\pi(t-t')} dt'. \tag{2.11}$$

The final evaluation becomes more transparent when the integration variable is changed from t' to $x = 2\pi(N+1/2)(t'-t)/T$ which transforms (2.11) into

$$I(t) = f(t) \lim_{N\longrightarrow\infty} \frac{1}{\pi} \int_{-\epsilon\pi(N+1/2)/T}^{\epsilon\pi(N+1/2)/T} \frac{\sin x}{x} dx = f(t) \frac{1}{\pi} \int_{-\infty}^{\infty} \frac{\sin x}{x} dx = f(t). \tag{2.12}$$

This establishes the delta function character of the Fourier series kernel. Equivalently, we have proven that for any smooth function $f(t)$ the Fourier series

$$f(t) = \sum_{n=-\infty}^{\infty} \hat{f}_n e^{i2\pi nt/T} \tag{2.13}$$

with coefficients given by (2.2) converges in the interval $-T/2 < t < T/2$.

2.1.2 Convergence at Step Discontinuities

Note that in the preceding limiting argument we have excluded the endpoints of the interval, i.e., we have shown convergence only in the open interval. In fact, as we shall shortly see, pointwise convergence can in general not be achieved by a Fourier series at $t = \pm T/2$ even for a function with smooth behavior in the open interval. It turns out that convergence at the endpoints is intimately related to convergence at a step discontinuity, to which we now turn our attention. Thus suppose our function possesses a finite number of step discontinuities in the (open) interval under consideration. We can then represent it as a sum comprising a smooth function $f_s(t)$ and a sum of step functions as in (1.280). In order not to encumber the development with excessive notation we confine the discussion to one typical discontinuity, say at $t = t_1$, and write

$$f(t) = f_s(t) + \left[f\left(t_1^+\right) - f\left(t_1^-\right)\right] U(t-t_1). \tag{2.14}$$

The Fourier coefficients follow from (2.2) so that

$$\hat{f}_n = \frac{1}{T} \int_{-T/2}^{T/2} f_s(t) e^{-i2\pi nt/T} dt + \frac{\left[f\left(t_1^+\right) - f\left(t_1^-\right)\right]}{T} \int_{t_1}^{T/2} e^{-i2\pi nt/T} dt \tag{2.15}$$

and substitution in (2.1) yields the partial sum

$$f^N(t) = \int_{-T/2}^{T/2} f_s(t') \frac{\sin[2\pi(N+1/2)(t-t')/T]}{T\sin[\pi(t-t')/T]} dt' + \left[f\left(t_1^+\right) - f\left(t_1^-\right)\right] \lambda_N(t), \tag{2.16}$$

where

$$\lambda_N(t) = \int_{t_1}^{T/2} \frac{\sin\left[2\pi\left(N+1/2\right)\left(t-t'\right)/T\right]}{T\sin\left[\pi\left(t-t'\right)/T\right]}dt' \ . \tag{2.17}$$

The limiting form of the first integral on the right of (2.16) as $N \longrightarrow \infty$ has already been considered so that

$$\lim_{N\longrightarrow\infty} f^N(t) = f_s(t) + \left[f\left(t_1^+\right) - f\left(t_1^-\right)\right] \lim_{N\longrightarrow\infty} \lambda_N(t) \tag{2.18}$$

and only the last limit introduces novel features. Confining our attention to this term we distinguish three cases: the interval $-T/2 < t < t_1$, wherein $t' \neq t$ so that the RLL applies, the interval $t_1 < t < T/2$, and the point of discontinuity $t = t_1$. In the first case $\lambda_N(t)$ approaches zero. In the second case we divide the integration interval into three subintervals as in (2.9). Proceeding in identical fashion we find that $\lambda_N(t)$ approaches unity. For $t = t_1$ we subdivide the integration interval into two subintervals as follows:

$$\begin{aligned}\lambda_N(t_1) &= \int_{t_1}^{t_1+\epsilon/2} \frac{\sin\left[2\pi\left(N+1/2\right)\left(t_1-t'\right)/T\right]}{T\sin\left[\pi\left(t_1-t'\right)/T\right]}dt' \\ &\quad + \int_{t_1+\epsilon/2}^{T/2} \frac{\sin\left[2\pi\left(N+1/2\right)\left(t_1-t'\right)/T\right]}{T\sin\left[\pi\left(t_1-t'\right)/T\right]}dt',\end{aligned} \tag{2.19}$$

where again ϵ is an arbitrarily small positive quantity. In the second integral $t' \neq t_1$ so that again the RLL applies and we obtain zero in the limit. Hence the limit is given by the first integral which we compute as follows:

$$\begin{aligned}\lim_{N\longrightarrow\infty}\lambda_N(t_1) &= \lim_{N\longrightarrow\infty}\int_{t_1}^{t_1+\epsilon/2} \frac{\sin\left[2\pi\left(N+1/2\right)\left(t_1-t'\right)/T\right]}{T\sin\left[\pi\left(t_1-t'\right)/T\right]}dt' \\ &= \lim_{N\longrightarrow\infty}\int_0^{\frac{\pi(2N+1)\epsilon}{2T}} \frac{\sin x}{\pi\left(2N+1\right)\sin\frac{x}{2N+1}}dx \\ &= \lim_{N\longrightarrow\infty}\int_0^{\frac{\pi(2N+1)\epsilon}{2T}} \frac{\sin x}{\pi x}dx = \int_0^{\infty}\frac{\sin x}{\pi x}dx = \frac{1}{2}.\end{aligned} \tag{2.20}$$

Summarizing the preceding results we have

$$\lim_{N\longrightarrow\infty}\lambda_N(t) = \begin{cases} 0\ ; & -T/2 < t < t_1, \\ 1/2\ ; & t = t_1, \\ 1\ ; & t_1 < t < T/2. \end{cases} \tag{2.21}$$

Returning to (2.18) and taking account of the continuity of $f_s(t)$ we have the final result

$$\lim_{N\longrightarrow\infty} f^N(t_1) = \frac{1}{2}\left[f\left(t_1^+\right) + f\left(t_1^-\right)\right]. \tag{2.22}$$

Clearly this generalizes to any number of finite discontinuities within the expansion interval. Thus, for a piecewise differentiable function with step discontinuities the Fourier series statement (2.13) should be replaced by

$$\frac{1}{2}\left[f\left(t^+\right) + f\left(t^-\right)\right] = \sum_{-\infty}^{\infty}\hat{f}_n e^{i2\pi nt/T}. \tag{2.23}$$

Although the limiting form (2.23) tells us what happens when the number of terms in the series is infinite, it does not shed any light on the behavior of the partial approximating sum for finite N. To assess the rate of convergence we should examine (2.17) as a function of t with increasing N. For this purpose let us introduce the function

$$\mathrm{Si}\, s(x,N) = \int_0^x \frac{\sin[(N+1/2)\theta]}{2\sin(\theta/2)} d\theta \tag{2.24}$$

so that the dimensionless parameter x is a measure of the distance from the step discontinuity ($x = 0$). The integrand in (2.24) is just the sum $(1/2)\sum_{n=-N}^{n=N} \exp(-in\theta)$ which we integrate term by term and obtain the alternative form

$$\mathrm{Si}\, s(x,N) = \frac{x}{2} + \sum_{n=1}^{N} \frac{\sin(nx)}{n}. \tag{2.25}$$

Note that for any N the preceding gives $\mathrm{Si}\, s(\pi,N) = \pi/2$. As $N \to \infty$ with $0 < x < \pi$ this series converges to $\pi/2$. A plot of (2.25) for $N = 10$ and $N = 20$ is shown in Fig. 2.2. For larger values of N the oscillatory behavior of $\mathrm{Si}\, s(y,N)$

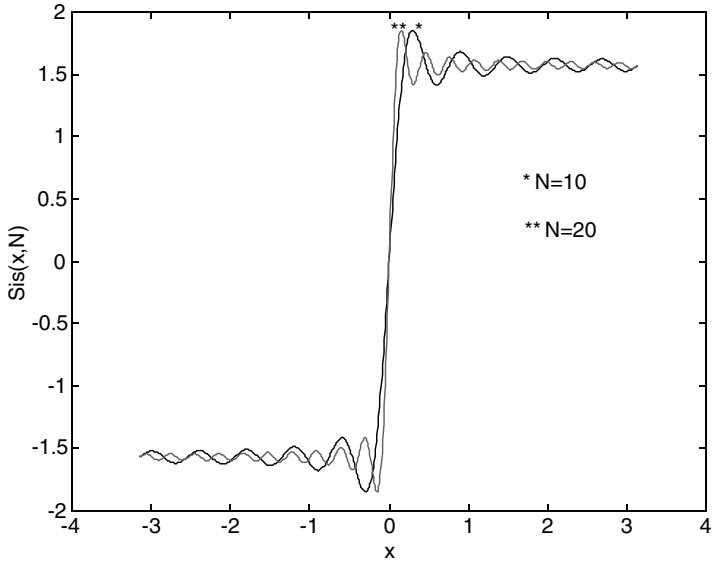

Figure 2.2: FS convergence at a step discontinuity for N=10 and N=20

damps out and the function approaches the asymptotes $\pm\pi/2$ for $y \neq 0$. Note that as N is increased the peak amplitude of the oscillations does not diminish but migrates toward the location of the step discontinuity, i.e., $y = 0$. The numerical value of the overshoot is ± 1.852 or about 18% above (below) the positive (negative) asymptote. When expressed in terms of (2.25), (2.17) reads

$$\lambda_N(t) = \frac{1}{\pi}\mathrm{Si}\, s[(T/2-t)2\pi/T, N] - \frac{1}{\pi}\mathrm{Si}\, s[(t_1-t)2\pi/T, N]. \tag{2.26}$$

Taking account of the limiting forms of (2.25) we note that as long as $t < T/2$ in the limit as $N \to \infty$ the contribution from the first term on the right of (2.26) approaches 1/2, while the second term tends to $-1/2$ for $t < t_1$,1/2 for $t > t_1$ and 0 for $t = t_1$, in agreement with the limiting forms enumerated in (2.21).

Results of sample calculations of $\lambda_N(t)$ (with $t_1 = 0$) for $N = 10$, 20, and 50 are plotted in Fig. 2.3. Examining these three curves we again observe that increasing N does not lead to a diminution of the maximum amplitude of the

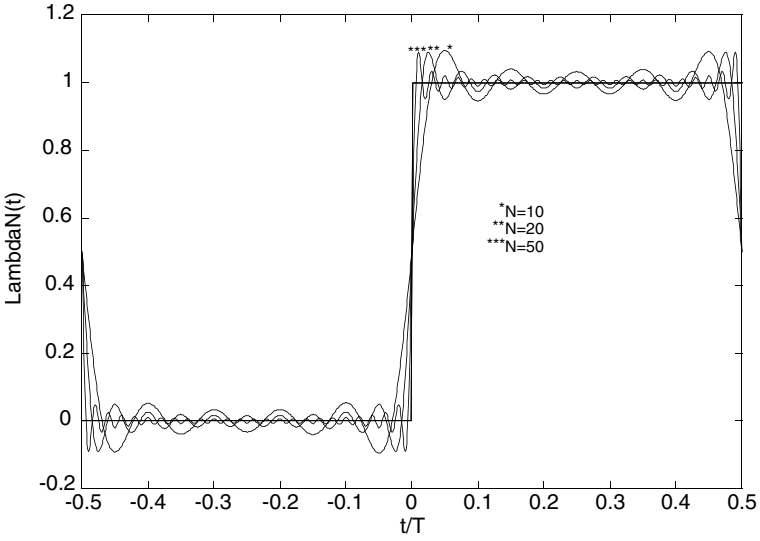

Figure 2.3: Convergence at a step discontinuity

oscillations. On the contrary, except for a compression of the timescale, the oscillations for $N = 50$ have essentially the same peak amplitudes as those for $N = 10$ and in fact exhibit the same overshoot as in Fig. 2.2. Thus N appears to enter into the argument in (2.22) merely as scaling factor of the abscissa, so that the magnitude of the peak overshoot appears to persist no matter how large N is chosen. The reason for this behavior can be demonstrated analytically by approximating (2.24) for large N. We do this by first changing the variable of integration in (2.24) to $y = (N + 1/2)\theta$ to obtain

$$\mathrm{Si}\, s(x, N) = \int_0^{(N+1/2)x} \frac{\sin y}{(2N+1)\sin[y/(2N+1)]} dy. \qquad (2.26^*)$$

Before proceeding with the next algebraic step we note that as $N \to \infty$ the numerator in (2.24) will be a rapidly oscillating sinusoid so that its contributions to the integral will mutually cancel except for those in the neighborhood of small θ. In terms of the variables in (2.26*) this means that for large N the argument $y/(2N + 1)$ of the sine function will remain small. In that case we may replace the sine by its argument which leads to the asymptotic form

$$\mathrm{Si}[s(N, x)] \;\sim\; \mathrm{Si}[(N + 1/2)x], \qquad (2.26^{**})$$

where $\mathrm{Si}(z)$ is the sine integral function defined in (1.278e) and plotted in Fig. 1.15. If we use this asymptotic form in (2.26), we get

$$\lambda_N(t) = \frac{1}{\pi}\,\mathrm{Si}[(N+1/2)(T/2-t)2\pi/T] - \frac{1}{\pi}\,\mathrm{Si}[(N+1/2)(t_1-t)2\pi/T],$$

which shows directly that N enters as a scaling factor of the abscissa. Thus as the number of terms in the approximation becomes infinite the oscillatory behavior in Fig. 2.3 compresses into two vanishingly small time intervals which in the limit may be represented by a pair of infinitely thin spikes at $t = 0^+$ and $t = 0^-$. Since in the limit these spikes enclose zero area we have here a direct demonstration of convergence in the mean (i.e., the LMS error rather than the error itself tending to zero with increasing N). This type of convergence, characterized by the appearance of an overshoot as a step discontinuity is approached, is referred to as the Gibbs phenomenon, in honor of Willard Gibbs, one of the America's greatest physicists. Gibbs phenomenon results whenever an LMS approximation is employed for a function with step discontinuities and is by no means limited to approximations by sinusoids (i.e., Fourier series). In fact the numerical example in Fig. 1.11 demonstrates it for Legendre Polynomials.

Another aspect of the Gibbs phenomenon worth mentioning is that it affords an example of nonuniform convergence. For as we have seen $\lim N \to \infty$ $\lambda_N(t_1) \to 1/2$. On the other hand, the limit approached when N is allowed to approach infinity first and the function subsequently evaluated at t as it is made to approach t_1 (say, through positive values) is evidently unity. Expressed in symbols, these two alternative ways of approaching the limit are

$$\lim_{N\longrightarrow\infty}\lim_{t\longrightarrow t_1^+}\lambda_N(t) = 1/2, \qquad (2.26^{***}\text{a})$$

$$\lim_{t\longrightarrow t_1^+}\lim_{N\longrightarrow\infty}\lambda_N(t) = 1. \qquad (2.26^{***}\text{b})$$

In other words, the result of the limiting process depends on the order in which the limits are taken, a characteristic of nonuniform convergence. We can view (2.26***) as a detailed interpretation of the limiting processes implied in the Fourier series at step discontinuities which the notation (2.23) does not make explicit.

2.1.3 Convergence at Interval Endpoints

The preceding discussion applies only to convergence properties of the Fourier series within the open interval. To complete the discussion of convergence we must still consider convergence at the interval endpoints $\pm T/2$. We start with the approximate form (2.20) (c.f. Fig. 2.3) which, together with the periodicity of $\lambda_N(t)$ based on the exact form (2.17), gives

$$\lim_{N\longrightarrow\infty}\lambda_N(\pm T/2) = 1/2.$$

Thus in view of (2.16) we have at the endpoints

$$\begin{aligned} & \lim_{N\to\infty} f^N(\pm T/2) \\ = & \lim_{N\to\infty} \int_{-T/2}^{T/2} f_s(t') \frac{\sin\left[2\pi\left(N+1/2\right)\left(\pm T/2-t'\right)/T\right]}{T\sin\left[\pi\left(\pm T/2-t'\right)/T\right]} dt' \\ & + \frac{\left[f\left(t_1^+\right)+f\left(t_1^-\right)\right]}{2}. \end{aligned} \tag{2.27}$$

Since the observation points $\pm T/2$ coincide with the integration limits, the limiting procedure following (2.9) is not directly applicable. Rather than examining the limiting form of the integral in (2.27) directly, it is more instructive to infer the limit in the present case from (2.24) and the periodicity of the Fourier series kernel. This periodicity permits us to increment the integration limits in (2.27) by an arbitrary amount, say τ, provided we replace $f_s(t)$ by its periodic extension

$$f_s^{ext}(t) = \sum_{n=-\infty}^{n=\infty} f_s(t-nT). \tag{2.28}$$

With this extension the endpoints $\pm T/2$ now become the interior points in an infinite sequence of expansion intervals $\ldots\ (\tau-3T/2, \tau-T/2)$, $(\tau-T/2, \tau+T/2)\ \ldots$. These intervals are all of length T and may be viewed as centered at $t=\tau\pm nT$, as may be inferred from Fig. 2.4. We note that unless $f_s(T/2) = f_s(-T/2)$ the periodic extension of the originally smooth $f_s(t)$ will have a step discontinuity at the new interior points of the amount $f_s(-T/2)-f_s(T/2)$. Thus with a suitable shift of the expansion interval and the replacement of

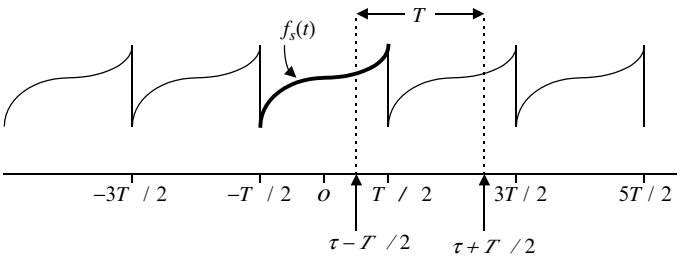

Figure 2.4: Step discontinuity introduced by a periodic extension of $f_s(t)$

$f_s(t')$ by the $f_s^{ext}(t')$ in (2.28) we can mimic the limiting process employed following (2.17) without change. Carrying this out we get an identical result at each endpoint, viz., $[f_s(-T/2)+f_s(T/2)]/2$. Clearly as far as any "real" discontinuity at an interior point of the original expansion interval is concerned, say at $t=t_1$, its contribution to the limit is obtainable by simply adding the last term in (2.27). Hence

$$\lim_{N\to\infty} f^N(\pm T/2) = \frac{f(-T/2)+f(T/2)}{2}. \tag{2.29}$$

Of course, as in the convergence at an interior discontinuity point, the limit (2.29) gives us only part of the story, since it sidesteps the very important issue of Gibbs oscillations for finite N. A representative example of what happens when the given function assumes different values at the two endpoints is demonstrated by the Fourier expansion of e^{-t} as shown in Fig. 2.5, where the expansion interval is $0, 1$, and 21 terms ($N = 10$) are employed. Clearly the convergence at $t = 0$ and $t = 1$ is quite poor. This should be contrasted with the plot in Fig. 2.6 which shows the expansion of $e^{-|t-1/2|}$ over the same interval

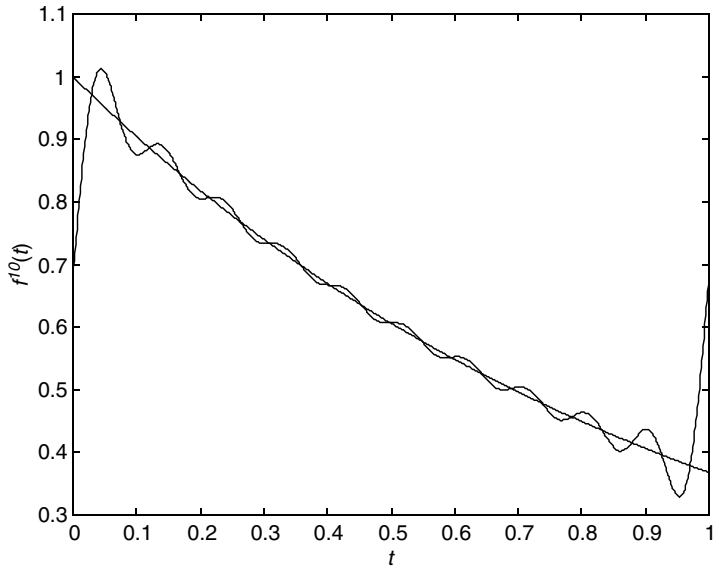

Figure 2.5: Fourier series approximation of e^{-t} with 21 sinusoids

and the same number of expansion functions. When the discontinuity occurs in the interior of the interval, the convergence is also marred by the Gibbs oscillations as illustrated in Fig. 2.7 for the pulse $p_{.5}(t - .5)$, again using 21 sinusoids. Fig. 2.8 shows a stem diagram of the magnitude of the Fourier coefficients $\hat{f}_n$ plotted as a function of $(m = n + 10,\ n = -10, -9, \ldots 11)$. Such Fourier coefficients are frequently referred to as (discrete) spectral lines and are intimately related to the concept of the frequency spectrum of a signal as will be discussed in detail in connection with the Fourier integral.

2.1.4 Delta Function Representation

The convergence properties of Fourier series can be succinctly phrased in terms of delta functions. Thus the Fourier series kernel can be formally represented by the statement

$$\lim_{N\to\infty} \frac{\sin\left[2\pi\left(N + 1/2\right)\left(t - t'\right)/T\right]}{T\sin\left[\pi\left(t - t'\right)/T\right]} = \sum_{k=-\infty}^{\infty} \delta\left(t - t' - kT\right). \tag{2.30}$$

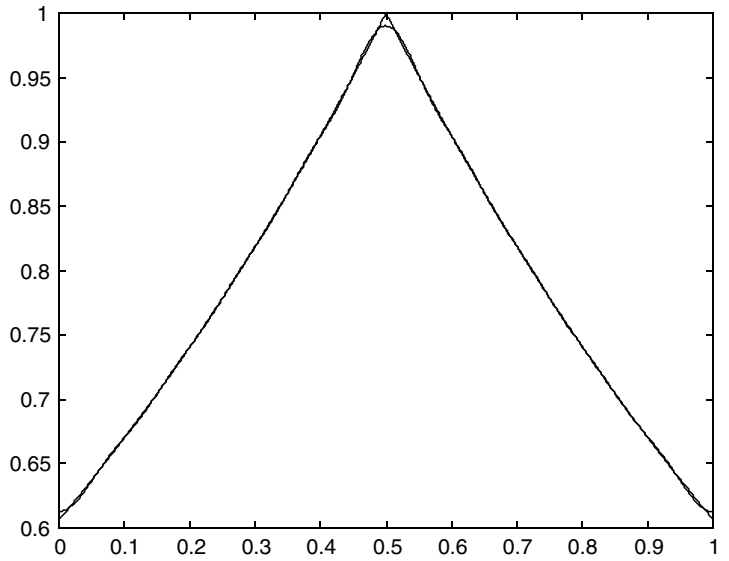

Figure 2.6: Fourier series approximation of $e^{-|t-1/2|}$ with 21 sinusoids

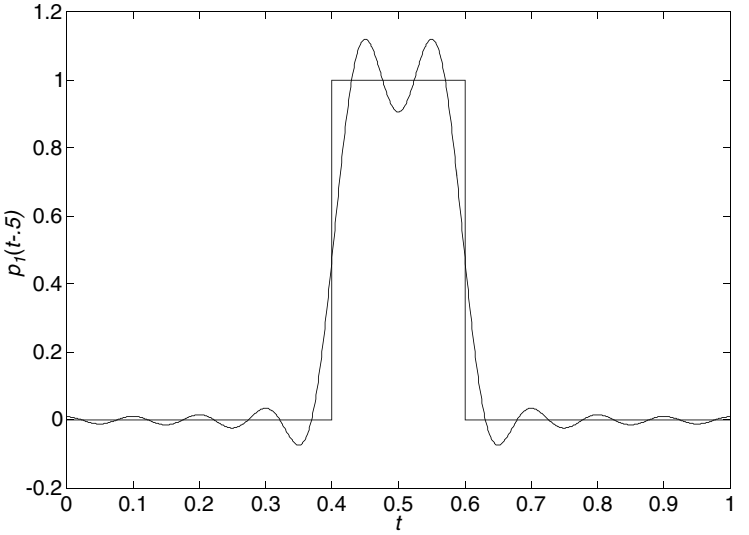

Figure 2.7: Fourier series approximation of a pulse using 21 terms

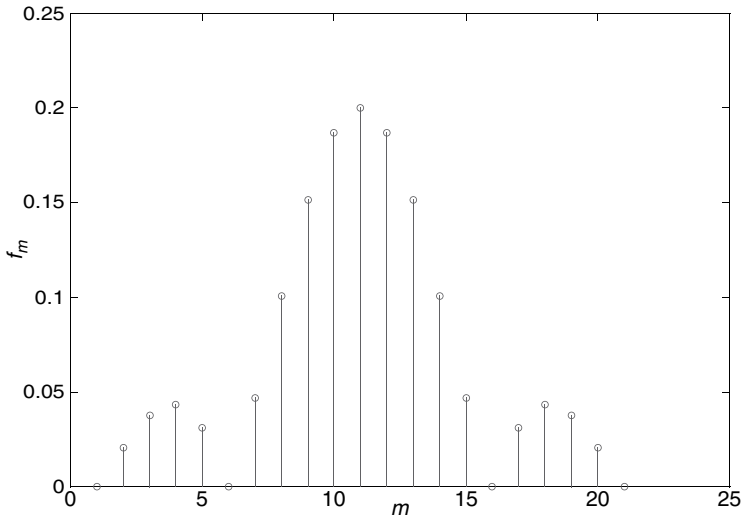

Figure 2.8: Magnitude of Fourier series coefficients for the pulse in Fig. 2.7

Alternatively, we can replace the kernel by the original geometric series and write

$$\sum_{n=-\infty}^{\infty} \left(\frac{1}{\sqrt{T}} e^{i2\pi nt/T}\right) \left(\frac{1}{\sqrt{T}} e^{i2\pi nt'/T}\right)^* = \frac{1}{T} \sum_{n=-\infty}^{\infty} e^{i2\pi n\left(t-t'\right)/T} = \sum_{k=-\infty}^{\infty} \delta\left(t - t' - kT\right). \tag{2.31}$$

These expressions, just as the corresponding completeness statements for general orthogonal sets discussed in 1.7.1, are to be understood as formal notational devices invented for efficient analytical manipulations; their exact meaning is to be understood in terms of the limiting processes discussed in the preceding subsection.

2.1.5 The Fejer Summation Technique

The poor convergence properties exhibited by Fourier series at step discontinuities due to the Gibbs phenomenon can be ameliorated if one is willing to modify the expansion coefficients (spectral lines) by suitable weighting factors. The technique, generally referred to as "windowing," involves the multiplication of the Fourier series coefficients by a suitable (spectral) "window" and summation of the new trigonometric sum having modified coefficients. In general, the new series will not necessarily converge to the original function over the entire interval. The potential practical utility of such a scheme rests on the fact the approximating sum may represent certain features of the given function that

are of particular interest better than the original series. This broad subject is treated in detail in books specializing in spectral estimation. Here we merely illustrate the technique with the so-called Fejer summation approach, wherein the modified trigonometric sum actually does converge to the original function. In fact this representation converges uniformly to the given function and thus completely eliminates the Gibbs phenomenon.

The Fejer [16] summation approach is based on the following result from the theory of limits. Given a sequence f^N such that $\lim_{N\to\infty} f^N \to f$ exists, the arithmetic average

$$\sigma_M = \frac{1}{M+1}\sum_{N=0}^{M} f^N \tag{2.32}$$

approaches the same limit as $M \to \infty$, i.e.,

$$\lim_{M\to\infty} \sigma_M \to f. \tag{2.33}$$

In the present case we take for $f^N = f^N(t)$, i.e., the partial Fourier series summation. Thus if this partial sum approaches $f(t)$ as $N \to \infty$, the preceding theorem states that $\sigma_M = \sigma_M(t)$ will also converge to $f(t)$. Since $f^N(t)$ is just a finite sum of sinusoids we should be able to find a closed-form expression for $\sigma_M(t)$ by a geometrical series summation. Thus

$$\begin{aligned}\sigma_M(t) &= \frac{1}{M+1}\{\hat{f}_0 + \left[\hat{f}_0 + \hat{f}_1 e^{i2\pi t/T} + \hat{f}_{-1}e^{-i2\pi t/T}\right] + \\ &\quad \left[\begin{array}{c}\hat{f}_0 + \hat{f}_1 e^{i2\pi t/T} + \hat{f}_2 e^{i2(2\pi t/T)} + \\ \hat{f}_{-1}e^{-i2\pi t/T} + \hat{f}_{-2}e^{-i2(2\pi t/T)}\end{array}\right] + \ldots\}.\end{aligned}$$

This can be rewritten as follows:

$$\begin{aligned}\sigma_M(t) &= \frac{1}{M+1}\{(M+1)\hat{f}_0 + M\left(\hat{f}_1 e^{i2\pi t/T} + \hat{f}_{-1}e^{-i2\pi t/T}\right) + \\ &\quad (M-1)\left(\hat{f}_2 e^{i2(2\pi t/T)} + \hat{f}_{-2}e^{-i2(2\pi t/T)}\right) + \ldots\} \\ &= \frac{1}{M+1}\{(M+1)\hat{f}_0 + \sum_{k=1}^{M}\hat{f}_k(M-k+1)e^{ik(2\pi t/T)} \\ &\quad + \sum_{k=1}^{M}\hat{f}_{-k}(M-k+1)e^{-ik(2\pi t/T)}\}.\end{aligned}$$

After changing the summation index from k to $-k$ in the last sum we get

$$\sigma_M(t) = \sum_{k=-M}^{M}\hat{f}_k\left(1 - \frac{|k|}{M+1}\right)e^{ik(2\pi t/T)}, \tag{2.34}$$

which we now identify as the expansion of the function $\sigma_M(t)$ in terms of $2M+1$ trigonometric (exponential) functions. We note that expansion coefficients

are obtained by multiplying the Fourier series coefficients $\hat{f}_k$ by the triangular spectral window

$$\hat{w}_k\,(M) = 1 - \frac{|k|}{M+1} \quad k = 0, \pm 1, \pm 2, \ldots \pm M. \tag{2.35}$$

We can view (2.34) from another perspective if we substitute the integral representation (2.3) of the partial sum $f^N\,(t)$ into (2.32) and carry out the summation on the Fourier series kernel (2.5). Thus after setting $\xi = 2\pi(t-t')/T$ we get the following alternative form:

$$\begin{aligned} \sigma_M\,(t) &= \frac{1}{M+1}\int_{-T/2}^{T/2}\sum_{N=0}^{M}\frac{\sin\left[(N+1/2)\,\xi\right]}{T\sin\left[\xi/2\right]}f\,(t')\,dt' \\ &= \frac{1}{M+1}\int_{-T/2}^{T/2}\frac{f\,(t')\,dt'}{T\sin(\xi/2)}\sum_{N=0}^{M}\left(\frac{e^{i(N+1/2)\xi}}{2i} - \frac{e^{-i(N+1/2)\xi}}{2i}\right). \end{aligned} \tag{2.36}$$

Using the formula

$$\sum_{N=0}^{M} e^{iN\xi} = e^{i\xi M/2}\frac{\sin\left[(M+1)\,\xi/2\right]}{\sin\left[\xi/2\right]}$$

to sum the two geometric series transforms (2.36) into

$$\sigma_M\,(t) = \int_{-T/2}^{T/2}\frac{\sin^2\left[(M+1)\,\pi(t-t')/T\right]}{T(M+1)\sin^2\left[\pi(t-t')/T\right]}f\,(t')\,dt'. \tag{2.37}$$

This representation of $\sigma_M\,(t)$ is very much in the spirit of (2.3). Indeed in view of (2.33) $\sigma_M\,(t)$ must converge to the same limit as the associated Fourier series. The new kernel function

$$K_M(t-t') = \frac{\sin^2\left[(M+1)\,\pi(t-t')/T\right]}{T(M+1)\sin^2\left[\pi(t-t')/T\right]} \tag{2.38}$$

is called the Fejer kernel and (2.34) the Fejer sum. Just like the Fourier series kernel the Fejer kernel is periodic with period T so that in virtue of (2.33) we may write

$$\lim_{M\to\infty}\frac{\sin^2\left[(M+1)\,\pi(t-t')/T\right]}{T(M+1)\sin^2\left[\pi(t-t')/T\right]} = \sum_{k=-\infty}^{\infty}\delta\,(t-t'-kT)\,. \tag{2.39}$$

Alternatively with the aid of limiting arguments similar to those employed in (2.11) and (2.12) one can easily verify (2.39) directly by evaluating the limit in (2.37) as $M \to \infty$.

Figure 2.9 shows the approximation achieved with the Fejer sum (2.34) (or its equivalent (2.37)) for $f\,(t) = U\,(t-0.5)$ with 51 sinusoids ($M = 25$). Also shown for comparison is the partial Fourier series sum for the same value of M.

Note that in the Fejer sum the Gibbs oscillations are absent but that the approximation underestimates the magnitude of the jump at the discontinuity. In effect, to achieve a good fit to the "corners" at a jump discontinuity the penalty one pays with the Fejer sum is that more terms are needed than with a Fourier sum to approximate the smooth portions of the function. To get some idea of the rate of convergence to the "corners" plots of Fejer sums for $M = 10, 25, 50$, and 100 are shown in Fig. 2.10, where (for $t > 0.5$) $\sigma_{10}(t) < \sigma_{25}(t) < \sigma_{50}(t) < \sigma_{100}(t)$.

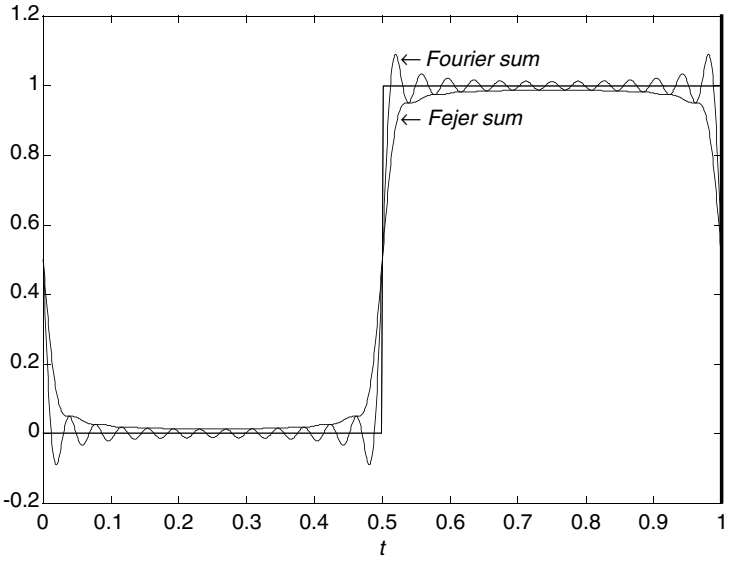

Figure 2.9: Comparison of Fejer and Fourier convergence

In passing we remark that the Fejer sum (2.34) is not a partial Fourier series sum because the expansion coefficients themselves, $\hat{\sigma}_k = \hat{w}_k(M)\,\hat{f}_k$ are functions of M. Trigonometric sums of this type are not unique. In fact by forming the arithmetic mean of the Fejer sum itself

$$\sigma_M^{(1)}(t) = \frac{1}{M+1}\sum_{N=0}^{M}\sigma_N(t) \tag{2.40}$$

we can again avail ourselves of the limit theorem in (2.32) and (2.33) and conclude that the partial sum $\sigma_M^{(1)}(t)$ must approach $f(t)$ in the limit of large M, i.e.,

$$\lim_{M\to\infty}\sigma_M^{(1)}(t) = f(t). \tag{2.41}$$

For any finite M we may regard $\sigma_M^{(1)}(t)$ as the second-order Fejer approximation. Upon replacing M by N in (2.34) and substituting for $\sigma_N(t)$ we can easily carry

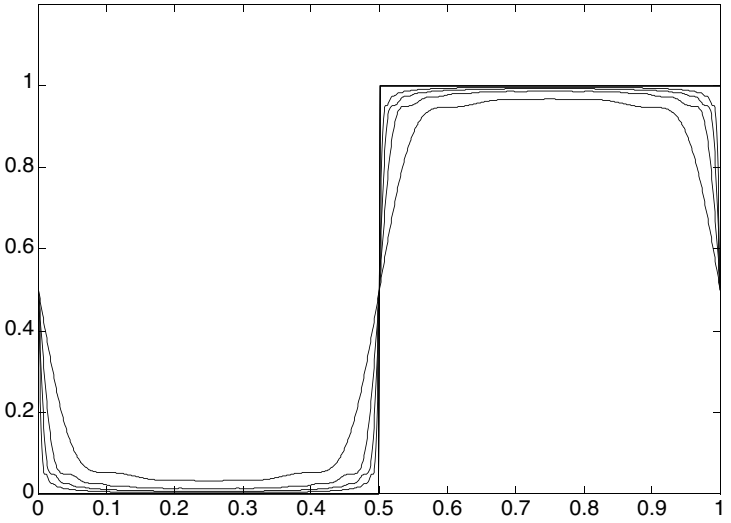

Figure 2.10: Convergence of the Fejer approximation

out one of the sums and write the final result in the form

$$\sigma_M^{(1)}(t) = \sum_{k=-M}^{M} \hat{f}_k \hat{w}_k^{(1)}(M)\, e^{ik(2\pi t/T)}, \tag{2.42}$$

where

$$\hat{w}_k^{(1)}(M) = \frac{1}{M+1} \sum_{n=1}^{M-|k|+1} \frac{n}{|k|+n}\ ,\ \ k = 0, \pm 1, \pm 2, \ldots \pm M \tag{2.43}$$

is the new spectral window. We see that we no longer have the simple linear taper that obtains for the first-order Fejer approximation. Unfortunately this sum does not appear to lend itself to further simplification. A plot of (2.43) in the form of a stem diagram is shown in Fig. 2.11 for $M = 12$. Figure 2.12 shows plots of the first- and second-order Fejer approximations for a rectangular pulse using $M = 25$. We see that the second-order approximation achieves a greater degree of smoothing but underestimates the pulse amplitude significantly more than does the first-order approximation. Apparently to reduce the amplitude error to the same level as achieved with the first-order approximation much larger spectral width (values of M) are required. This is consistent with the concave nature of the spectral taper in Fig. 2.11 which, for the same bandwidth, will tend to remove more energy from the original signal spectrum than a linear taper.

Clearly higher order Fejer approximations can be generated recursively with the formula

$$\sigma_M^{(m)}(t) = \frac{1}{M+1} \sum_{k=0}^{M} \sigma_k^{(m-1)}(t)\,, \tag{2.44a}$$

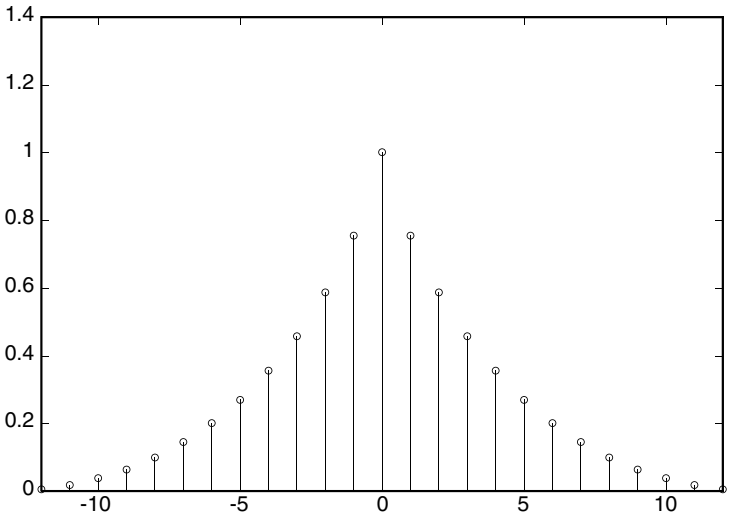

Figure 2.11: Second-order Fejer spectral window

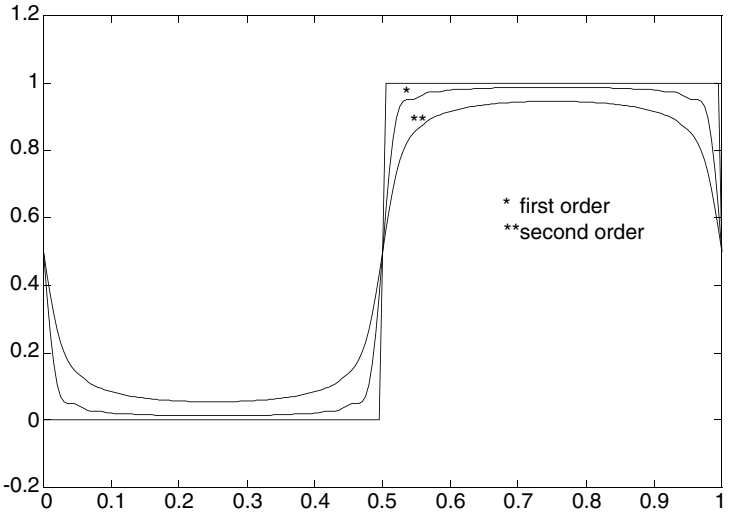

Figure 2.12: First- and second-order Fejer approximations

wherein $\sigma_k^{(0)}(t) \equiv \sigma_k(t)$. It should be noted that Fejer approximations of all orders obey the limiting property

$$\lim_{M\to\infty} \sigma_M^{(m-1)}(t) = \frac{1}{2}[f(t^+) + f(t^-)]\ ;\ \ m = 1, 2, 3, \ldots. \tag{2.44b}$$

i.e., at step discontinuities the partial sums converge to the arithmetic average of the given function, just like ordinary Fourier series. The advantage of higher

order Fejer approximations is that they provide for a greater degree of smoothing in the neighborhood of step discontinuities. This is achieved at the expense of more expansion terms (equivalently, requiring wider bandwidths) to reach a given level of approximation accuracy.

2.1.6 Fundamental Relationships Between the Frequency and Time Domain Representations

Parseval Formula

Once all the Fourier coefficients of a given function are known they may be used, if desired, to reconstruct the original function. In fact, the specification of the coefficients and the time interval within which the function is defined is, in principle, equivalent to the specification of the function itself. Even though the $\hat{f}_n$ are components of the infinite-dimensional vector

$$\mathbf{f} = [\ldots \hat{f}_n \ldots]^T, \tag{2.45}$$

we can still interpret them as the projections of the signal $f(t)$ along the basis functions $e^{i2\pi nt/T}$ and think of them geometrically as in Fig. 1.3. Because each $\hat{f}_n$ is uniquely associated with a radian frequency of oscillation ω_n, with $\omega_n/2\pi = n/T\ Hz$, $\mathbf{f}$ is said to constitute the frequency domain representation of the signal, and the elements of $\mathbf{f}$ the signal (line) spectrum. A very important relationship between the frequency domain and the time domain representations of the signal is Parseval formula

$$\frac{1}{T}\int_{-T/2}^{T/2} |f(t)|^2\, dt = \sum_{n=-\infty}^{n=\infty} \left|\hat{f}_n\right|^2. \tag{2.46}$$

This follows as a special case of (1.305) and is a direct consequence of the LMS error in the approximation tending to zero. With $\mathbf{f}' \equiv \sqrt{T}\mathbf{f}$ we can rewrite (2.46) using the notation

$$(f, f) = \|\mathbf{f}'\|^2, \tag{2.47}$$

which states that the norm in the frequency domain is identical to that in the time domain. Since physically the time average on the left of (2.46) may generally be interpreted as the average signal power (or some quantity proportional to it), Parseval formula in effect states that the average power in the time and frequency domains is preserved.

Given the two functions, $f(t)$ and $g(t)$ within the interval $-T/2, T/2$ with Fourier coefficients $\hat{f}_n$ and $\hat{g}_n$, it is not hard to show (problem 2-2) that (2.46) generalizes to

$$\frac{1}{T}\int_{-T/2}^{T/2} f(t)\, g^*(t)\, dt = \sum_{n=-\infty}^{n=\infty} \hat{f}_n \hat{g}_n^*. \tag{2.48}$$

Time and Frequency Domain Convolution

An important role in linear system analysis is played by the convolution integral. From the standpoint of Fourier series this integral is of the form

$$h(t) = \frac{1}{T}\int_{-T/2}^{T/2} f(\tau)\, g(t-\tau)\, d\tau. \tag{2.49}$$

We now suppose that the Fourier series coefficients $\hat{f}_n$ and $\hat{g}_n$ of $f(t)$ and $g(t)$, defined within $-T/2, T/2$, are known. What will be the Fourier coefficients $\hat{h}_m$ of $h(t)$ when expanded in the same interval? The answer is readily obtained when we represent $f(\tau)$ by its Fourier series (2.13) and similarly $g(t-\tau)$. Thus

$$\begin{aligned} h(t) &= \frac{1}{T}\int_{-T/2}^{T/2} \sum_{n=-\infty}^{\infty} \hat{f}_n e^{i2\pi n\tau/T} \sum_{m=-\infty}^{\infty} \hat{g}_m e^{i2\pi m(t-\tau)/T} d\tau \\ &= \frac{1}{T}\sum_{m=-\infty}^{\infty} \hat{g}_m e^{i2\pi mt/T} \sum_{n=-\infty}^{\infty} \hat{f}_n \int_{-T/2}^{T/2} e^{i2\pi(n-m)\tau/T} d\tau \\ &= \frac{1}{T}\sum_{m=-\infty}^{\infty} \hat{g}_m e^{i2\pi mt/T} \sum_{n=-\infty}^{\infty} \hat{f}_n T\delta_{nm} \\ &= \sum_{m=-\infty}^{\infty} \hat{g}_m \hat{f}_m e^{i2\pi mt/T} = \sum_{m=-\infty}^{\infty} \hat{h}_m e^{i2\pi mt/T} \end{aligned} \tag{2.50}$$

from which we identify $\hat{h}_m = \hat{g}_m \hat{f}_m$. A dual situation frequently arises when we need the Fourier coefficients of the product of the two functions, e.g., $q(t) \equiv f(t)\, g(t)$. Here we can proceed similarly

$$\begin{aligned} q(t) &\equiv f(t)\, g(t) \\ &= \sum_{n=-\infty}^{\infty} \hat{f}_n e^{i2\pi nt/T} \sum_{m=-\infty}^{\infty} \hat{g}_m e^{i2\pi mt/T} \\ &= \sum_{n=-\infty}^{\infty} \sum_{m=-\infty}^{\infty} \hat{f}_n \hat{g}_m e^{i2\pi(n+m)t/T} \\ &= \sum_{n=-\infty}^{\infty} \sum_{k=-\infty}^{\infty} \hat{f}_n \hat{g}_{k-n} e^{i2\pi kt/T} \\ &= \sum_{n=-\infty}^{\infty} \left(\sum_{m=-\infty}^{\infty} \hat{f}_m \hat{g}_{n-m} \right) e^{i2\pi nt/T} = \sum_{n=-\infty}^{\infty} \hat{q}_n e^{i2\pi nt/T}, \end{aligned} \tag{2.51}$$

where in the last step we identify the Fourier coefficient of $q(t)$ as $\hat{q}_n = \sum_{m=-\infty}^{\infty} \hat{f}_m \hat{g}_{n-m}$ which is a convolution sum formed with the Fourier coefficients of the two functions.

Symmetries

Frequently (but not always) the signal in the time domain will be real. In that case the formula for the coefficients gives

$$\hat{f}_{-n} = \hat{f}_n^*, \tag{2.52}$$

which means that the magnitude of the line spectrum is symmetrically disposed with respect to the index $n = 0$. Simplifications also arise when the signal is either an even or an odd function with respect to $t = 0$. In case of an even function $f(t) = f(-t)$ we obtain

$$\hat{f}_n = \frac{2}{T} \int_0^{T/2} f(t) \cos(2\pi nt/T)\, dt \tag{2.53}$$

and since $\hat{f}_{-n} = \hat{f}_n$ the Fourier series reads

$$f(t) = \hat{f}_0 + 2 \sum_{n=1}^{\infty} \hat{f}_n \cos(2\pi nt/T)\,. \tag{2.54}$$

In case of an odd function $f(t) = -f(-t)$ the coefficients simplify to

$$\hat{f}_n = \frac{-i2}{T} \int_0^{T/2} f(t) \sin(2\pi nt/T)\, dt \tag{2.55}$$

and since $\hat{f}_{-n} = -\hat{f}_n$ we have for the Fourier series

$$f(t) = i2 \sum_{n=1}^{\infty} \hat{f}_n \sin(2\pi nt/T)\,. \tag{2.56}$$

It is worth noting that (2.53-2.54) hold for complex functions in general, independent of (2.52).

2.1.7 Cosine and Sine Series

In our discussion of convergence of Fourier series we noted that whenever a function assumes unequal values at the interval endpoints its Fourier series coverages at either endpoint to the arithmetic mean of the two endpoint values. An illustration of how the approximation manifests itself when finite partial sums are involved may be seen from the plot in Fig. 2.5 for an exponential function. It turns out that these pathological convergence properties can actually be eliminated by a judicious choice of the expansion interval. The approach rests on the following considerations. Suppose function $f(t)$ to be expanded is defined in the interval $0, T$ while the nature of its periodic extension is outside the domain of the problem of interest and, consequently, at our disposal. In that case we may artificially extend the expansion interval to $-T, T$ and define a function over this new interval as $f(|t|)$, as shown in Fig. 2.13. This function is continuous

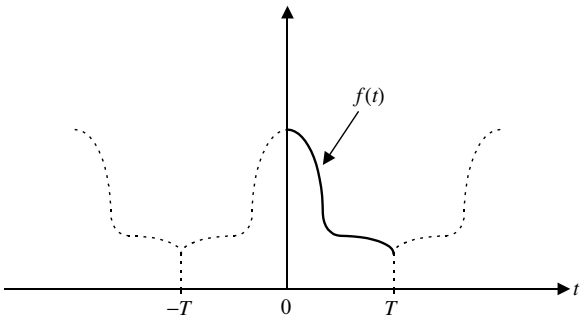

Figure 2.13: Extension of the function for the cosine series

at $t = 0$ and moreover assumes identical values at $-T$ and T. Hence its periodic extension is also continuous at these endpoints which means that its Fourier series will converge uniformly throughout the closed interval $-T, T$ to $f(|t|)$ and, in particular, to the prescribed function $f(t)$ throughout the desired range $0 \leq t \leq T$. Of course, since $f(|t|)$ is even with respect to $t = 0$, this Fourier series contains only cosine terms. However, because the expansion interval is $2T$ rather than T, the arguments of the expansion functions are $\pi nt/T$ rather than $2\pi nt/T$. Hence

$$\begin{aligned} \hat{f}_n &= \frac{1}{2T}\int_{-T}^{T} f(|t|)\cos(\pi nt/T)\,dt \\ &= \frac{1}{T}\int_{0}^{T} f(t)\cos(\pi nt/T)\,dt. \end{aligned} \tag{2.57}$$

The Fourier cosine series reads

$$\begin{aligned} f(t) &= \hat{f}_0 + 2\sum_{n=1}^{\infty}\hat{f}_n\cos(\pi nt/T) \\ &= \sum_{n=0}^{\infty}\hat{f}_n^c\cos(\pi nt/T), \end{aligned} \tag{2.58}$$

where

$$\hat{f}_n^c = \begin{cases} \frac{1}{T}\int_0^T f(t)\,dt\ ;\ n = 0, \\ \frac{2}{T}\int_0^T f(t)\cos(\pi nt/T)\,dt\ ; n > 0. \end{cases} \tag{2.59}$$

The approximation to e^{-t} using a cosine series comprised of 10 terms is plotted in Fig. 2.14. We note a significant improvement in the approximation over that obtained with the conventional partial Fourier series sum in Fig. 2.5, where 21 terms are employed to approximate the same function.

It should be noted that the coefficients of the cosine series (2.59) are nothing more than the solution to the normal equations for the LMS problem phrased in terms of the cosine functions

$$\phi_n^c(t) = \cos(\pi nt/T),\ n = 0, 1, 2, \ldots \tag{2.60}$$

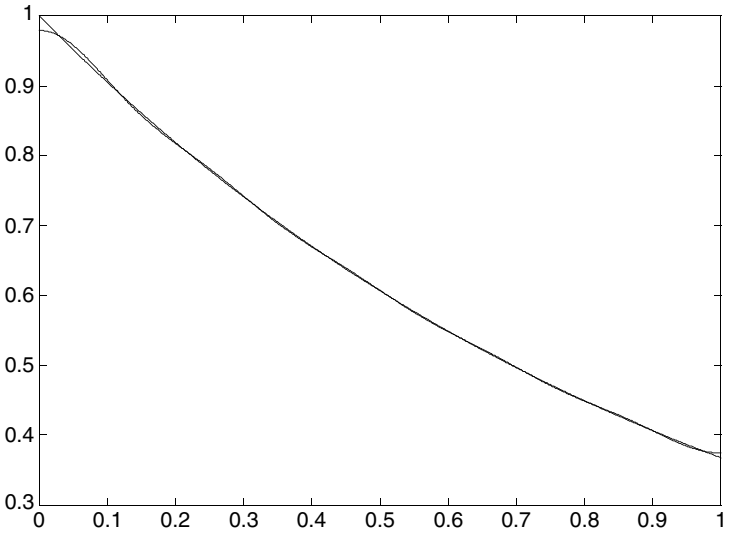

Figure 2.14: Cosine series approximation (N=10)

As may be verified directly, they are orthogonal over the interval $0, T$. In our compact notation this reads

$$(\phi_n^c, \phi_m^c) = (T/\varepsilon_n)\,\delta_{nm},$$

where we have introduced the abbreviation

$$\varepsilon_n = \begin{cases} 1; n = 0, \\ 2\ ; n > 0, \end{cases}$$

which is usually referred to as the Neumann symbol.

The convergence properties of the cosine series at points of continuity and at jump discontinuities within the interval are identical to those of the complete Fourier series from which, after all, the cosine series may be derived. The cosine expansion functions form a complete set in the space of piecewise differentiable functions whose derivatives must vanish at the interval endpoints. This additional restriction arises because of the vanishing of the derivative of $\cos(\pi nt/T)$ at $t = 0$ and $t = T$. In accordance with (1.303), the formal statement of completeness may be phrased in terms of an infinite series of products of the orthonormal expansion functions $\sqrt{\varepsilon_n/T}\phi_n^c(t)$ as follows:

$$\delta(t - t') = \sum_{n=0}^{\infty} \sqrt{\frac{\varepsilon_n}{T}} \cos(\pi nt/T) \sqrt{\frac{\varepsilon_n}{T}} \cos(\pi nt'/T). \tag{2.61}$$

Sine Series

If instead of an even extension of $f(t)$ into the interval $-T, 0$ as in Fig. 2.13, we employ an odd extension, as in Fig. 2.15, and expand the function $f(|t|)\,sign(t)$ in a Fourier series within the interval $-T, T$, we find that the cosine terms

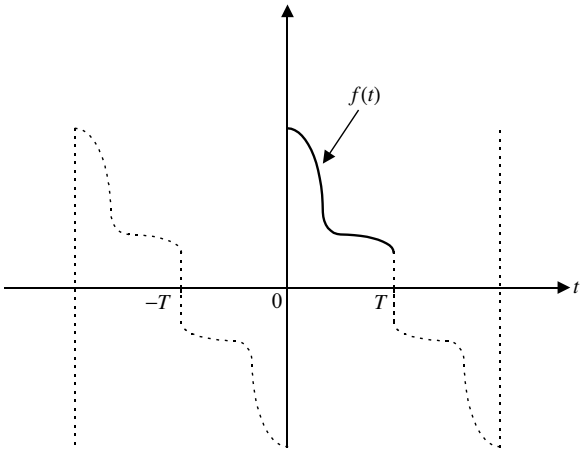

Figure 2.15: Function extension for sine series

vanish and the resulting Fourier series is comprised entirely of sines. Within the original interval $0, T$ it converges to the prescribed function $f(t)$ and constitutes the so-called sine series expansion, to wit,

$$f(t) = \sum_{n=0}^{\infty} \hat{f}_n^s \sin(\pi n t/T), \tag{2.62}$$

where

$$\hat{f}_n^s = \frac{2}{T} \int_0^T f(t) \sin(\pi n t/T)\, dt. \tag{2.63}$$

Evidently because the sine functions vanish at the interval endpoints the sine series will necessarily converge to zero there. Since at a discontinuity a Fourier series always converges to the arithmetic mean of the left and right endpoint values, we see from Fig. 2.15 that the convergence of the sine series to zero at the endpoints does not require that the prescribed function also vanishes there. Of course, if this is not the case, only LMS convergence is guaranteed at the endpoints and an approximation by a finite number of terms will be vitiated by the Gibbs effect. A representative illustration of the expected convergence behavior in such cases can be had by referring to Fig. 2.5. For this reason the sine series is to be used only with functions that vanish at the interval endpoints. In such cases convergence properties very similar to those of cosine series are achieved. A case in point is the approximation shown in Fig. 2.6.

The sine expansion functions

$$\phi_n^s(t) = \sin(\pi n t/T), \ n = 1, 2, 3, \ldots \tag{2.64}$$

possess the orthogonality properties

$$(\phi_n^s, \phi_m^s) = (T/2)\, \delta_{nm}; \tag{2.65}$$

they form a complete set in the space of piecewise differentiable functions that vanish at the interval endpoints. Again the formal statement of this completeness may be summarized by the delta function representation

$$\delta(t-t') = \sum_{n=0}^{\infty} \sqrt{\frac{2}{T}} \sin(\pi n t/T) \sqrt{\frac{2}{T}} \sin(\pi n t'/T). \tag{2.66}$$

2.1.8 Interpolation with Sinusoids

Interpolation Using Exponential Functions

Suppose $f(t)$ can be represented exactly by the sum

$$f(t) = \sum_{n=-N}^{N} c_n e^{i\frac{2\pi n t}{T}} \;;\; 0 \le t \le T. \tag{2.67}$$

If $f(t)$ is specified at $M = 2N+1$ points within the given interval (2.67) can be viewed as a system of M linear equations for the M unknown coefficients c_n. A particularly simple formula for the coefficients results if we suppose that the function is specified on uniformly spaced points within the interval. To derive it we first change the summation index in (2.67) from n to $m = N+n$ to obtain

$$f(t) = \sum_{m=0}^{2N} c_{m-N} e^{i\frac{2\pi(m-N)t}{T}} \quad . \tag{2.68}$$

With $t = \ell\Delta t$ and $\Delta t = T/M$ (2.68) becomes

$$f(\ell\Delta t) = \sum_{m=0}^{M-1} c_{m-N} e^{i\frac{2\pi(m-N)\ell}{M}}. \tag{2.69}$$

From the geometric series $\sum_{m=0}^{M-1} e^{im\alpha} = e^{i\alpha(M-1)/2} \sin(M\alpha/2) / \sin(\alpha/2)$ we readily establish the orthogonality relationship

$$\sum_{\ell=0}^{M-1} e^{i\frac{2\pi\ell(m-k)}{M}} = M\delta_{mk}. \tag{2.70}$$

Upon multiplying both sides of (2.69) by $e^{-i\frac{2\pi\ell k}{M}}$ and summing on ℓ and using (2.70) we obtain the solution for the coefficients

$$c_{m-N} = \frac{1}{M} \sum_{\ell=0}^{M-1} f(\ell\Delta t)\, e^{-i\frac{2\pi\ell(m-N)}{M}}. \tag{2.71}$$

Reverting to the index n and $M = 2N+1$ the preceding is equivalent to

$$c_n = \frac{1}{2N+1} \sum_{\ell=0}^{2N} f(\ell\Delta t)\, e^{-i\frac{2\pi\ell n}{2N+1}}. \tag{2.72}$$

On the other hand we know that the solution for c_n in (2.67) is also given by the integral

$$c_n = \frac{1}{T}\int_0^T f(t)e^{-i\frac{2\pi nt}{T}}dt. \tag{2.73}$$

If in (2.72) we replace $1/(2N+1)$ by its equivalent $\Delta t/T$, we can interpret (2.71) as a Riemann sum approximation to (2.73). However we know from the foregoing that (2.72) is in fact an exact solution of (2.69). Thus whenever $f(t)$ is comprised of a finite number of sinusoids the Riemann sum will represent the integral (2.73) exactly provided $2N+1$ is chosen equal to or greater than the number of sinusoids. Evidently, if the number of sinusoids is exactly $2N+1$, the c_n as computed using either (2.73) or (2.72) must be identically zero whenever $|n| > N$. If $f(t)$ is a general piecewise differentiable function, then (2.67) with the coefficients determined by (2.72) provides an interpolation to $f(t)$ in terms of sinusoids. In fact by substituting (2.72) into (2.67) and again summing a geometric series we obtain the following explicit interpolation formula:

$$f(t) = \sum_{\ell=0}^{M-1} f(\ell\Delta t)\,\frac{\sin\left[\pi\left(\frac{t}{\Delta t}-\ell\right)\right]}{M\sin\left[\frac{\pi}{M}\left(\frac{t}{\Delta t}-\ell\right)\right]}. \tag{2.74}$$

Unlike the LMS approximation problem underlying the classical Fourier series, the determination of the coefficients in the interpolation problem does not require the evaluation of integrals. This in itself is of considerable computational advantage. How do interpolation-type approximations compare with LMS approximations? Figure 2.16 shows the interpolation of e^{-t} achieved with 11 sinusoids while Fig. 2.17 shows the approximation with the same number of sinusoids using the LMS approximation. We note that the fit is comparable in the two cases except at the endpoints where, as we know, the LMS approximation necessarily converges to $\left(1+e^{-1}\right)/2$. As the number of terms in the interpolation is increased the fit within the interval improves. Nevertheless, the interpolated function continues to show considerable undamped oscillatory behavior near the endpoints as shown by the plot in Fig. 2.18.

Interpolation Using Cosine Functions

Recalling the improvement in the LMS approximation achieved with the cosine series over the complete Fourier expansion, we might expect a similar improvement in case of interpolation. This turns out actually to be the case. As will be demonstrated, the oscillatory behavior near the endpoints in Fig. 2.18 can be completely eliminated and a substantially better fit to the prescribed function achieved throughout the entire approximating interval using an alternative interpolation that employs only cosine functions, i.e., an interpolation formula based on (2.58) rather than (2.67). In this case we set the interpolation interval to

$$\Delta t = T/(M-1/2) \tag{2.75}$$

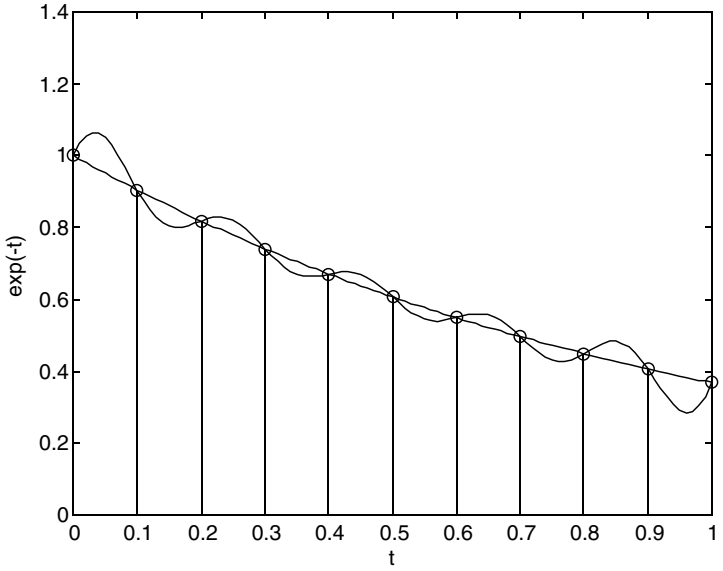

Figure 2.16: Interpolation of e^{-t} using 11 sinusoids

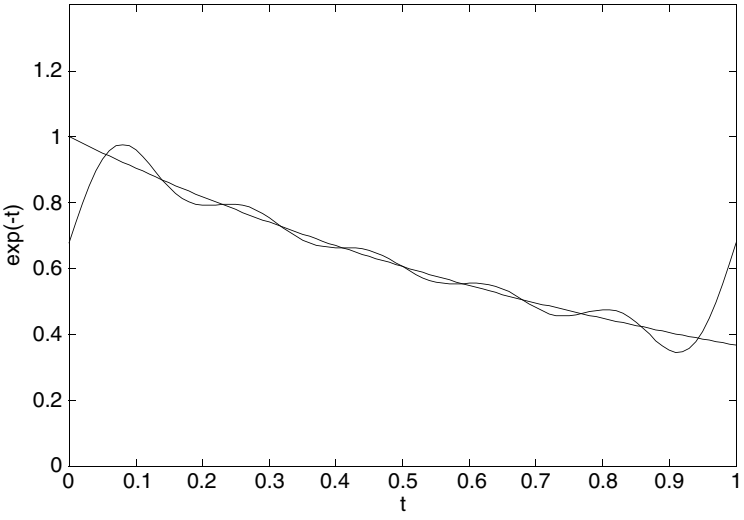

Figure 2.17: LMS approximation to e^{-t} using 11 sinusoids

and with $t = m\Delta t$ in (2.58) we obtain

$$f\left(m\Delta t\right) = \sum_{n=0}^{M-1} c_n^c \cos\left[\pi nm/\left(M-1/2\right)\right] \quad ; \quad m = 0, 1, 2, \ldots M-1, \qquad (2.76)$$

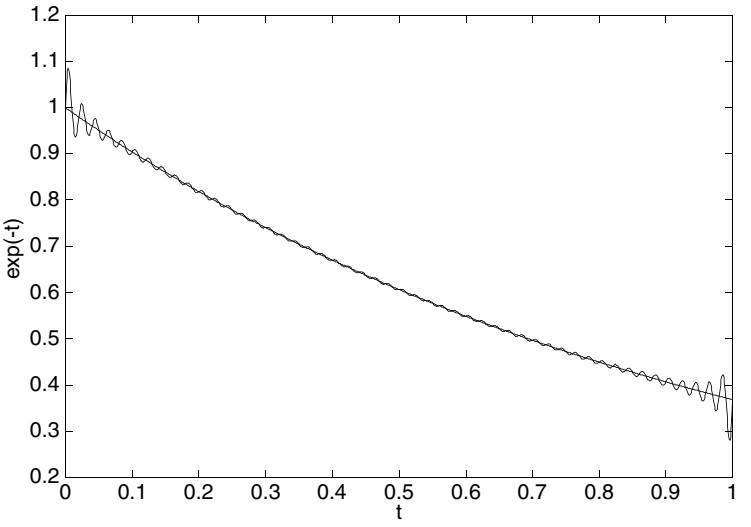

Figure 2.18: Interpolation of e^{-t} using 101 sinusoids

where the c_n^c are the unknown coefficients. The solution for the c_n^c is made somewhat easier if one first extends the definition of $f(m\Delta t)$ to negative indices as in Fig. 2.13 and rewrites (2.76) in terms of complex exponentials. Thus

$$f(m\Delta t) = \sum_{n=-(M-1)}^{M-1} c_n'^c e^{i2\pi nm/(2M-1)} \;\; ; \;\; m = 0, \pm 1, \pm 2, \ldots \pm (M-1), \quad (2.77)$$

where in addition to $f(m\Delta t) = f(-m\Delta t)$ we postulated that $c_n^c = c_{-n}^c$ and defined

$$c_n'^c = \begin{cases} c_0^c \; ; \; n = 0, \\ c_n^c/2 \; ; \; n \neq 0. \end{cases} \quad (2.78)$$

Again using the geometric series sum formula we have the orthogonality

$$\begin{aligned} \sum_{n=-(M-1)}^{M-1} e^{i2\pi n(m-k)/(2M-1)} &= \frac{\sin[\pi(m-k)]}{\sin[\pi(m-k)/(2M-1)]} \\ &\equiv (2M-1)\,\delta_{mk} \end{aligned} \quad (2.79)$$

with the aid of which the solution for the $c_n'^c$ in (2.78) follows at once:

$$\begin{aligned} c_n'^c &= \frac{1}{2M-1} \sum_{m=-(M-1)}^{M-1} f(m\Delta t)\, e^{-i2\pi nm/(2M-1)} \\ &= \frac{1}{2M-1} \sum_{m=0}^{M-1} \varepsilon_m f(m\Delta t) \cos[2\pi nm/(2M-1)] \end{aligned}$$

$$= \frac{1}{M-1/2}\sum_{m=0}^{M-1}(\varepsilon_m/2)\, f(m\Delta t)\cos[\pi nm/(M-1/2)]\,.$$

Taking account of (2.78) we obtain the final result

$$c_n^c = \frac{2}{M-1/2}\sum_{m=0}^{M-1}(\varepsilon_n\varepsilon_m/4)\, f(m\Delta t)\cos[\pi nm/(M-1/2)]\,;\ n=0,1,2,\ldots M-1. \tag{2.80}$$

The final interpolation formula now follows through a direct substitution of (2.80) into

$$f(t) = \sum_{n=0}^{M-1} c_n^c \cos(\pi nt/T)\,. \tag{2.81}$$

After summation over n we obtain

$$f(t) = \frac{1}{M-1/2}\sum_{m=0}^{M-1}(\varepsilon_m/2)\, f(m\Delta t)\left\{1 + k_M(t/\Delta t - m) + k_M(t/\Delta t + m)\right\}, \tag{2.82}$$

where

$$k_M(t) = \cos\left(\frac{\pi M}{2M-1}t\right)\frac{\sin\left[\frac{\pi(M-1))}{2(M-1/2)}t\right]}{\sin\left[\frac{\pi}{2(M-1/2)}t\right]}. \tag{2.83}$$

Fig. 2.19 shows the interpolation of e^{-t} using 11 cosine functions.

The improvement over the interpolation wherein both sines and cosines were employed, Fig. 2.16, is definitely noticeable. A more important issue with general sinusoids is the crowding toward the interval endpoints as in Fig. 2.18. With the cosine interpolation these oscillations are completely eliminated, as may be seen from the plot in Fig. 2.20.

By choosing different distributions of the locations and sizes of the interpolation intervals the interpolation properties can be tailored to specific classes of functions. Of course, a nonuniform distribution of interpolation intervals will in general not lead to analytically tractable forms of expansion coefficients and will require a numerical matrix inversion. We shall not deal with nonuniform distribution of intervals. There is, however, a slightly different way of specifying a uniform distribution of interpolation intervals from the one we have just considered which is worth mentioning since it leads to formulas for the so-called discrete cosine transform commonly employed in data and image compression work. Using the seemingly innocuous modification of (2.75) to

$$\Delta t = \frac{T}{2M} \tag{2.84}$$

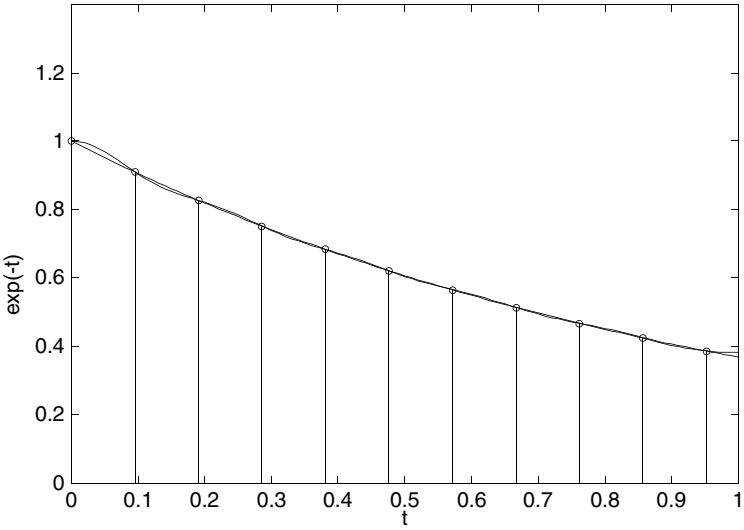

Figure 2.19: Interpolation of e^{-t} with 11 cosine functions

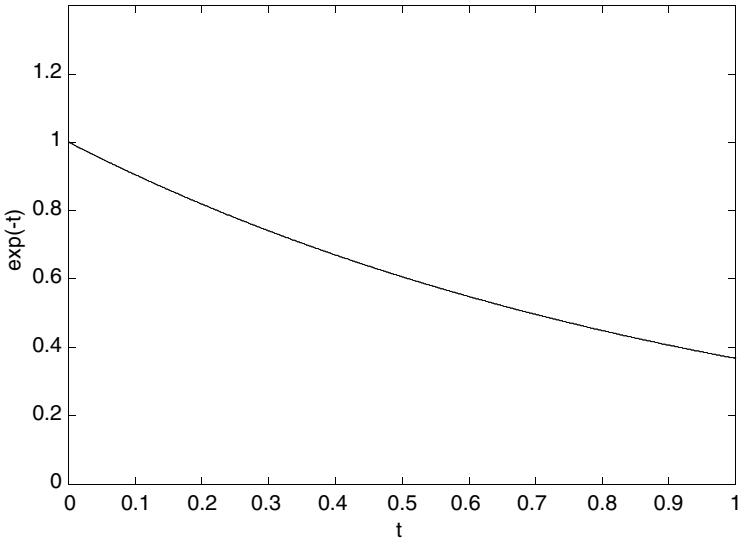

Figure 2.20: Interpolation of e^{-t} with 101 cosine functions

and forcing the first and the last step size to equal $\Delta t/2$ we replace (2.76) by

$$f\left[\Delta t\left(m+1/2\right)\right]=\sum_{n=0}^{M-1}\hat{c}_{n}^{c}\cos\left[\pi n\left(2m+1\right)/2M\right]\quad;\quad m=0,1,2,\ldots M-1. \tag{2.85}$$

With the aid of the geometrical sum formula we can readily verify the orthogonality relationship

$$\sum_{m=0}^{M-1} \cos\left[\pi n\left(2m+1\right)/2M\right] \cos\left[\pi k\left(2m+1\right)/2M\right] = \frac{M}{\varepsilon_n}\delta_{nk} \tag{2.86}$$

with the aid of which we solve for the coefficients in (2.85):

$$\hat{c}_n^c = \frac{\varepsilon_n}{M} \sum_{m=0}^{M-1} f\left[\Delta t\left(m+1/2\right)\right] \cos\left[\pi n\left(2m+1\right)/2M\right]. \tag{2.87}$$

Replacing c_n^c in (2.81) by $\hat{c}_n^c$ of (2.87) yields the interpolation formula

$$f\left(t\right) = \frac{1}{M} \sum_{m=0}^{M-1} f\left[\Delta t\left(m+1/2\right)\right] \left[1 + \hat{k}_M\left(\tau^+\right) + \hat{k}_M\left(\tau^-\right)\right], \tag{2.88}$$

where

$$\tau^+ = t/\Delta t - (m+1/2) \tag{2.88a}$$

$$\tau^- = t/\Delta t + (m+1/2) \tag{2.88b}$$

and

$$\hat{k}_M\left(t\right) = \cos(\pi t/2) \frac{\sin\left(\frac{\pi(M-1)}{2M}t\right)}{\sin\left(\frac{\pi}{2M}t\right)}. \tag{2.89}$$

Equation (2.85) together with (2.87) is usually referred to as the discrete cosine transform pair. Here we have obtained it as a by-product along our route toward a particular interpolation formula comprised of cosine functions.

2.1.9 Anharmonic Fourier Series

Suppose we approximate the signal $f(t)$ in the LMS sense by a sum of sinusoids with radian frequencies $\mu_1, \mu_2, \ldots \mu_N$ which are not necessarily harmonically related. Assuming the signal is specified in the interval $a \le t \le b$ we write this approximating sum as follows:

$$f(t) \sim \sum_{n=1}^{N} \hat{f}_n \psi_n\left(t\right), \tag{2.90}$$

wherein

$$\psi_n\left(t\right) = A_n \sin \mu_n t + B_n \cos \mu_n t \tag{2.91}$$

and A_n and B_n are suitable normalization constants. It is not hard to show that as long as all the μ_n are distinct the Gram matrix $\Gamma_{nm} = (\psi_n, \psi_m)$ is nonsingular so that the normal equations yield a unique set of expansion coefficients $\hat{f}_n$. Of course their computation would be significantly simplified if

it were possible to choose a sets of radian frequencies μ_n such that the Gram matrix is diagonal, or, equivalently, that the ψ_n are orthogonal over the chosen interval. We know that this is always the case for harmonically related radian frequencies. It turns out that orthogonality also obtains when the radian frequencies are not harmonically related provided they are chosen such that for a given pair of real constants α and β the $\psi_n(t)$ satisfy the following endpoint conditions:

$$\psi_n(a) = \alpha\psi_n'(a), \tag{2.92a}$$
$$\psi_n(b) = \beta\psi_n'(b). \tag{2.92b}$$

To prove orthogonality we first observe that the $\psi_n(t)$ satisfy the differential equation of the harmonic oscillator, i.e.,

$$\frac{d^2\psi_n}{dt^2} + \mu_n^2\psi_n = 0, \tag{2.93}$$

where we may regard the ψ_n as an eigenvector and μ_n^2 as the eigenvalue of the differential operator $-d^2\psi_n/\,dt^2$. Next we multiply (2.93) by ψ_m and integrate the result over $a \le t \le b$ to obtain

$$\psi_m \frac{d\psi_n}{dt}\Big|_a^b - \int_a^b \frac{d\psi_m}{dt}\frac{d\psi_n}{dt}dt + \mu_n^2\int_a^b \psi_m\psi_n dt = 0, \tag{2.94}$$

where the second derivative has been eliminated by an integration by parts. An interchange of indices in (2.94) gives

$$\psi_n \frac{d\psi_m}{dt}\Big|_a^b - \int_a^b \frac{d\psi_n}{dt}\frac{d\psi_m}{dt}dt + \mu_m^2\int_a^b \psi_n\psi_m dt = 0 \tag{2.95}$$

and subtraction of (2.95) from (2.94) yields

$$\psi_m \frac{d\psi_n}{dt}\Big|_a^b - \psi_n \frac{d\psi_m}{dt}\Big|_a^b = \left(\mu_n^2 - \mu_m^2\right)\int_a^b \psi_n\psi_m dt. \tag{2.96}$$

We now observe that substitution of the endpoint conditions (2.92) into the left side of (2.96) yields zero. This implies orthogonality provided we assume that for $n \neq m$ μ_m and μ_n are distinct. For then

$$\int_a^b \psi_n\psi_m dt = 0 \ ; \ n \neq m. \tag{2.97}$$

The fact that the eigenvalues μ_n^2 are distinct follows from a direct calculation. To compute the eigenvalues we first substitute (2.91) into (2.92) which yields the following set of homogeneous algebraic equations:

$$\left(\sin\mu_n a - \alpha\mu_n\cos\mu_n a\right)A_n + \left(\cos\mu_n a + \alpha\mu_n\sin\mu_n a\right)B_n = 0, \tag{2.98a}$$
$$\left(\sin\mu_n b - \beta\mu_n\cos\mu_n b\right)A_n + \left(\cos\mu_n a + \alpha\mu_n\sin\mu_n a\right)B_n = 0. \tag{2.98b}$$

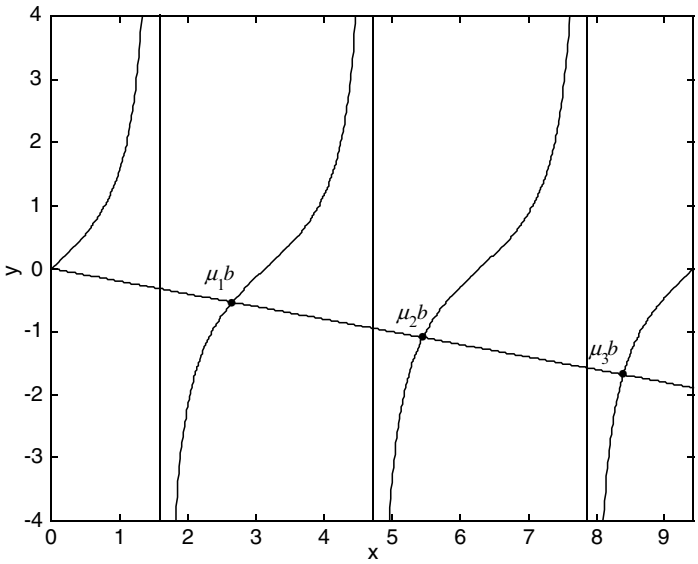

Figure 2.21: Diagram of the transcendental equation $-0.2x = \tan x$

A nontrivial solution for A_n and B_n is only possible if the determinant of the coefficients vanishes. Computing this determinant and setting the result to zero yield the following equation for μ_n :

$$(\beta - \alpha)\mu_n \cos[\mu_n(b-a)] - (1 + \alpha\beta\mu_n^2) \sin[\mu_n(b-a)] = 0. \tag{2.99}$$

This transcendental equation possesses an infinite set of distinct positive simple zeros μ_n. For an arbitrary set of parameters these roots can only be determined numerically. Many standard root finding algorithms are available for this purpose. Generally these are iterative techniques that require a "good" first guess of the root. In case of (2.99) an approximate location to start the iteration can be got from a graphical construction. We illustrate it for $\alpha = 0$ and $a = 0$ in which case (2.99) becomes $\beta\mu_n \cos \mu_n b - \sin \mu_n b = 0$, which is equivalent to

$$\beta\mu_n = \tan(\mu_n b). \tag{2.100}$$

Defining the nondimensional variable $x = \mu_n b$ in (2.100) we obtain the roots from the intersection of the straight line $y = x\beta/b$ with the curves defined by the various branches of $y = \tan x$ as shown in Fig. 2.21 for $\beta/b = -0.2$. The first three roots expressed in terms of the nondimensional quantities $\mu_1 b, \mu_2 b$ and $\mu_3 b$ may be read off the abscissa. When $\alpha = 0$ and $a = 0$ (2.98a) requires that $B_n = 0$ so that the expansion functions that correspond to the solutions of (2.100) are

$$\psi_n(t) = A_n \sin \mu_n t. \tag{2.101}$$

Setting $A_n = 1$ we compute the normalization constant

$$Q_n = \int_0^b \sin^2 \mu_n t dt = \int_0^b \frac{1 - \cos 2\mu_n t}{2} dt$$

$$= \left(b/2 - \frac{\sin 2\mu_n b}{4\mu_n}\right) = \frac{b}{2}(1 - \frac{\sin \mu_n b \cos \mu_n b}{\mu_n b}).$$

The expansion coefficients in (2.90) for this case are

$$\hat{f}_n = \frac{2}{b}\left(1 - \frac{\sin \mu_n b \cos \mu_n b}{\mu_n b}\right)^{-1} \int_0^b f(t) \sin \mu_n t dt. \tag{2.102}$$

From Fig. 2.21 we note that as n increases the abscissas of the points where the straight line intersects the tangent curves approach $\pi/2(2n-1) \approx n\pi$. Hence for large n the radian frequencies of the anharmonic expansion (2.90) are asymptotically harmonic, i.e.,

$$\underset{n\sim\infty}{\mu_n} \sim n\pi/b. \tag{2.103}$$

Taking account of (2.103) in (2.102) we also observe that for large n formula (2.102) represents the expansion coefficient of a sine Fourier series (2.63). Thus the anharmonic character of the expansion appears to manifest itself only for finite number of terms. Hence we would expect that the convergence properties of anharmonic expansions to be essentially the same as harmonic Fourier series.

An anharmonic series may be taken as a generalization of a Fourier series. For example, it reduces to the (harmonic) sine series in (2.62) when $\alpha = \beta = 0$ and when $\alpha = \beta \to \infty$ to the (harmonic) cosine series (2.58), provided $f(a) \neq 0$ and $f(b) \neq 0$. When the endpoint conditions (2.92) are replaced by a periodicity condition we obtain the standard Fourier series.

2.2 The Fourier Integral

2.2.1 LMS Approximation by Sinusoids Spanning a Continuum

Instead of approximating $f(t)$ by a sum of $2N+1$ sinusoids with discrete frequencies $\omega_n = 2\pi n/T$ we now suppose that the frequencies ω span a continuum between $-\Omega$ and Ω. With

$$f^{\Omega}(t) = \int_{-\Omega}^{\Omega} \hat{f}(\omega) e^{i\omega t} d\omega \tag{2.104}$$

we seek a function $\hat{f}(\omega)$ such that the MS error

$$\varepsilon_{\Omega}(T) \equiv \int_{-T/2}^{T/2} \left| f(t) - f^{\Omega}(t) \right|^2 dt \tag{2.105}$$

is minimized. As we know, this minimization leads to the normal equation (1.99), where we identify $\phi(\omega, t) = e^{i\omega t}, a = -T/2, b = T/2$, so that with the aid of (1.100) we obtain

$$\int_{-T/2}^{T/2} f(t) e^{-i\omega t} dt = \int_{-\Omega}^{\Omega} \hat{f}(\omega') \frac{2\sin\left[(\omega - \omega')T/2\right]}{(\omega - \omega')} d\omega'. \tag{2.106}$$

Thus unlike in the case of a discrete set of sinusoids the unknown "coefficients" $\hat{f}(\omega')$ now span a continuum. In fact, according to (2.106), to find $\hat{f}(\omega')$ we must solve an integral equation.

2.2.2 Transition to an Infinite Observation Interval: The Fourier Transform

For any finite time interval T the solution of (2.106) for $\hat{f}(\omega')$ can be expressed in terms of spheroidal functions [23]. Here we confine our attention to the case of an infinite time interval, which is the conventional domain of the Fourier integral. In that case we can employ the limiting form of the Fourier kernel in (1.269) (with Ω replaced by $T/2$) so that the right side of (2.106) becomes

$$\lim_{T\longrightarrow\infty}\int_{-\Omega}^{\Omega}\hat{f}(\omega')\,\frac{2\sin\left[(\omega-\omega')\,T/2\right]}{(\omega-\omega')}d\omega'=2\pi\hat{f}(\omega)\,. \tag{2.107}$$

Hence as the expansion interval in the time domain is allowed to approach infinity the solution of (2.106) reads

$$\int_{-\infty}^{\infty}f(t)\,e^{-i\omega t}dt=F(\omega), \tag{2.108}$$

where we have set $F(\omega)=2\pi\hat{f}(\omega)$ which shall be referred to as the Fourier Integral (or the Fourier transform) of $f(t)$. Substituting this in (2.104) and integrating with respect to ω we get

$$f^{\Omega}(t)=\int_{-\infty}^{\infty}f(t')\,\frac{\sin\left[(t-t')\,\Omega\right]}{\pi\,(t-t')}dt'. \tag{2.109}$$

The corresponding LMS error $\varepsilon_{\Omega\,\min}$ is

$$\begin{aligned}\varepsilon_{\Omega\,\min}&=\left(f-f^{\Omega},f-f^{\Omega}\right)\\&=(f,f)-\left(f,f^{\Omega}\right)\geq 0,\end{aligned} \tag{2.110}$$

where the inner products are taken over the infinite time domain and account has been taken of the projection theorem (1.75). Substituting for f^{Ω} from (2.104) the preceding is equivalent to

$$\begin{aligned}\varepsilon_{\Omega\,\min}&=\int_{-\infty}^{\infty}|f(t)|^2\,dt-\int_{-\infty}^{\infty}f^*(t)\,dt\int_{-\Omega}^{\Omega}\hat{f}(\omega)\,e^{i\omega t}d\omega\\&=\int_{-\infty}^{\infty}|f(t)|^2\,dt-2\pi\int_{-\Omega}^{\Omega}\left|\hat{f}(\omega)\right|^2d\omega\\&=\int_{-\infty}^{\infty}|f(t)|^2\,dt-\frac{1}{2\pi}\int_{-\Omega}^{\Omega}|F(\omega)|^2\,d\omega\geqslant 0,\end{aligned} \tag{2.111}$$

which is the Bessel inequality for the Fourier transform. As $\Omega\longrightarrow\infty$ the integrand in (2.109) approaches a delta function and in accordance with (1.285)

we have

$$\lim_{\Omega \longrightarrow \infty} f^{\Omega}(t) = \frac{1}{2}\left[f\left(t^{+}\right) + f\left(t^{-}\right)\right] \tag{2.112}$$

or, equivalently, using (2.104) with $F(\omega) = 2\pi \hat{f}(\omega)$

$$\lim_{\Omega \longrightarrow \infty} \frac{1}{2\pi} \int_{-\Omega}^{\Omega} F(\omega)\, e^{i\omega t} d\omega = \frac{1}{2}\left[f\left(t^{+}\right) + f\left(t^{-}\right)\right]. \tag{2.113}$$

At the same time the MS error in (2.111) approaches zero and we obtain

$$\int_{-\infty}^{\infty} |f(t)|^2 \, dt = \frac{1}{2\pi} \int_{-\infty}^{\infty} |F(\omega)|^2 \, d\omega, \tag{2.114}$$

which is Parseval theorem for the Fourier transform. Equation (2.113) is usually written in the abbreviated form

$$f(t) = \frac{1}{2\pi} \int_{-\infty}^{\infty} F(\omega)\, e^{i\omega t} d\omega \tag{2.115}$$

and is referred to as the inverse Fourier transform or the Fourier transform inversion formula. It will be frequently convenient to designate both (2.115) and the direct transform (2.108) by the concise statement

$$f(t) \overset{\mathcal{F}}{\Longleftrightarrow} F(\omega). \tag{2.116}$$

In addition, we shall at times find it useful to express the direct and inverse transform pair as

$$\mathcal{F}\{f(t)\} = F(\omega), \tag{2.117}$$

which is just an abbreviation of the statement "the Fourier transform of $f(t)$ is $F(\omega)$." We shall adhere to the convention of designating the time domain signal by a lowercase letter and its Fourier transform by the corresponding uppercase letter.

2.2.3 Completeness Relationship and Relation to Fourier Series

Proceeding in a purely formal way we replace $F(\omega)$ in (2.115) by (2.108) and interchange the order of integration and obtain

$$f(t) = \int_{-\infty}^{\infty} f(t') \left\{ \frac{1}{2\pi} \int_{-\infty}^{\infty} e^{i\omega\left(t-t'\right)} d\omega \right\} dt'. \tag{2.118}$$

The quantity in braces can now be identified as the delta function

$$\delta(t - t') = \frac{1}{2\pi} \int_{-\infty}^{\infty} e^{i\omega\left(t-t'\right)} d\omega, \tag{2.119}$$

which is a slightly disguised version of (1.254). To see this we merely have to rewrite (2.119) as the limiting form

$$\lim_{\Omega \longrightarrow \infty} \frac{1}{2\pi} \int_{-\Omega}^{\Omega} e^{i\omega(t-t')} d\omega$$

and note that for any finite Ω the integration yields $\sin[\Omega(t-t')]/\pi(t-t')$.

The representation (2.119) bears a formal resemblance to the completeness relationship for orthonormal discrete function sets, (1.302), and, more directly, to the completeness statement for Fourier series in (2.31). This resemblance can be highlighted by rewriting (2.119) to read

$$\delta(t-t') = \int_{-\infty}^{\infty} \left(\frac{1}{\sqrt{2\pi}} e^{i\omega t}\right) \left(\frac{1}{\sqrt{2\pi}} e^{i\omega t'}\right)^* d\omega \tag{2.120}$$

so that a comparison with (2.31) shows that the functions $\phi_\omega(t) \equiv 1/\sqrt{2\pi} exp(i\omega t)$ play an analogous role to the orthonormal functions $\phi_n(t) \equiv 1/\sqrt{T} exp(2\pi int/T)$ provided we view the continuous variable ω in (2.120) as proportional to a summation index. In fact a direct comparison of the variables between (2.31) and (2.120) gives the correspondence

$$\omega \quad \longleftrightarrow \quad \frac{2\pi n}{T} \tag{2.121a}$$

$$d\omega \quad \longleftrightarrow \quad \frac{2\pi}{T}. \tag{2.121b}$$

Thus as the observation period T of the signal increases, the quantity $2\pi/T$ may be thought of as approaching the differential $d\omega$ while the discrete spectral lines occurring at $2\pi n/T$ merge into a continuum corresponding to the frequency variable ω. Moreover the orthogonality over the finite interval $-T/2, T/2$, as in (1.213), becomes in the limit as $T \longrightarrow \infty$

$$\begin{aligned} \delta(\omega-\omega') &= \frac{1}{2\pi} \int_{-\infty}^{\infty} e^{it(\omega-\omega')} dt \\ &= \int_{-\infty}^{\infty} \left(\frac{1}{\sqrt{2\pi}} e^{it\omega}\right) \left(\frac{1}{\sqrt{2\pi}} e^{it\omega'}\right)^* dt \end{aligned} \tag{2.122}$$

i.e., the identity matrix represented by the Kronecker symbol δ_{mn} goes over into a delta function, which is the proper identity transformation for the continuum.

A more direct but qualitative connection between the Fourier series and the Fourier transform can be established if we suppose that the function $f(t)$ is initially truncated to $|t| < T/2$ in which case its Fourier transform is

$$F(\omega) = \int_{-T/2}^{T/2} f(t) e^{-i\omega t} dt. \tag{2.123}$$

The coefficients in the Fourier series that represents this function within the interval $-T/2, T/2$ can now be expressed as $\hat{f}_n = F(2\pi n/T)/T$ so that

$$f(t) = \sum_{n=-\infty}^{\infty} F(2\pi n/T) e^{i2\pi nt/T} \left(\frac{1}{T}\right). \tag{2.124}$$

Thus in view of (2.121) we can regard the Fourier transform inversion formula (2.115) as a limiting form of (2.124) as $T \longrightarrow \infty$. Figure 2.22 shows the

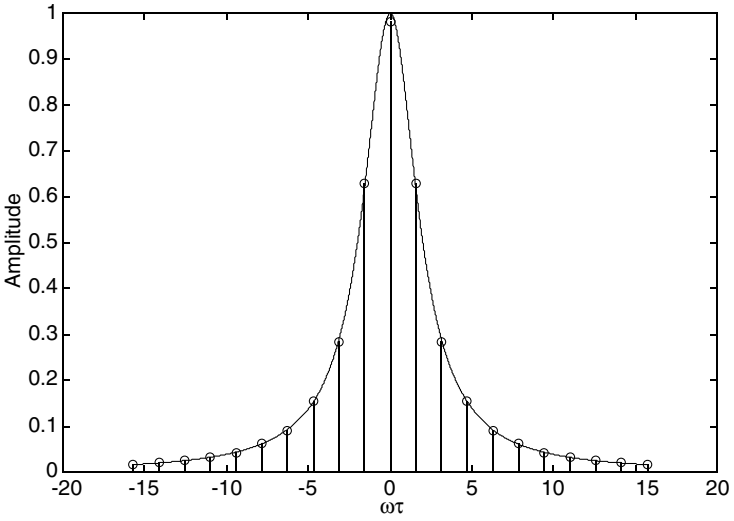

Figure 2.22: Continuous and discrete spectra

close correspondence between the discrete spectrum defined by Fourier series coefficients and the continuous spectrum represented by the Fourier transform. The time domain signal is the exponential $\exp -2\,|t/\tau|$. For the discrete spectrum the time interval is truncated to $-T/2 \leq t \leq T/2$ (with $T/2\tau = 2$) and the Fourier series coefficients $\left|(T/\tau)\,\hat{f}_n\right|$ (stem diagram) plotted as a function of $2\pi n\tau/T$. Superposed for comparison is the continuous spectrum represented by $4/\left[4 + (\omega\tau)^2\right]$, the Fourier transform of $(1/\tau)\exp -2\,|t/\tau|$.

2.2.4 Convergence and the Use of CPV Integrals

The convergence properties of the Fourier integral are governed by the delta function kernel (2.109). In many respects they are qualitatively quite similar to the convergence properties of Fourier series kernel (2.5). For example, as we shall show explicitly in 2.2.7, the convergence at points of discontinuity is again accompanied by the Gibbs oscillatory behavior. The one convergence issue that does not arise with Fourier series, but is unavoidable with the Fourier Integral, relates to the behavior of the functions at infinity, a problem we had already dealt with in Chap. 1 in order to arrive at the limit statement (1.269). There we found that it was sufficient to require that $f\,(t)$ satisfy (1.266) which, in particular, is satisfied by square integrable functions (Problem 1-18). Unfortunately this constraint does not apply to several idealized signals that have been found to be of great value in simplifying system analysis. To accommodate these signals, the convergence of the Fourier transform has to

be examined on a case-by-case basis. In certain cases this requires a special definition of the limiting process underlying the improper integrals that define the Fourier transform and its inverse. In the following we provide a brief account of this limiting process.

An improper integral of the form $\int_{-\infty}^{\infty} f(t)\,dt$, unless stated to the contrary, implies the limit (1.278c)

$$\lim_{T_1\to\infty}\lim_{T_2\to\infty}\int_{-T_1}^{T_2} f(t)\,dt, \tag{2.125}$$

which means that integral converges when the upper and lower limits approach infinity independently. This definition turns out to be too restrictive in many situations of physical interest. An alternative and more encompassing definition is the following:

$$\lim_{T\to\infty}\int_{-T}^{T} f(t)\,dt. \tag{2.126}$$

Here we stipulate that upper and lower limits must approach infinity at the same rate. It is obvious that (2.126) implies (2.125). The converse is, however, not true. The class of functions for which the integral exists in the sense of (2.126) is much larger than under definition (2.125). In particular, all (piecewise differentiable) bounded odd functions are integrable in the sense of (2.126) and the integral yields zero. Under these circumstances (2.125) would generally diverge, unless of course the growth of the function at infinity is suitably restricted. When the limit is taken symmetrically in accordance with (2.126) the integral is said to be defined in terms of the Cauchy Principal Value (CPV). We have in fact already employed this definition implicitly on several occasions, in particular in (2.113). A somewhat different form of the CPV limit is also of interest in Fourier transform theory. This form arises whenever the integral is improper in virtue of one or more simple pole singularities within the integration interval. For example, the integral $\int_{-2}^{8}\frac{dt}{t-1}$ has a singularity at $t=1$ where the integrand becomes infinite. The first inclination would be to consider this integral simply as divergent. On the other hand since the integrand changes sign as one moves through the singularity it is not unreasonable to seek a definition of a limiting process which would facilitate the mutual cancellation of the positive and negative infinite contributions. For example, suppose we define

$$I(\epsilon_1,\epsilon_2)=\int_{-2}^{1-\epsilon_1}\frac{dt}{t-1}+\int_{1+\epsilon_2}^{8}\frac{dt}{t-1},$$

where ϵ_1 and ϵ_2 are small positive numbers so that the integration is carried out up to and past the singularity. By direct calculation we find $I(\epsilon_1,\epsilon_2)=\ln(7\epsilon_1/3\epsilon_2)$. We see that if we let ϵ_1 and ϵ_2 approach zero independently the integral diverges. On the other by setting $\epsilon_1=\epsilon_2=\epsilon$ the result is always finite. Apparently when the singularity is approached symmetrically from both sides

results in a cancellation of the positive and negative infinite contributions and yield a convergent integral. The formal expression for the limit is

$$\lim_{\epsilon\to 0}\left\{\int_{-2}^{1-\epsilon}\frac{dt}{t-1}+\int_{1+\epsilon}^{8}\frac{dt}{t-1}\right\}=\ln(7/3).$$

This limiting procedure constitutes the CPV definition of the integral whenever the singularity falls within the integration interval. Frequently a special symbol is used to indicate a CPV evaluation. We shall indicate it by prefixing the letter P to the integration symbol. Thus $P\int_{-2}^{8}\frac{dt}{t-1}=\ln(7/3)$. When more than one singularity is involved the CPV limiting procedure must be applied to each. For example,

$$\begin{aligned} I &= P\int_{-5}^{9}\frac{dt}{(t-1)(t-2)} \\ &= \lim_{\epsilon\to 0}\left\{\int_{-5}^{1-\epsilon}\frac{dt}{(t-1)(t-2)}+\int_{1+\varepsilon}^{2-\varepsilon}\frac{dt}{(t-1)(t-2)}\right. \\ &\quad \left.+\int_{2+\varepsilon}^{9}\frac{dt}{(t-1)(t-2)}\right\} \\ &= \ln 3/4. \end{aligned}$$

The following example illustrates the CPV evaluation of an integral with infinite limits of integration:

$$\begin{aligned} I &= P\int_{-\infty}^{\infty}\frac{dt}{t-2}=\lim_{\epsilon\to 0\ T\to\infty}\left\{\int_{-T}^{2-\epsilon}\frac{dt}{t-2}+\int_{2+\epsilon}^{T}\frac{dt}{t-2}\right\} \\ &= \lim_{\epsilon\to 0\ T\to\infty}\ln\frac{(2-\epsilon-2)(T-2)}{(-T-2)(2+\varepsilon-2)}=0. \end{aligned}$$

Note that the symbol P in this case pertains to a CPV evaluation at $t=-\infty$ *and* $t=\infty$. A generic form of an integral that is frequently encountered is

$$I=P\int_{a}^{b}\frac{f(t)}{t-q}dt, \tag{2.127}$$

where $a<q<b$ and $f(t)$ is a bounded function within a,b and differentiable at $t=q$. We can represent this integral as a sum of an integral of a bounded function and a CPV integral which can be evaluated in closed form as follows:

$$\begin{aligned} I &= P\int_{a}^{b}\frac{f(t)-f(q)+f(q)}{t-q}dt \\ &= \int_{a}^{b}\frac{f(t)-f(q)}{t-q}dt+f(q)\,P\int_{a}^{b}\frac{dt}{t-q} \\ &= \int_{a}^{b}\frac{f(t)-f(q)}{t-q}dt+f(q)\ln\frac{b-q}{q-a}. \end{aligned} \tag{2.128}$$

Note that the integrand in the first integral in the last expression is finite at $t = q$ so that the integral can be evaluated, if necessary, numerically using standard techniques.

Let us now apply the CPV procedure to the evaluation of the Fourier transform of $f(t) = 1/t$. Even though a signal of this sort might appear quite artificial it will be shown to play a pivotal role in the theory of the Fourier transform. Writing the transform as a CPV integral we have

$$F(\omega) = P\int_{-\infty}^{\infty} \frac{e^{-i\omega t}}{t} dt = P\int_{-\infty}^{\infty} \frac{\cos\omega t}{t} dt - iP\int_{-\infty}^{\infty} \frac{\sin\omega t}{t} dt.$$

Since $P\int_{-\infty}^{\infty} \frac{\cos\omega t}{t} dt = 0$, and $\frac{\sin\omega t}{t}$ is free of singularities we have

$$F(\omega) = -i\int_{-\infty}^{\infty} \frac{\sin\omega t}{t} dt \tag{2.129}$$

Recalling that $\int_{-\infty}^{\infty} \frac{\sin x}{x} dx = \pi$ we obtain by setting $\omega t = x$ in (2.129)

$$\frac{1}{\pi}\int_{-\infty}^{\infty} \frac{\sin\omega t}{t} dt = sign(\omega) = \begin{cases} 1\ ;\ \omega > 0, \\ -1\ ;\ \omega < 0. \end{cases} \tag{2.130}$$

Thus we arrive at the transform pair

$$\frac{1}{\pi t} \overset{\mathcal{F}}{\Longleftrightarrow} -isign(\omega). \tag{2.131}$$

By using the same procedure for the inverse transform of $1/\omega$ we arrive at the pair

$$sign(t) \overset{\mathcal{F}}{\Longleftrightarrow} \frac{2}{i\omega}. \tag{2.132}$$

Several idealized signals may be termed canonical in that they form the essential building blocks in the development of analytical techniques for evaluation of Fourier transforms and also play a fundamental role in the characterization of linear system. One such canonical signal is the sign function just considered. We consider several others in turn.

2.2.5 Canonical Signals and Their Transforms

The Delta Function

That Fourier transform of $\delta(t)$ equals 1 follows simply from the basic property of the delta function as an identity transformation. The consistency of this with the inversion formula follows from (2.119). Hence

$$\delta(t) \overset{\mathcal{F}}{\Longleftrightarrow} 1. \tag{2.133}$$

In identical fashion we get

$$1 \overset{\mathcal{F}}{\Longleftrightarrow} 2\pi\delta(\omega). \tag{2.134}$$

The Unit Step Function

From the identity $U(t) = \frac{1}{2}[1 + sign(t)]$ we get in conjunction with (2.132) and (2.134)

$$U(t) \overset{\mathcal{F}}{\Longleftrightarrow} \pi\delta(\omega) + \frac{1}{i\omega}. \tag{2.135}$$

The Rectangular Pulse Function

Using the definition for $p_T(t)$ in (1.6-40b) we obtain by direct integration the pair

$$p_T(t) \overset{\mathcal{F}}{\Longleftrightarrow} \frac{2\sin(\omega T)}{\omega}, \tag{2.136}$$

where we again find the familiar Fourier integral kernel. If, on the other hand, $p_\Omega(\omega)$ describes a rectangular frequency window, then a direct evaluation of the inverse transform yields

$$\frac{\sin(\Omega t)}{\pi t} \overset{\mathcal{F}}{\Longleftrightarrow} p_\Omega(\omega). \tag{2.137}$$

The transition of (2.137) to (2.133) as $\Omega \to \infty$ and of (2.136) to (2.134) as $T \to \infty$ should be evident.

Triangular Pulse Function

Another signal that we should like to add to our catalogue of canonical transforms is the triangular pulse $q_T(t)$ defined in (1.278d) for which we obtain the pair

$$q_T(t) \overset{\mathcal{F}}{\Longleftrightarrow} \frac{T\sin^2(\omega T/2)}{(\omega T/2)^2}. \tag{2.137*}$$

Exponential Functions

Since the Fourier transform is a representation of signals in terms of exponentials we would expect exponential functions to play a special role in Fourier analysis. In the following we distinguish three cases: a purely imaginary argument, a purely real argument with the function truncated to the positive time axis, and a real exponential that decays symmetrically for both negative and positive times. In the first case we get from the definition of the delta function (2.119) and real ω_0

$$e^{i\omega_0 t} \overset{\mathcal{F}}{\Longleftrightarrow} 2\pi\delta(\omega - \omega_0). \tag{2.138}$$

This result is in perfect consonance with the intuitive notion that a single tone, represented in the time domain by a unit amplitude sinusoidal oscillation of infinitely long duration, should correspond in the frequency domain to a single number, i.e., the frequency of oscillation, or, equivalently, by a spectrum consisting of a single spectral line. Here this spectrum is represented symbolically by a delta function at $\omega = \omega_0$. Such a single spectral line, just like the

corresponding tone of infinite duration, are convenient abstractions never realizable in practice. A more realistic model should consider a tone of finite duration, say $-T < t < T$. We can do this either by truncating the limits of integration in the evaluation of the direct transform, or, equivalently, by specifying this truncation in terms of the pulse function $p_T(t)$. The resulting transform pair then reads

$$p_T(t)e^{i\omega_0 t} \overset{\mathcal{F}}{\Longleftrightarrow} \frac{2\sin\left[(\omega-\omega_0)\,T\right]}{(\omega-\omega_0)}, \tag{2.139}$$

so that the form of the spectrum is the Fourier kernel (2.136) whose peak has been shifted to ω_0. One can show that slightly more than 90% of the energy is contained within the frequency band defined by the first two nulls on either side of the principal peak. It is therefore reasonable to take this bandwidth as the nominal spectral linewidth of the tone. Thus we see that a tone of duration $2T$ has a spectral width of $2\pi/T$ which is sometimes referred to as the Rayleigh resolution limit. This inverse relationship between the signal duration and spectral width is of fundamental importance in spectral analysis. Its generalization to a wider class of signals is embodied in the so-called uncertainty principle discussed in 2.5.1.

With $\alpha > 0$ and the exponential truncated to the nonnegative time axis we get

$$e^{-\alpha t}U\left(t\right) \overset{\mathcal{F}}{\Longleftrightarrow} \frac{1}{\alpha+i\omega}. \tag{2.140}$$

For the exponential $e^{-\alpha|t|}$ defined over the entire real line the transform pair reads

$$e^{-\alpha|t|} \overset{\mathcal{F}}{\Longleftrightarrow} \frac{2\alpha}{\alpha^2+\omega^2}. \tag{2.141}$$

Formula (2.140) also holds when α is replaced by the complex number $p_0 = \alpha - i\omega_0$ where ω_0 is real. A further generalization follows if we differentiate the right side of (2.140) $n-1$ times with respect to ω. The result is

$$\frac{t^{n-1}}{(n-1)!}e^{-p_0 t}U\left(t\right) \overset{\mathcal{F}}{\Longleftrightarrow} \frac{1}{\left(p_0+i\omega\right)^n}; \quad n \geq 1. \tag{2.142}$$

Using this formula in conjunction with the partial fraction expansion technique constitutes one of the basic tools in the evaluation of inverse Fourier transforms of rational functions.

Gaussian Function

A rather important idealized signal is the Gaussian function

$$f(t) = \frac{1}{\sqrt{2\pi\sigma_t^2}}e^{-\frac{t^2}{2\sigma_t^2}},$$

where we have adopted the normalization $\left(\sqrt{f},\sqrt{f}\right)=1$. We compute its FT as follows:

$$\begin{aligned} F(\omega) &= \frac{1}{\sqrt{2\pi\sigma_t^2}}\int_{-\infty}^{\infty} e^{-\frac{t^2}{2\sigma_t^2}} e^{-i\omega t}dt = \frac{1}{\sqrt{2\pi\sigma_t^2}}\int_{-\infty}^{\infty} e^{-\frac{1}{2\sigma_t^2}\left[t^2+2i\omega\sigma_t^2 t\right]}dt \\ &= \frac{e^{-\frac{1}{2}\sigma_t^2\omega^2}}{\sqrt{2\pi\sigma_t^2}}\int_{-\infty}^{\infty} e^{-\frac{1}{2\sigma_t^2}\left[t+i\omega\sigma_t^2\right]^2}dt = \frac{e^{-\frac{1}{2}\sigma_t^2\omega^2}}{\sqrt{2\pi\sigma_t^2}}\int_{-\infty+i\omega\sigma_t^2}^{\infty+i\omega\sigma_t^2} e^{-\frac{z^2}{2\sigma_t^2}}dz. \end{aligned}$$

The last integral may be interpreted as an integral in the complex z plane with the path of integration running along the straight line with endpoints $(-\infty+i\omega\sigma_t^2, \infty+i\omega\sigma_t^2)$. Since the integrand is analytic in the entire finite z plane we can shift this path to run along the axis of reals so that

$$\int_{-\infty+i\omega\sigma_t^2}^{\infty+i\omega\sigma_t^2} e^{-\frac{z^2}{2\sigma_t^2}}dz = \int_{-\infty}^{\infty} e^{-\frac{z^2}{2\sigma_t^2}}dz = \sqrt{2\pi\sigma_t^2}.$$

Thus we obtain the transform pair

$$\frac{1}{\sqrt{2\pi\sigma_t^2}} e^{-\frac{t^2}{2\sigma_t^2}} \overset{\mathcal{F}}{\Longleftrightarrow} e^{-\frac{1}{2}\sigma_t^2\omega^2}. \tag{2.142*}$$

Note that except for a scale factor the Gaussian function is its own FT. Here we see another illustration of the inverse relationship between the signal duration and bandwidth. If we take σ_t as the nominal duration of the pulse in the time domain, then a similar definition for the effective bandwidths of $F(\omega)$ yields $\sigma_\omega = 1/\sigma_t$.

2.2.6 Basic Properties of the FT

Linearity

The Fourier transform is a linear operator which means that for any set of functions $f_n(t)$ $n=1,2,\ldots N$ and corresponding transforms $F_n(\omega)$ we have

$$\mathcal{F}\left\{\sum_{n=1}^{N}\alpha_n f_n(t)\right\} = \sum_{n=1}^{N}\alpha_n F_n(\omega),$$

where the α_n are constants. This property is referred to as the superposition principle. We shall return to it in Chap. 3 when we discuss linear systems. This superposition principle carries over to a continuous index. Thus if

$$f(\xi,t) \overset{\mathcal{F}}{\Longleftrightarrow} F(\xi,\omega)$$

holds for a continuum of values of ξ, then

$$\mathcal{F}\left\{\int f(\xi,t)\,d\xi\right\} = \int F(\xi,\omega)\,d\xi.$$

Symmetries

For any Fourier transform pair

$$f(t) \overset{\mathcal{F}}{\Longleftrightarrow} F(\omega)$$

we also have, by a simple substitution of variables,

$$F(t) \overset{\mathcal{F}}{\Longleftrightarrow} 2\pi f(-\omega). \tag{2.143}$$

For example, using this variable replacement in (2.141), we obtain

$$\frac{\alpha}{\pi(\alpha^2 + t^2)} \overset{\mathcal{F}}{\Longleftrightarrow} e^{-\alpha|\omega|}. \tag{2.143*}$$

The Fourier transform of the complex conjugate of a function follows through the variable replacement

$$f^*(t) \overset{\mathcal{F}}{\Longleftrightarrow} F^*(-\omega). \tag{2.144}$$

Frequently we shall be interested in purely real signals. If $f(t)$ is real, the preceding requires

$$F^*(-\omega) = F(\omega). \tag{2.145}$$

If we decompose $F(\omega)$ into its real and imaginary parts

$$F(\omega) = R(\omega) + iX(\omega), \tag{2.146}$$

we note that (2.145) is equivalent to

$$R(\omega) = R(-\omega), \tag{2.147a}$$
$$X(\omega) = -X(-\omega), \tag{2.147b}$$

so that for a real signal the real part of the Fourier transforms is even function while the imaginary part an odd function of frequency. The even and odd symmetries carry over to the amplitude and phase of the transform. Thus writing

$$F(\omega) = A(\omega) e^{i\theta(\omega)}, \tag{2.148}$$

wherein

$$A(\omega) = |F(\omega)| = \sqrt{[R(\omega)]^2 + [X(\omega)]^2}, \tag{2.149a}$$
$$\theta(\omega) = \tan^{-1}\frac{X(\omega)}{R(\omega)}, \tag{2.149b}$$

we have in view of (2.147)

$$A(\omega) = A(-\omega) \tag{2.150a}$$
$$\theta(\omega) = -\theta(-\omega). \tag{2.150b}$$

As a result the inversion formula can be put into the form

$$\begin{aligned} f(t) &= \frac{1}{\pi}\int_0^\infty A(\omega)\cos[\omega t+\theta(\omega)]\,d\omega \\ &= \Re e\left\{\frac{1}{2\pi}\int_0^\infty 2F(\omega)\,e^{i\omega t}d\omega\right\}. \end{aligned} \tag{2.151}$$

The last expression shows that a real physical signal can be represented as the real part of a fictitious complex signal whose spectrum equals twice the spectrum of the real signal for positive frequencies but is identically zero for negative frequencies. Such a complex signal is referred to as an analytic signal, a concept that finds extensive application in the study of modulation to be discussed in 2.3.

Time Shift and Frequency Shift

For any real T we have

$$f(t-T) \overset{\mathcal{F}}{\Longleftrightarrow} F(\omega)\,e^{-i\omega T} \tag{2.152}$$

and similarly for any real ω_0

$$f(t)\,e^{i\omega_0 t} \overset{\mathcal{F}}{\Longleftrightarrow} F(\omega-\omega_0). \tag{2.153}$$

The last formula is the quantification of the modulation of a high frequency CW carrier by a baseband signal comprised of low frequency components. For example, for the carrier of $A\cos(\omega_0 t+\theta_0)$ and a baseband signal $f(t)$ we get

$$f(t)\,A\cos(\omega_0 t+\theta_0) \overset{\mathcal{F}}{\Longleftrightarrow} \frac{A}{2}e^{i\theta_0}F(\omega-\omega_0)+\frac{A}{2}e^{-i\theta_0}F(\omega+\omega_0). \tag{2.154}$$

If we suppose that $F(\omega)$ is negligible outside the band defined by $|\omega|<\Omega$, and also assume that $\omega_0>2\Omega$, the relationship among the spectra in (2.154) may be represented schematically as in Fig. 2.23

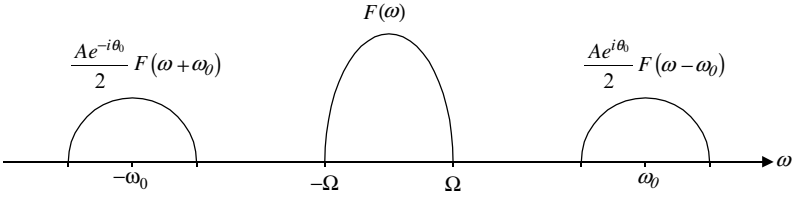

Figure 2.23: Modulation by a CW carrier

Differentiation

If $f(t)$ is everywhere differentiable, then a simple integration by parts gives

$$\begin{aligned}\int_{-\infty}^{\infty} f'(t)\, e^{-i\omega t} dt &= f(t)\, e^{-i\omega t}\big|_{-\infty}^{\infty} + i\omega \int_{-\infty}^{\infty} f(t)\, e^{-i\omega t} dt \\ &= i\omega F(\omega). \end{aligned} \tag{2.155}$$

Clearly if $f(t)$ is differentiable n times we obtain by repeated integration

$$f^{(n)}(t) \overset{\mathcal{F}}{\Longleftrightarrow} (i\omega)^n F(\omega). \tag{2.156}$$

Actually this formula may still be used even if $f(t)$ is only piecewise differentiable and discontinuous with discontinuous first and even higher order derivatives at a countable set of points. We merely have to replace $f^{(n)}(t)$ with a generalized derivative defined in terms of singularity functions, an approach we have already employed for the first derivative in (1.280). For example, the Fourier transform of (1.280) is

$$f'(t) \overset{\mathcal{F}}{\Longleftrightarrow} i\omega F(\omega) = \mathcal{F}\{f_s'(t)\} + \sum_k \left[f\left(t_k^+\right) - f\left(t_k^-\right)\right] e^{-i\omega t_k}. \tag{2.157}$$

In the special case of only one discontinuity at $t = 0$ and $f(0^-) = 0$ (2.157) becomes

$$f_s'(t) \overset{\mathcal{F}}{\Longleftrightarrow} i\omega F(\omega) - f\left(0^+\right). \tag{2.158}$$

What about the Fourier transform of higher order derivatives? Clearly if the first derivative is continuous at $t = 0$, the Fourier transform of $f_s''(t)$ may be obtained by simply multiplying the right side of (2.158) by $i\omega$. However in case of a discontinuity in the first derivative the magnitude of the jump in the derivative must be subtracted. Again assuming $f'(0^-) = 0$ we have

$$f_s''(t) \overset{\mathcal{F}}{\Longleftrightarrow} i\omega\left[i\omega F(\omega) - f\left(0^+\right)\right] - f'\left(0^+\right). \tag{2.159}$$

Higher order derivatives can be handled similarly.

Since an $n-th$ order derivative in the time domain transforms in the frequency domain to a multiplication by $(i\omega)^n$, the Fourier transform of any linear differential operator with constant coefficients is a polynomial in $i\omega$. This feature makes the Fourier transform a natural tool for the solution of linear differential equations with constant coefficients. For example, consider the following differential equation:

$$x''(t) + 2x'(t) + x(t) = 0. \tag{2.160}$$

We seek a solution for $x(t)$ for $t \geq 0$ with initial conditions $x(0^+) = 2$ and $x'(0^+) = 6$. Then

$$\begin{aligned} x'(t) &\overset{\mathcal{F}}{\Longleftrightarrow} i\omega X(\omega) - 2 \\ x''(t) &\overset{\mathcal{F}}{\Longleftrightarrow} -\omega^2 X(\omega) - i\omega 2 - 6. \end{aligned}$$

The solution for $X(\omega)$ reads

$$X(\omega) = \frac{i2\omega + 10}{-\omega^2 + i2\omega + 1},$$

while the signal $x(t)$ is to be computed from

$$x(t) = \frac{1}{2\pi}\int_{-\infty}^{\infty} \frac{i2\omega + 10}{-\omega^2 + i2\omega + 1} e^{i\omega t} d\omega. \tag{2.161}$$

The integral can be evaluated by contour integration as will be shown in 2.4.4 (see also (A.96) in the Appendix).

Inner Product Invariance

We compute the inner product of two functions in the time domain and with the aid of the inversion formulas transform it into an inner product in the frequency domain as follows:

$$\begin{aligned}
(f_1, f_2) &= \int_{-\infty}^{\infty} f_1^*(t) f_2(t)\, dt \\
&= \int_{-\infty}^{\infty} \left\{ \frac{1}{2\pi}\int_{-\infty}^{\infty} F_1^*(\omega) e^{-i\omega t} d\omega \frac{1}{2\pi}\int_{-\infty}^{\infty} F_2(\omega') e^{i\omega' t} d\omega' \right\} dt \\
&= \frac{1}{2\pi}\int_{-\infty}^{\infty}\int_{-\infty}^{\infty} F_1^*(\omega) F_2(\omega') \left\{ \frac{1}{2\pi}\int_{-\infty}^{\infty} e^{i(\omega'-\omega)t} dt \right\} d\omega' d\omega \\
&= \frac{1}{2\pi}\int_{-\infty}^{\infty}\int_{-\infty}^{\infty} F_1^*(\omega) F_2(\omega') \delta(\omega - \omega')\, d\omega' d\omega \\
&= \frac{1}{2\pi}\int_{-\infty}^{\infty} F_1^*(\omega) F_2(\omega)\, d\omega.
\end{aligned}$$

The final result may be summarized to read

$$\int_{-\infty}^{\infty} f_1^*(t) f_2(t)\, dt = \frac{1}{2\pi}\int_{-\infty}^{\infty} F_1^*(\omega) F_2(\omega)\, d\omega, \tag{2.162}$$

which is recognized as a generalization of Parseval's formula.

Convolution

We have already encountered the convolution of two functions in connection with Fourier series, (2.49). Since in the present case the time domain encompasses the entire real line the appropriate definition is

$$h(t) = \int_{-\infty}^{\infty} f(\tau) g(t - \tau)\, d\tau.$$

We shall frequently employ the abbreviated notation

$$\int_{-\infty}^{\infty} f(\tau) g(t - \tau)\, d\tau = f * g. \tag{2.163}$$

Note that

$$\int_{-\infty}^{\infty} f(\tau)\, g(t-\tau)\, d\tau = \int_{-\infty}^{\infty} g(\tau)\, f(t-\tau)\, d\tau$$

as one can readily convince oneself through a change of the variable of integration. This can also be expressed as $f * g = g * f$, i.e., the convolution operation is commutative. In view of (2.152) $g(t-\tau) \overset{\mathcal{F}}{\Longleftrightarrow} G(\omega)\, e^{-i\omega\tau}$ so that

$$\int_{-\infty}^{\infty} f(\tau)\, g(t-\tau)\, d\tau \overset{\mathcal{F}}{\Longleftrightarrow} \int_{-\infty}^{\infty} f(\tau)\, G(\omega)\, e^{-i\omega\tau} d\tau = F(\omega)\, G(\omega). \quad (2.164)$$

In identical manner we establish that

$$f(t)\, g(t) \overset{\mathcal{F}}{\Longleftrightarrow} \frac{1}{2\pi} \int_{-\infty}^{\infty} F(\eta)\, G(\omega-\eta)\, d\eta = \frac{1}{2\pi} F * G. \quad (2.165)$$

Integration

When the Fourier transform is applied to integro-differential equations one sometimes needs to evaluate the transform of the integral of a function. For example with $g(t) = \int_{-\infty}^{t} f(\tau)\, d\tau$ we would like to determine $G(\omega)$ in terms of $F(\omega)$. We can do this by first recognizing that $\int_{-\infty}^{t} f(\tau)\, d\tau = \int_{-\infty}^{\infty} f(\tau)\, U(t-\tau)\, d\tau$. Using (2.164) and (2.135) we have

$$\int_{-\infty}^{\infty} f(\tau)\, U(t-\tau)\, d\tau \overset{\mathcal{F}}{\Longleftrightarrow} F(\omega) \left[\pi\delta(\omega) + \frac{1}{i\omega}\right]$$

with the final result

$$\int_{-\infty}^{t} f(\tau)\, d\tau \overset{\mathcal{F}}{\Longleftrightarrow} \pi F(0)\, \delta(\omega) + \frac{F(\omega)}{i\omega} = G(\omega). \quad (2.166)$$

Note that the integral implies $g'(t) = f(t)$ so that

$$i\omega G(\omega) = F(\omega). \quad (2.167)$$

This is certainly compatible with (2.166) since $\omega\delta(\omega) = 0$. However the solution of (2.167) for $G(\omega)$ by simply dividing both sides by $i\omega$ is in general not permissible since $G(\omega) \neq F(\omega)/i\omega$ unless $F(0) = 0$.

Causal Signals and the Hilbert Transform [16]

Let

$$f_e(t) = \frac{f(t) + f(-t)}{2}, \quad (2.168a)$$

$$f_o(t) = \frac{f(t) - f(-t)}{2}, \quad (2.168b)$$

so that $f(t) = f_e(t) + f_o(t)$ for any signal. Since $f_e(t) = f_e(-t)$ and $f_o(t) = -f_o(-t)$ (2.168a) and (2.168b) are referred to as the even and odd parts of $f(t)$, respectively. Now

$$\begin{aligned}\mathcal{F}\{f_e(t)\} &= \frac{1}{2}\int_{-\infty}^{\infty}[f(t)+f(-t)][\cos(\omega t)-i\sin(\omega t)]\,dt \\ &= \int_{-\infty}^{\infty} f(t)\cos(\omega t)\,dt \end{aligned} \tag{2.169a}$$

and

$$\begin{aligned}\mathcal{F}\{f_o(t)\} &= \frac{1}{2}\int_{-\infty}^{\infty}[f(t)-f(-t)][\cos(\omega t)-i\sin(\omega t)]\,dt \\ &= -i\int_{-\infty}^{\infty} f(t)\sin(\omega t)\,dt. \end{aligned} \tag{2.169b}$$

In view of the definition (2.146), for a real $f(t)$ (2.169a) and (2.169b) are equivalent to

$$f_e(t) \overset{\mathcal{F}}{\Longleftrightarrow} R(\omega), \tag{2.170a}$$

$$f_o(t) \overset{\mathcal{F}}{\Longleftrightarrow} iX(\omega). \tag{2.170b}$$

In the following we shall be concerned only with real signals.

As will be discussed in Chap. 3, signals that vanish for negative values of the argument play a special role in linear time-invariant systems. Such signals are said to be causal. Suppose $f(t)$ is a causal signal. Then according to (2.168)

$$f(t) = \begin{cases} 2f_e(t) = 2f_o(t) & ;t>0, \\ 0 & ;t<0. \end{cases} \tag{2.171}$$

Evidently the even and odd parts are not independent for

$$\begin{aligned} f_e(t) &= f_o(t) \;\; ;t>0, \\ f_e(t) &= -f_o(t) \;\; ;t<0,. \end{aligned}$$

which can be rephrased in more concise fashion with the aid of the *sign* function as follows:

$$f_o(t) = sign(t)\, f_e(t) \tag{2.172a}$$

$$f_e(t) = sign(t)\, f_o(t). \tag{2.172b}$$

Taking account of (2.170), (2.132), and (2.165) Fourier Transformation of both sides of (2.172) results in the following pair of equations:

$$X(\omega) = -\frac{1}{\pi}P\int_{-\infty}^{\infty}\frac{R(\eta)\,d\eta}{\omega-\eta}, \tag{2.173a}$$

$$R(\omega) = \frac{1}{\pi}P\int_{-\infty}^{\infty}\frac{X(\eta)\,d\eta}{\omega-\eta}. \tag{2.173b}$$

These relations show explicitly that the real and imaginary parts of the Fourier transform of a causal signal may not be prescribed independently. For example if we know $R(\omega)$, then $X(\omega)$ can be determined uniquely by (2.173a). Since $P\int_{-\infty}^{\infty}\frac{d\eta}{\omega-\eta}=0$, an $R(\omega)$ that is constant for all frequencies gives a null result for $X(\omega)$. Consequently, (2.173b) determines $R(\omega)$ from $X(\omega)$ only within a constant.

The integral transform $\frac{1}{\pi}P\int_{-\infty}^{\infty}\frac{R(\eta)d\eta}{\omega-\eta}$ is known as the Hilbert Transform which shall be denoted by $\mathcal{H}\{R(\omega)\}$. Using this notation we rewrite (2.173) as

$$X(\omega) = -\mathcal{H}\{R(\omega)\}, \tag{2.174a}$$

$$R(\omega) = \mathcal{H}\{X(\omega)\}. \tag{2.174b}$$

Since (2.174b) is the inverse of (2.174a) the inverse Hilbert transform is obtained by a change in sign. As an example, suppose $R(\omega)=p_{\Omega}(\omega)$. Carrying out the simple integration yields

$$X(\omega)=\frac{1}{\pi}\ln\left|\frac{\omega-\Omega}{\omega+\Omega}\right|, \tag{2.175}$$

which is plotted in Fig. 2.24. The Hilbert Transform in the time domain is defined similarly. Thus for a signal $f(t)$

$$\mathcal{H}\{f(t)\}=\frac{1}{\pi}P\int_{-\infty}^{\infty}\frac{f(\tau)\,d\tau}{t-\tau}. \tag{2.176}$$

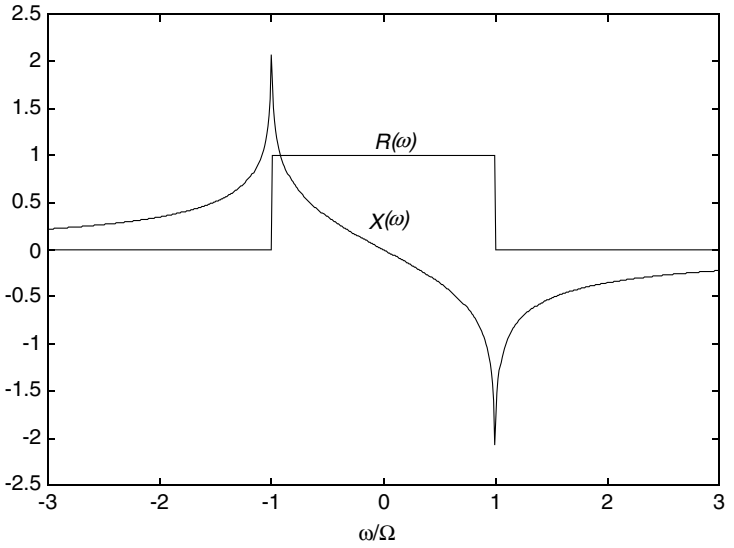

Figure 2.24: $R(\omega)$ and its Hilbert transform

Particularly simple results are obtained for Hilbert transforms of sinusoids. For example, with $f(t) = \cos(\omega t)$ (with ω a real constant) we have

$$\begin{aligned}\frac{1}{\pi}P\int_{-\infty}^{\infty}\frac{\cos(\omega\tau)\,d\tau}{t-\tau} &= \frac{1}{\pi}P\int_{-\infty}^{\infty}\frac{\cos[\omega(t-\tau)]\,d\tau}{\tau}\\ &= \cos(\omega t)\,\frac{1}{\pi}P\int_{-\infty}^{\infty}\frac{\cos(\omega\tau)\,d\tau}{\tau}\\ &\quad + \sin(\omega t)\,\frac{1}{\pi}P\int_{-\infty}^{\infty}\frac{\sin(\omega\tau)\,d\tau}{\tau}.\end{aligned}$$

We note that the first of the two preceding integrals involves an odd function and therefore vanishes, while in virtue of (2.132) the second integral yields $sign(\omega)$. Hence

$$\mathcal{H}\{\cos(\omega t)\} = sign(\omega)\sin(\omega t). \tag{2.177}$$

In identical fashion we obtain

$$\mathcal{H}\{\sin(\omega t)\} = -sign(\omega)\cos(\omega t). \tag{2.178}$$

We shall have occasion to employ the last two formulas in connection with analytic signal representations.

The Hilbert transform finds application in signal analysis, modulation theory, and spectral analysis. In practical situations the evaluation of the Hilbert transform must be carried out numerically for which purpose direct use of the defining integral is not particularly efficient. The preferred approach is to carry out the actual calculations in terms of the Fourier transform which can be computed efficiently using the FFT algorithm. To see how this may be arranged, let us suppose that $R(\omega)$ is given and we wish to find $X(\omega)$. By taking the inverse FT we first find $f_e(t)$, in accordance with (2.170a). In view of (2.171), if we now multiply the result by 2, truncate it to nonnegative t, and take the direct FT, we should obtain $F(\omega)$. Thus

$$2f_e(t)\,U(t) \overset{\mathcal{F}}{\Longleftrightarrow} F(\omega) \tag{2.179}$$

and $X(\omega)$ follows by taking the imaginary part of $F(\omega)$. In summary we have

$$\mathcal{H}\{R\} = -\Im m\left\{\int_0^{\infty} 2\mathcal{F}^{-1}\{R\}\,e^{-i\omega t}dt\right\} = -X(\omega), \tag{2.180}$$

where

$$\mathcal{F}^{-1}\{R\} \equiv \frac{1}{2\pi}\int_{-\infty}^{\infty} R(\omega')\,e^{i\omega' t}d\omega'.$$

Initial and Final Value Theorems

Again assume that $f(t)$ is a causal signal and that it is piecewise differentiable for all $t > 0$. Then

$$\begin{aligned}\mathcal{F}\{f'(t)\} &= \int_{0^+}^{\infty} f'(t)\,e^{-i\omega t}dt = f(t)\,e^{-i\omega t}\,|_{0^+}^{\infty} + i\omega\int_{0^+}^{\infty} f(t)\,e^{-i\omega t}dt\\ &= i\omega F(\omega) - f\left(0^+\right).\end{aligned}$$

Since by assumption $f'(t)$ exists for $t > 0$, or, equivalently, $f(t)$ is smooth, $\mathcal{F}\{f'(t)\}$ approaches zero as $\omega \to \infty$ (c.f. (2.158)). Under these conditions the last equation yields

$$\lim_{\omega\to\infty} i\omega F(\omega) = f\left(0^+\right), \tag{2.181}$$

a result known as the initial value theorem. Note that $f_e(0) \equiv f(0)$ but according to (2.171) $2\, f_e(0) = f\left(0^+\right)$. Hence

$$f(0) = \frac{1}{2} f\left(0^+\right), \tag{2.182}$$

which is consistent with the fact that the FT converges to the arithmetic mean of the step discontinuity.

Consider now the limit

$$\begin{aligned}\lim_{\omega\to 0}\left[i\omega F(\omega) - f\left(0^+\right)\right] &= \lim_{\omega\to 0}\int_{0^+}^{\infty} f'(t)\, e^{-i\omega t} dt \\ &= \int_{0^+}^{\infty} f'(t) \lim_{\omega\to 0}\left[e^{-i\omega t}\right] dt \\ &= \lim_{t\to\infty} f(t) - f\left(0^+\right).\end{aligned}$$

Upon cancelling $f\left(0^+\right)$ we get

$$\lim_{\omega\to 0}\left[i\omega F(\omega)\right] = \lim_{t\to\infty} f(t), \tag{2.183}$$

which is known as the final value theorem.

Fourier Series and the Poisson Sum Formula

Given a function $f(t)$ within the finite interval $-T/2, T/2$ we can represent it either as a Fourier integral, (2.123), comprised of a continuous spectrum of

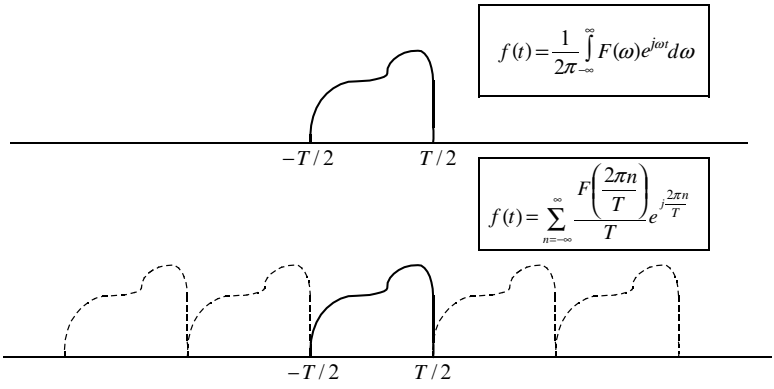

Figure 2.25: Fourier integral and Fourier series representations

sinusoids, or as a Fourier series, (2.124), comprised of discrete harmonically related sinusoids. In the former case the representation converges to zero outside the interval in question while in the latter case we obtain a periodic repetition (extension) of the given function, as illustrated in Fig. 2.25. The significant point to note here is that the Fourier series coefficients are given by the FT formula. Note also that the Fourier transform of $f(t)$ and its periodic extension (taken over the entire real-time axis) is a infinite series comprised of delta functions, i.e.,

$$\sum_{n=-\infty}^{\infty} \hat{f}_n e^{i2\pi nt/T} \overset{\mathcal{F}}{\Longleftrightarrow} 2\pi \sum_{n=-\infty}^{\infty} \hat{f}_n \delta\left(\omega - 2\pi n/T\right). \tag{2.184}$$

In the following we present a generalization of (2.124), known as the Poisson sum formula wherein the function $f(t)$ may assume nonzero values over the entire real line. We start by defining the function $g(t)$ through the sum

$$g(t) = \sum_{n=-\infty}^{\infty} f(t - nT). \tag{2.185}$$

It is easy to see that $g(t)$ is periodic with period T. We take the FT to obtain

$$\sum_{n=-\infty}^{\infty} f(t - nT) \overset{\mathcal{F}}{\Longleftrightarrow} \sum_{n=-\infty}^{\infty} F(\omega) e^{-i\omega nT}.$$

In view of (2.31) the sum of exponentials can be replaced by a sum comprised of delta functions. Thus

$$\begin{aligned} \sum_{n=-\infty}^{\infty} F(\omega) e^{-i\omega nT} &= \sum_{\ell=-\infty}^{\infty} F(\omega) 2\pi\delta(\omega T - 2\pi\ell) \\ &= \frac{2\pi}{T} \sum_{\ell=-\infty}^{\infty} F(2\pi\ell/T)\, \delta(\omega - 2\pi\ell/T). \end{aligned}$$

Inverting the FT gives

$$\sum_{\ell=-\infty}^{\infty} F(2\pi\ell/T)/T e^{i2\pi\ell t/T} \overset{\mathcal{F}}{\Longleftrightarrow} \frac{2\pi}{T} \sum_{\ell=-\infty}^{\infty} F(2\pi\ell/T)\, \delta(\omega - 2\pi\ell/T).$$

Since the left side in the last expression must be identical to (2.185) we are justified in writing

$$\sum_{n=-\infty}^{\infty} f(t - nT) = \sum_{\ell=-\infty}^{\infty} F(2\pi\ell/T)/T e^{i2\pi\ell t/T}, \tag{2.186}$$

which is the desired Poisson sum formula.

As an example, suppose $f(t) = 1/(1 + t^2)$. Then $F(\omega) = \pi e^{-|\omega|}$ (see (2.143*)) and with $T = 2\pi$ we get

$$\sum_{n=-\infty}^{\infty} \frac{1}{1 + (t - 2\pi n)^2} = \frac{1}{2} \sum_{\ell=-\infty}^{\infty} e^{-(|\ell| - i\ell t)} = \frac{e^2 - 1}{2\left[e^2 - 2e\cos(t) + 1\right]}. \tag{2.187}$$

2.2.7 Convergence at Discontinuities

The convergence of the FT at a step discontinuity exhibits the Gibbs oscillatory behavior similar to Fourier series. Thus suppose $f(t)$ has step discontinuities at $t = t_k$, $k = 1, 2, \ldots$ and we represent it as in (1.282). Then with $f^{\Omega}(t)$ as in (2.109) we have

$$\begin{aligned} f^{\Omega}(t) &= f_s^{\Omega}(t) + \sum_k \left[f\left(t_k^+\right) - f\left(t_k^-\right) \right] \int_{t_k}^{\infty} \frac{\sin\left[(t-t')\,\Omega\right]}{\pi\,(t-t')} dt' \\ &= f_s^{\Omega}(t) + \sum_k \left[f\left(t_k^+\right) - f\left(t_k^-\right) \right] \frac{1}{\pi} \int_{-\infty}^{(t-t_k)\Omega} \frac{\sin x}{x} dx \\ &= f_s^{\Omega}(t) + \sum_k \left[f\left(t_k^+\right) - f\left(t_k^-\right) \right] \left[\frac{1}{2} + \frac{1}{\pi} \mathrm{Si}\left[(t-t_k)\,\Omega\right] \right]. \quad (2.188) \end{aligned}$$

As $\Omega \to \infty$ the $f_s^{\Omega}(t)$ tends uniformly to $f_s(t)$ whereas the convergence of each member in the sum is characterized by the oscillatory behavior of the sine

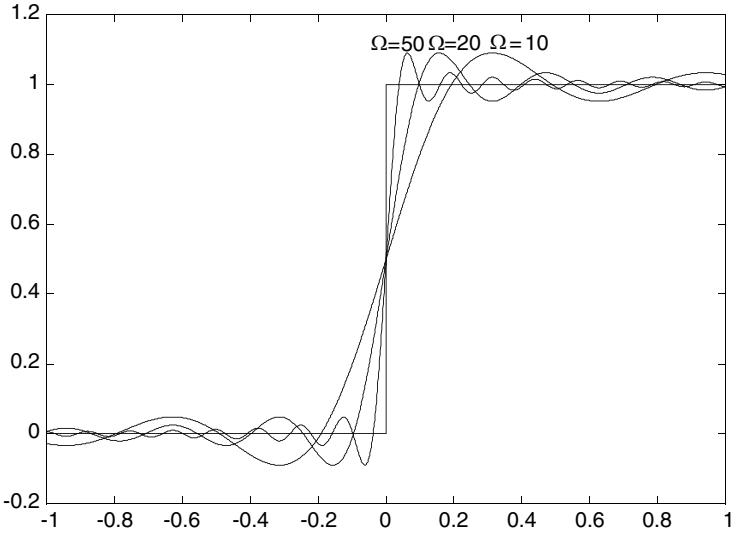

Figure 2.26: Convergence of the Fourier transform at a step discontinuity

integral function. This is illustrated in Fig. 2.26 which shows a unit step together with plots of $1/2 + (1/\pi)\,\mathrm{Si}(\Omega t)$ for $\Omega = 10, 20$, and 50.

2.2.8 Fejer Summation

In 2.1.5 it was shown that the Gibbs oscillations at step discontinuities arising in partial sums of Fourier series can be suppressed by employing the Fejer summation technique. An analogous procedure works for the Fourier Integral where

instead of (2.32) we must resort to the following fundamental theorem from the theory of limits. Given a function $f(\Omega)$ integrable over any finite interval $0, \Omega$ we define, by analogy with (2.135), the average σ_Ω by

$$\sigma_\Omega = \frac{1}{\Omega}\int_0^\Omega f(\Omega)d\Omega. \tag{2.189}$$

It can be shown that if $\lim_{\Omega\longrightarrow\infty} f(\Omega) = f$ exists then so does $\lim_{\Omega\longrightarrow\infty} \sigma_\Omega = f$. Presently for the function $f(\Omega)$ we take the partial "sum" $f^{\Omega}(t)$ in (2.109) and denote the left side of (2.189) by $\sigma_\Omega(t)$. If we suppose that $\lim_{\Omega\longrightarrow\infty} f^{\Omega}(t) = \frac{1}{2}\left[f(t^+) + f(t^-)\right]$, then by the above limit theorem we also have

$$\lim_{\Omega\longrightarrow\infty} \sigma_\Omega(t) = \frac{1}{2}\left[f(t^+) + f\left(t^-\right)\right]. \tag{2.190}$$

By integrating the right side of (2.109) with respect to Ω and using (2.189) we obtain

$$\sigma_\Omega(t) = \int_{-\infty}^{\infty} f(t')\,\frac{\sin^2\left[(\Omega/2)(t-t')\right]}{\pi(\Omega/2)(t-t')^2}dt'. \tag{2.191}$$

Unlike the kernel (2.38) in the analogous formula for Fourier series in (2.37), the kernel

$$K_\Omega(t-t') = \frac{\sin^2\left[(\Omega/2)(t-t')\right]}{\pi(\Omega/2)(t-t')^2} \tag{2.192}$$

is not periodic. We leave it exercise to show that

$$\lim_{\Omega\longrightarrow\infty} \frac{\sin^2\left[(\Omega/2)(t-t')\right]}{\pi(\Omega/2)(t-t')^2} = \delta(t-t'), \tag{2.193}$$

which may be taken as a direct verification of (2.190). A plot of the Fejer kernel together with the Fourier integral kernel is shown in Fig. 2.27, where the maximum of each kernel has been normalized to unity. Note that the Fejer kernel is always nonnegative with a wider main lobe than the Fourier kernel and exhibits significantly lower sidelobes. One can readily show that

$$\mathcal{F}\left\{\frac{\sin^2(\Omega/2)t}{\pi(\Omega/2)t^2}\right\} = \begin{cases} 1-\frac{|\omega|}{\Omega}; |\omega| < \Omega, \\ 0; |\omega| > \Omega. \end{cases} \tag{2.194}$$

Since the right side of (2.191) is a convolution in the time domain, its FT yields a product of the respective transforms. Therefore using (2.194) we can rewrite (2.191) as an inverse FT as follows:

$$\sigma_\Omega(t) = \frac{1}{2\pi}\int_{-\Omega}^{\Omega} F(\omega)\left(1-\frac{|\omega|}{\Omega}\right)e^{i\omega t}d\omega. \tag{2.195}$$

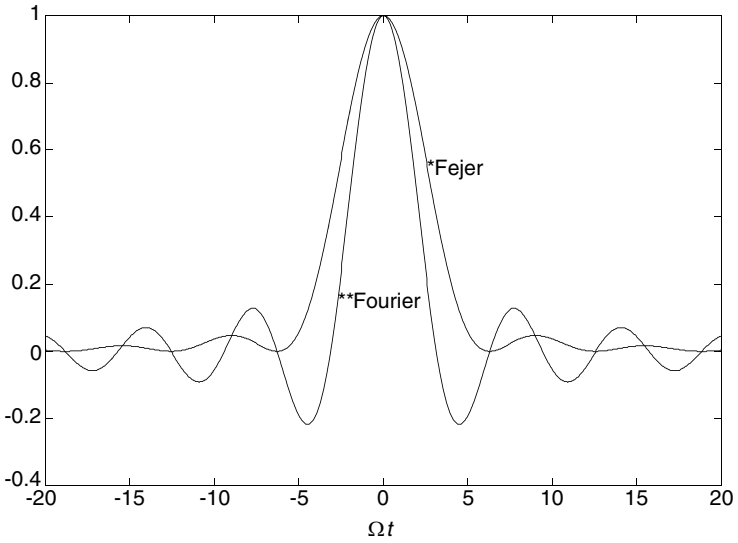

Figure 2.27: Fejer and Fourier integral kernels

We see that the Fejer "summation" (2.195) is equivalent to the multiplication of the signal transform $F(\omega)$ by the triangular spectral window:

$$W(\omega) = \left(1 - \frac{|\omega|}{\Omega}\right) p_\Omega(\omega) \tag{2.196}$$

quite analogous to the discrete spectral weighting of the Fourier series coefficients in (2.34). Figure 2.28 shows a rectangular pulse together with the Fejer and Fourier approximations using a spectral truncation of $\Omega = 40/T$. These results are seen to be very similar to those plotted in Fig. 2.9 for Fourier series. Just like for Fourier series, we can also introduce higher order Fejer approximations. For example, the second-order approximation $\sigma_\Omega^{(1)}(t)$ can be defined by

$$\sigma_\Omega^{(1)}(t) = \sigma_\Omega = \frac{1}{\Omega}\int_0^\Omega \sigma_a(t)\, da \tag{2.197}$$

again with the property

$$\lim_{\Omega \longrightarrow \infty} \sigma_\Omega^{(1)}(t) = \frac{1}{2}\left[f(t^+) + f\left(t^-\right)\right]. \tag{2.198}$$

Substituting (2.191) with Ω replaced by the integration variable a into (2.197) one can show that

$$\sigma_\Omega^{(1)}(t) = \int_{-\infty}^{\infty} f(t')\, K_\Omega^{(1)}(t - t')\, dt', \tag{2.199}$$

where

$$K_\Omega^{(1)}(t) = \frac{1}{\pi t^2}\int_0^{\Omega t} \frac{1 - \cos x}{x} dx. \tag{2.200}$$

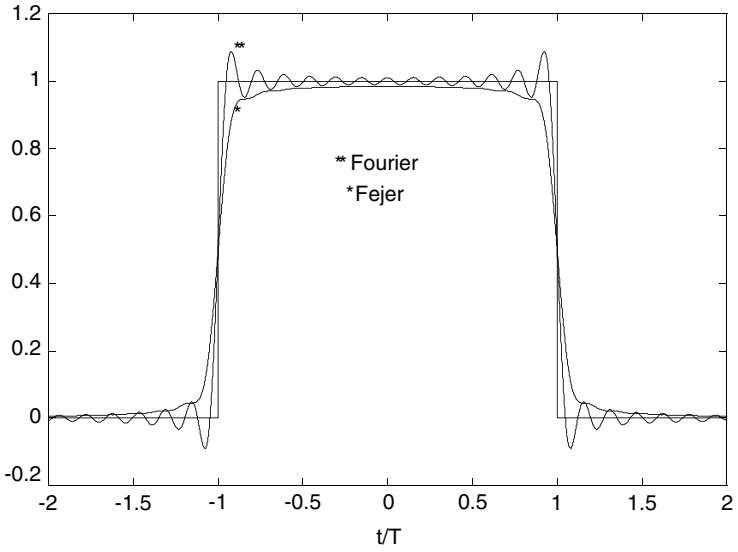

Figure 2.28: Comparison of Fejer and Fourier integral approximations

One can show directly that $\lim_{\Omega \longrightarrow \infty} K_{\Omega}^{(1)}(t) = \delta(t)$, consistent with (2.198). A plot of $4\pi K_{\Omega}^{(1)}(t)/\Omega^2$ as a function of Ωt together with the (first-order) Fejer and Fourier kernels is shown in Fig. 2.29. Unlike the Fourier Integral and the (first-order) Fejer kernels, $K_{\Omega}^{(1)}(t)$ decreases monotonically on both sides of the

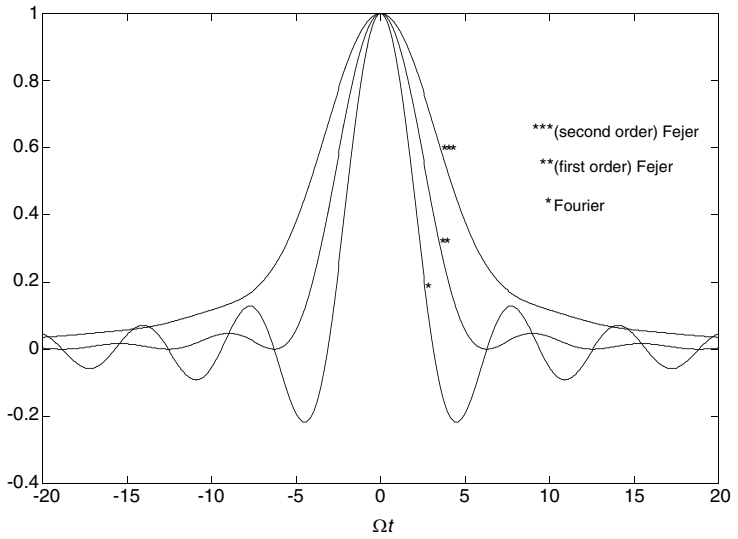

Figure 2.29: Comparison of Fourier and Fejer kernels

maximum, i.e., the functional form is free of sidelobes. At the same time its single lobe is wider than the main lobe of the other two kernels. It can be shown that for large Ωt

$$K_{\Omega}^{(1)}(t) \sim \frac{\ln(\Omega |t| \gamma)}{\pi (\Omega t)^2}, \tag{2.201}$$

where $\ln\gamma = 0.577215\ldots$ is the Euler constant. Because of the presence of the logarithmic term (2.201) represents a decay rate somewhere between that of the Fourier Integral kernel $(1/\Omega t)$ and that of the (first-order) Fejer kernel $\left(1/(\Omega t)^2\right)$.

The Fourier transform of $K_{\Omega}^{(1)}(t)$ furnishes the corresponding spectral window. An evaluation of the FT by directly transforming (2.200) is somewhat cumbersome. A simpler approach is the following:

$$\begin{aligned}\mathcal{F}\{K_{\Omega}^{(1)}(t)\} &= \mathcal{F}\{\frac{1}{\Omega}\int_0^{\Omega}\frac{\sin^2[(a/2)t]}{\pi(a/2)t^2}da\} = \frac{1}{\Omega}\int_0^{\Omega}\mathcal{F}\left\{\frac{\sin^2[(a/2)t]}{\pi(a/2)t^2}\right\}da \\ &= \frac{1}{\Omega}\int_0^{\Omega}\left(1-\frac{|\omega|}{a}\right)p_a(\omega)\,da = \begin{cases} \frac{1}{\Omega}\int_{|\omega|}^{\Omega}\left(1-\frac{|\omega|}{a}\right)da\ ;\ |\omega|<\Omega, \\ 0\ ;\ |\omega|>\Omega. \end{cases}\end{aligned}$$

The last integral is easily evaluated with the final result

$$\mathcal{F}\{K_{\Omega}^{(1)}(t)\} \equiv W^{(1)}(\omega) = \left\{1+\frac{|\omega|}{\Omega}\left(\ln\frac{|\omega|}{\Omega}-1\right)\right\}p_{\Omega}(\omega). \tag{2.202}$$

A plot of this spectral window is shown in Fig. 2.30 which is seen to be quite similar to its discrete counterpart in Fig. 2.11.

2.3 Modulation and Analytic Signal Representation

2.3.1 Analytic Signals

Suppose $z(t)$ is a real signal with a Fourier transform $Z(\omega) = A(\omega)\,e^{i\theta(\omega)}$. According to (2.151) this signal can be expressed as a real part of the complex signal whose Fourier transform vanishes for negative frequencies and equals twice the transform of the given real signal for positive frequencies. Presently we denote this complex signal by $w(t)$ so that

$$w(t) = \frac{1}{2\pi}\int_0^{\infty} 2Z(\omega)\,e^{i\omega t}d\omega, \tag{2.203}$$

whence the real and imaginary parts are, respectively,

$$\Re e\{w(t)\} = z(t) = \frac{1}{\pi}\int_0^{\infty} A(\omega)\cos[\omega t+\theta(\omega)]d\omega, \tag{2.204a}$$

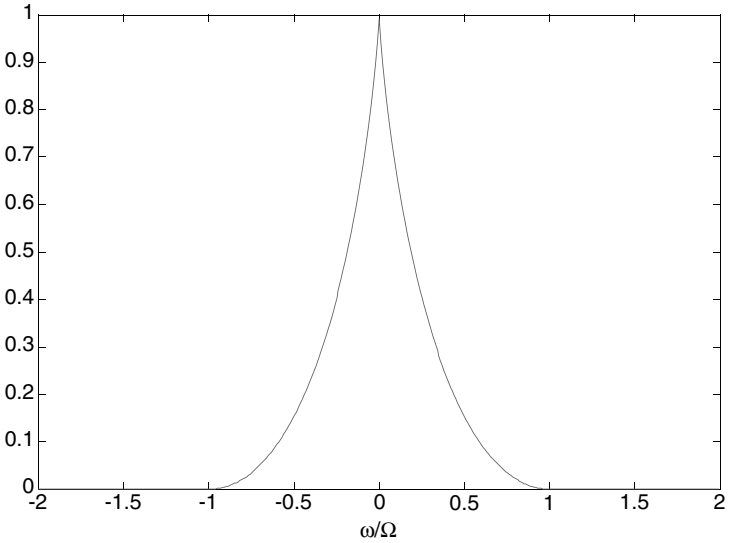

Figure 2.30: FT of second-order Fejer kernel

$$\Im m\left\{w\left(t\right)\right\} \quad = \quad \frac{1}{\pi}\int_0^\infty A(\omega)\sin[\omega t+\theta\left(\omega\right)]d\omega. \tag{2.204b}$$

We claim that $\Im m\left\{w\left(t\right)\right\}$, which we presently denote by $\hat{z}\ \left(t\right)$, is the Hilbert transform of $z\left(t\right)$, i.e.,

$$\hat{z}\ \left(t\right) = \frac{1}{\pi}P\int_{-\infty}^{\infty}\frac{z\left(\tau\right)}{t-\tau}d\tau. \tag{2.205}$$

Taking Hilbert transforms of both sides of (2.204a) and using trigonometric sum formulas together with (2.179) and (2.180) we obtain

$$\begin{aligned}
\hat{z}\ \left(t\right) &= \mathcal{H}\left\{z\left(t\right)\right\} = \mathcal{H}\left\{\frac{1}{\pi}\int_0^\infty A(\omega)\cos[\omega t+\theta\left(\omega\right)]d\omega\right\} \\
&= \frac{1}{\pi}\int_0^\infty A(\omega)\mathcal{H}\left\{\cos[\omega t+\theta\left(\omega\right)]\right\}d\omega \\
&= \frac{1}{\pi}\int_0^\infty A(\omega)\left(\cos\left[\theta\left(\omega\right)\right]\mathcal{H}\left\{\cos\left(\omega t\right)\right\}-\sin\left[\theta\left(\omega\right)\right]\mathcal{H}\left\{\sin\left(\omega t\right)\right\}\right)d\omega \\
&= \frac{1}{\pi}\int_0^\infty A(\omega)\left(\cos\left[\theta\left(\omega\right)\right]\sin\left(\omega t\right)+\sin\left[\theta\left(\omega\right)\right]\cos(\omega t)\right)d\omega \\
&= \frac{1}{\pi}\int_0^\infty A(\omega)\sin[\omega t+\theta\left(\omega\right)]d\omega = \Im m\left\{w\left(t\right)\right\}
\end{aligned}$$

as was to be demonstrated. As a by-product of this derivation we see that the evaluation of the Hilbert transform of any signal can always be carried

out entirely in terms of the FT, as already remarked in connection with the frequency domain calculation in (2.180).

The complex function

$$w(t) = z(t) + i\hat{z}\ (t) \tag{2.206}$$

of a real variable t is referred to as *an analytic signal*.[1] By construction the Fourier transform of such a signal vanishes identically for negative frequencies. This can also be demonstrated directly by Fourier transforming both sides of (2.206). This entails recognition of (2.205) as a convolution of $z(t)$ with $1/\pi t$ and use of (2.164) and (2.131). As a result we get the transform pair

$$\hat{z}(t) \overset{\mathfrak{F}}{\Longleftrightarrow} -i\ sign(\omega)\ \ Z(\omega). \tag{2.207}$$

Using this in the FT of (2.206) yields $W(\omega) = Z(\omega) + i[-i\ sign(\omega)\ \ Z(\omega)]$ which is equivalent to

$$W(\omega) = \begin{cases} 2Z(\omega)\ ;\ \omega > 0 \\ 0\ ;\ \omega < 0. \end{cases} \tag{2.208}$$

In practical situations a signal will invariably have negligible energy above a certain frequency. It is frequently convenient to idealize this by assuming that the FT of the signal vanishes identically above a certain frequency. Such a signal is said to be bandlimited (or effectively bandlimited). For example if $z(t)$ is bandlimited to $|\omega| < \omega_{\max}$ the magnitude of its FT may appear as shown in Fig. 2.31a. In conformance with (2.208) the magnitude of the Fourier spectrum of the corresponding analytic signal then appears as in Fig. 2.31b. It is common to refer to the spectrum in Fig. 2.31a as double sided and to that in Fig. 2.31b as the single sided. In practical applications the use of the latter is more common. The energy balance between the time and the frequency domains follows from Parseval theorem

$$\int_{-\infty}^{\infty} |w(t)|^2\, dt = \frac{2}{\pi} \int_0^{\omega_{\max}} |Z(\omega)|^2\, d\omega.$$

Because of (2.207) the energy of an analytic signal is shared equally by the real signal and its Hilbert transform.

2.3.2 Instantaneous Frequency and the Method of Stationary Phase

The analytic signal furnishes a means of quantifying the amplitude, phase, and frequency of signals directly in the time domain. We recall that these concepts have their primitive origins in oscillatory phenomena described by

[1] The term "analytic" refers to the fact that a signal whose Fourier transform vanishes for real negative values of frequency, i.e., is represented by the integral (2.203), is an analytic function of t in the upper half of the complex t plane (i.e., $\Im m(t) > 0$). (See Appendix, pages 341–348).

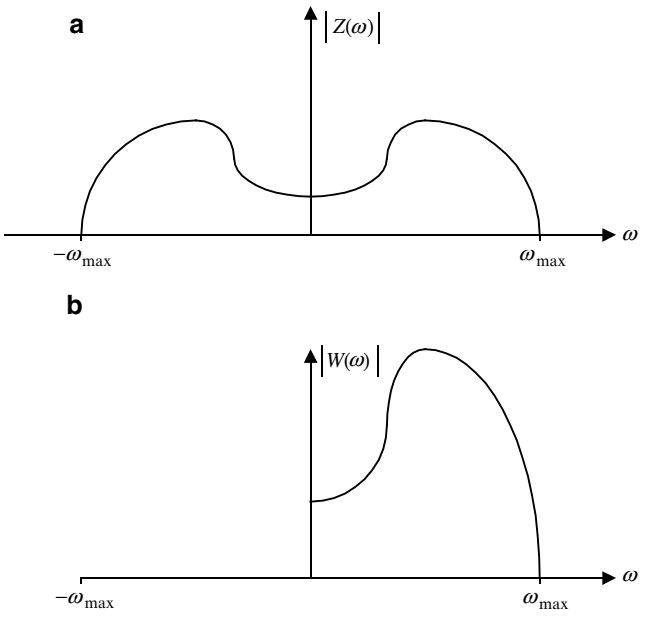

Figure 2.31: Spectrum of $z(t)$ and $z(t) + i\hat{z}(t)$

sinusoids. Thus we say that the signal $r\cos(\omega t + \psi_0)$ has amplitude r, frequency ω and a fixed phase reference ψ_0, where for purposes of analysis we sometimes find it more convenient to deal directly with a fictitious complex signal $r\exp[i(\omega t + \psi_0)]$ with the tacit understanding that physical processes are to be associated only with the real part of this signal. A generalization of this construct is an analytic signal. In addition to simplifying the algebra such complex notation also affords novel points of view. For example, the exponential of magnitude r and phase angle $\psi(t) = \omega t + \theta_0$ can be interpreted graphically as a phasor of length r rotating at the constant angular velocity $\omega = \frac{d}{dt}(\omega t + \theta_0)$. Classically for a general nonsinusoidal (real) signal $z(t)$ the concepts of frequency, amplitude, and phase are associated with each sinusoidal component comprising the signal Fourier spectrum, i.e., in this form these concepts appear to have meaning only when applied to each individual spectral component of the signal. On the other hand we can see intuitively that at least in special cases the concept of frequency must bear a close relationship to the rate of zero crossings of a real signal. For pure sinusoids this observation is trivial, e.g., the number of zero crossings of the signal $\cos(10t)$ per unit time is twice that of $\cos(5t)$. Suppose instead we take the signal $\cos\left(10t^2\right)$. Here the number of zero crossings varies linearly with time and the corresponding complex signal, as represented by the phasor $\exp\left[i\left(10t^2\right)\right]$, rotates at the rate $\frac{d}{dt}\left(10t^2\right) = 20t$ rps. Thus we conclude that the frequency of this signal varies linearly with time. The new concept here is that of *instantaneous frequency* which is clearly not identical with the frequency associated with each Fourier component of the signal (except of course in case of a pure sinusoid). We extend this definition to

arbitrary real signals $z(t)$ through an analytic signal constructed in accordance with (2.203). We write it presently in the form

$$w(t) = r(t)\, e^{i\psi(t)}, \tag{2.209}$$

where

$$r(t) = \sqrt{z^2(t) + \hat{z}^2(t)} \tag{2.210}$$

is the (real, nonnegative) time-varying amplitude, or envelope, $\psi(t)$ the instantaneous phase, and

$$\widetilde{\omega}(t) = \frac{d\psi}{dt} \tag{2.211}$$

the instantaneous frequency. Note also that the interpretation of $\widetilde{\omega}(t)$ as a zero crossing rate requires that it be nonnegative which is compatible with the analytic signal having only positive frequency components. To deduce the relationship between the instantaneous frequency and the signal Fourier spectrum let us formulate an estimate of the spectrum of $w(t)$:

$$W(\omega) = \int_{-\infty}^{\infty} r(t)\, e^{i[\psi(t)-\omega t]} dt. \tag{2.212}$$

We can, of course, not "evaluate" this integral without knowing the specific signal. However for signals characterized by a large time-bandwidth product we can carry out an approximate evaluation utilizing the so-called principle of stationary phase. To illustrate the main ideas without getting sidetracked by peripheral generalities consider the real part of the exponential in (2.212), i.e., $\cos[q(t)]$ with $q(t) = \psi(t) - \omega t$. Figure 2.32 shows a plot of $\cos[q(t)]$ for

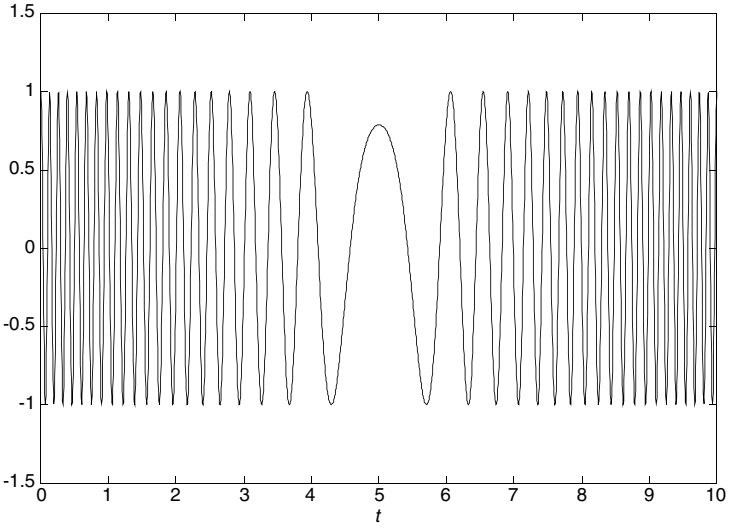

Figure 2.32: Plot of $\cos(5t^2 - 50t)$ (stationary point at $t = 5$)

the special choice $\psi(t) = 5t^2$ and $\omega = 50$. This function is seen to oscillate rapidly except in the neighborhood of $t = t_0 = 5 = \omega/10$ which point corresponds to $q'(5) = 0$. The value $t_0 = 5$ in the neighborhood of which the phase varies slowly is referred to as the stationary point of $q(t)$ (or a point of stationary phase). If we suppose that the function $r(t)$ is slowly varying relative to these oscillations, we would expect the contributions to an integral of the form $\int_{-\infty}^{\infty} r(t) \cos\left(5t^2 - 50t\right) dt$ from points not in the immediate vicinity of $t = 5$ to mutually cancel. Consequently the dominant contributions to the integral would arise only from the values of $r(t)$ and $\psi(t)$ in the immediate neighborhood of the point of stationary phase. We note in passing that in this example the product $t_0\omega = 250 >> 1$. It is not hard to show that the larger this dimensionless quantity (time bandwidth product) the narrower the time band within which the phase is stationary and therefore the more nearly localized the contribution to the overall integral. In the general case the stationary point is determined by

$$q'(t) = \psi'(t) - \omega = 0, \tag{2.213}$$

which coincides with the definition of the instantaneous frequency in (2.211). When we expand the argument of the exponential in a Taylor series about $t = t_0$ we obtain

$$q(t) = \psi(t_0) - \omega t_0 + \frac{1}{2}(t - t_0)^2 \psi''(t_0) + \dots \tag{2.214}$$

Similarly we have for $r(t)$

$$r(t) = r(t_0) + (t - t_0) r'(t_0) + \dots \tag{2.215}$$

In accordance with the localization principle just discussed we expect, given a sufficiently large ωt_0, that in the exponential function only the first two Taylor series terms need to be retained. Since $r(t)$ is assumed to be relatively slowly varying it may be replaced by $r(t_0)$. Therefore (2.212) may be approximated by

$$W(\omega) \sim r(t_0)\, e^{i[\psi(t_0) - \omega t_0]} \int_{-\infty}^{\infty} e^{i\frac{1}{2}(t-t_0)^2 \psi''(t_0)} dt. \tag{2.216}$$

When the preceding standard Gaussian integral is evaluated we obtain the final formula

$$\underset{\omega t_0 \sim \infty}{W(\omega)} \sim r(t_0)\, e^{i[\psi(t_0) - \omega t_0]} \sqrt{\frac{2\pi}{\left|\psi''(t_0)\right|}} e^{i\frac{\pi}{4} sign\left[\psi''(t_0)\right]}. \tag{2.217}$$

It should be noted that the variable t_0 is to be expressed in terms of ω by inverting (2.213), a procedure that in general is far from trivial. When this is done (2.217) provides an asymptotic approximation to the signal Fourier spectrum for large ωt_0.

To illustrate the relationship between the instantaneous frequency of a signal and its frequency content as defined by Fourier synthesis consider the signal

$$g(t) = \begin{cases} A\cos(at^2 + \beta t)\ ;\ 0 \le t \le T, \\ 0 \text{ elsewhere.} \end{cases}$$

whose instantaneous frequency increases linearly from $\omega_{\min} = \beta$ ($\beta > 0$) to $\omega_{\max} = 2aT + \beta$ rps. Based on this observation it appears reasonable to define the nominal bandwidth of this signal by $B = aT/\pi$ Hz. The relationship between B and the bandwidth as defined by the signal Fourier spectrum is more readily clarified in terms of the dimensionless parameters $M = 2BT$ (the nominal time-bandwidth product) and $r = \omega_{\min}/\omega_{\max} < 1$. Using these parameters we put the signal in the form

$$g(t) = \begin{cases} A\cos\left[\left(\frac{\pi}{2}M\right)(t/T)^2 + \pi\frac{M}{1-r}\left(\frac{t}{T}\right)\right]\ ;\ 0 \le t \le T, \\ 0 \text{ elsewhere.} \end{cases} \tag{2.218}$$

The FT of (2.218) can be expressed in terms of Fresnel integrals whose standard forms read

$$C(x) = \int_0^x \cos\left(\frac{\pi}{2}\xi^2\right) d\xi, \tag{2.219a}$$

$$S(x) = \int_0^x \sin\left(\frac{\pi}{2}\xi^2\right) d\xi. \tag{2.219b}$$

One then finds

$$\begin{aligned} G(\omega) = \frac{AT}{2\sqrt{M}} \Bigg[& e^{-i\frac{\pi}{2}M\left(\frac{r-f}{1-r}'\right)^2} [C\{\sqrt{M}\frac{1-f'}{1-r}\} + iS\{\sqrt{M}\frac{1-f'}{1-r}\} \\ & - C\{\sqrt{M}\frac{r-f'}{1-r}\} - iS\{\sqrt{M}\frac{r-f'}{1-r}\}] \\ & + e^{i\frac{\pi}{2}M\left(\frac{r+f}{1-r}'\right)^2} [C\{\sqrt{M}\frac{1+f'}{1-r}\} - iS\{\sqrt{M}\frac{1+f'}{1-r}\} \\ & - C\{\sqrt{M}\frac{r+f'}{1-r}\} + iS\{\sqrt{M}\frac{r+f'}{1-r}\}] \Bigg], \end{aligned} \tag{2.220}$$

where we have introduced the normalized frequency variable $f' = \omega(1-r)/2\pi B$. Using the asymptotic forms of the Fresnel integrals for large arguments, i.e., $C(\pm\infty) = \pm 1/2$ and $S(\pm\infty) = \pm 1/2$, we find that as the nominal time-bandwidth product $(M/2)$ approaches infinity, the rather cumbersome expression (2.220) assumes the simple asymptotic form

$$\underset{M\sim\infty}{G(\omega)} \sim \begin{cases} \frac{AT}{2}\sqrt{\frac{2}{M}}e^{-i\frac{\pi}{2}M\left(\frac{r-f}{1-r}'\right)^2}\ ; r < f' < 1, \\ \frac{AT}{2}\sqrt{\frac{2}{M}}e^{i\frac{\pi}{2}M\left(\frac{r+f}{1-r}'\right)^2}\ ; -1 < f' < -r, \\ 0\ ; |f'| > 1 \text{ and } |f'| < r. \end{cases} \tag{2.221}$$

From (2.221) we see that the FT of $g(t)$ approaches the constant $AT/2\sqrt{2/M}$ within the frequency band $r < |f'| < 1$ and vanishes outside this range, except at the band edges (i.e., $f' = \pm 1$ and $\pm r$) where it equals one-half this constant. Since $g(t)$ is of finite duration it is asymptotically simultaneously bandlimited and timelimited. Even though for any finite M the signal spectrum will not be bandlimited this asymptotic form is actually consistent with Parseval theorem. For applying Parseval formula to (2.221) we get

$$\frac{1}{2\pi}\int_{-\infty}^{\infty} |G(\omega)|^2 \, d\omega = \frac{A^2}{4}\frac{T}{B}2B = \left(A^2/2\right)T \tag{2.222}$$

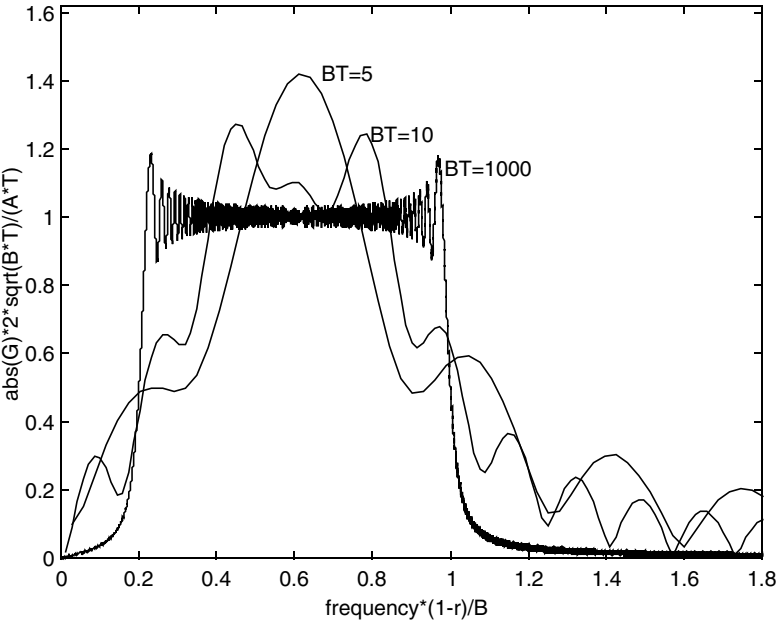

Figure 2.33: Magnitude of the FT of a linear FM pulse for different time-bandwidth products

On the other hand we recognize the last term as the asymptotic form (i.e., for large $\omega_0 T$) of the total energy of a sinusoid of fixed frequency, amplitude A, and duration T. Thus apparently if the time-bandwidth product is sufficiently large we may approximate the energy of a constant amplitude sinusoid with variable phase by the same simple formula $(A^2/2)T$. Indeed this result actually generalizes to signals of the form $A\cos[\phi(t)]$. How large must M be for (2.221) to afford a reasonable approximation to the signal spectrum? Actually quite large, as is illustrated by the plots in Fig. 2.33 for $BT = 5, 10$, and $1,000$, where the lower (nominal) band edge is defined by $r = 0.2$ and the magnitude of the asymptotic spectrum equals unity within $.2 < f' < 1$ and $1/2$ at $f' = .2$ and $f' = 1$.

2.3.3 Bandpass Representation

The construct of an analytic signal affords a convenient tool for describing the process of modulation of a low frequency (baseband) signal by a high frequency carrier as well as the demodulation of a transmitted bandpass signal down to baseband frequencies. We have already encountered a modulated signal in simplified form in connection with the frequency shifting properties of the FT in (2.154). Adopting now a more general viewpoint we take an arbitrary real signal $z\,(t)$ together with its Hilbert transform $\hat{z}\,(t)$ and a positive constant ω_0 to define two functions $x\,(t)$ and $y\,(t)$ as follows:

$$x\,(t) = z\,(t)\cos\,(\omega_0 t) + \hat{z}(t)\sin\,(\omega_0 t)\,, \tag{2.223a}$$

$$y\,(t) = -z\,(t)\sin\,(\omega_0 t) + \hat{z}(t)\cos\,(\omega_0 t)\,, \tag{2.223b}$$

which are easily inverted to yield

$$z\,(t) = x\,(t)\cos\,(\omega_0 t) - y(t)\sin\,(\omega_0 t) \tag{2.224a}$$

$$\hat{z}(t) = x\,(t)\sin\,(\omega_0 t) + y(t)\cos\,(\omega_0 t)\,. \tag{2.224b}$$

Equations (2.223) and (2.224) constitute a fundamental set of relations that are useful in describing rather general modulation and demodulation processes. In fact the form of (2.224a) suggests an interpretation of $z\,(t)$ as a signal modulated by a carrier of frequency ω_0 a special case of which is represented by the left side of (2.154). Comparison with (2.224a) yields $x\,(t) = Af(t)\cos(\theta_0)$ and $y\,(t) = Af(t)\sin(\theta_0)$. We note that in this special case $x\,(t)$ and $y(t)$ are linearly dependent which need not be true in general.

Let us now suppose that the only datum at our disposal is the signal $z\,(t)$ and that the carrier frequency ω_0 is left unspecified. As far as the mathematical representation (2.223) and (2.224) is concerned it is, of course, perfectly valid and consistent for any choice of (real) ω_0. However, if $x\,(t)$ and $y(t)$ in (2.223) are to represent baseband signals at the receiver resulting from the demodulation of $z\,(t)$ by the injection of a local oscillator with frequency ω_0, then the bandwidth of $x\,(t)$ and $y(t)$ (centered at $\omega = 0$) should certainly be less than $2\omega_0$. A more precise interrelation between the constraints on signal bandwidth and carrier frequency ω_0 is readily deduced from the FT of $x\,(t)$ and $y(t)$. Denoting these, respectively, by $X\,(\omega)$ and $Y\,(\omega)$, we obtain using (2.223) and (2.207)

$$X\,(\omega) = U(\omega_0 - \omega)Z\,(\omega - \omega_0) + U(\omega + \omega_0)Z\,(\omega + \omega_0)\,, \tag{2.225a}$$

$$Y\,(\omega) = iU(\omega_0 - \omega)Z\,(\omega - \omega_0) - iU(\omega + \omega_0)Z\,(\omega + \omega_0)\,. \tag{2.225b}$$

On purely physical grounds we would expect $Z\,(\omega)$ to be practically zero above some finite frequency, say $\omega_{\max}$. If the bandwidth of $X(\omega)$ and $Y(\omega)$ is to be limited to $|\omega| \leq \omega_0$, then $\omega_{\max} - \omega_0$ may not exceed ω_0. This follows directly from (2.225) or from the graphical superposition of the spectra shown in Fig. 2.34. In other words if $x\,(t)$ and $y(t)$ are to represent baseband signals, we must have

$$\omega_0 \geq \omega_{\max}/2. \tag{2.226}$$

When this constraint is satisfied the spectrum of $z(t)$ may in fact extend down to zero frequency (as, e.g., in Fig. 2.31a) so that theoretically the spectra of $x(t)$ and $y(t)$ are allowed to occupy the entire bandwidth $|\omega| \leq \omega_0$. However in practice there will generally also be a lower limit on the band occupancy of $Z(\omega)$, say $\omega_{\min}$. Thus the more common situation is that of a bandpass spectrum illustrated in Fig. 2.34 wherein the nonzero spectral energy of $z(t)$ occupies the band $\omega_{\min} < \omega < \omega_{\max}$ for positive frequencies and the band $-\omega_{\max} < \omega < -\omega_{\min}$ for negative frequencies.

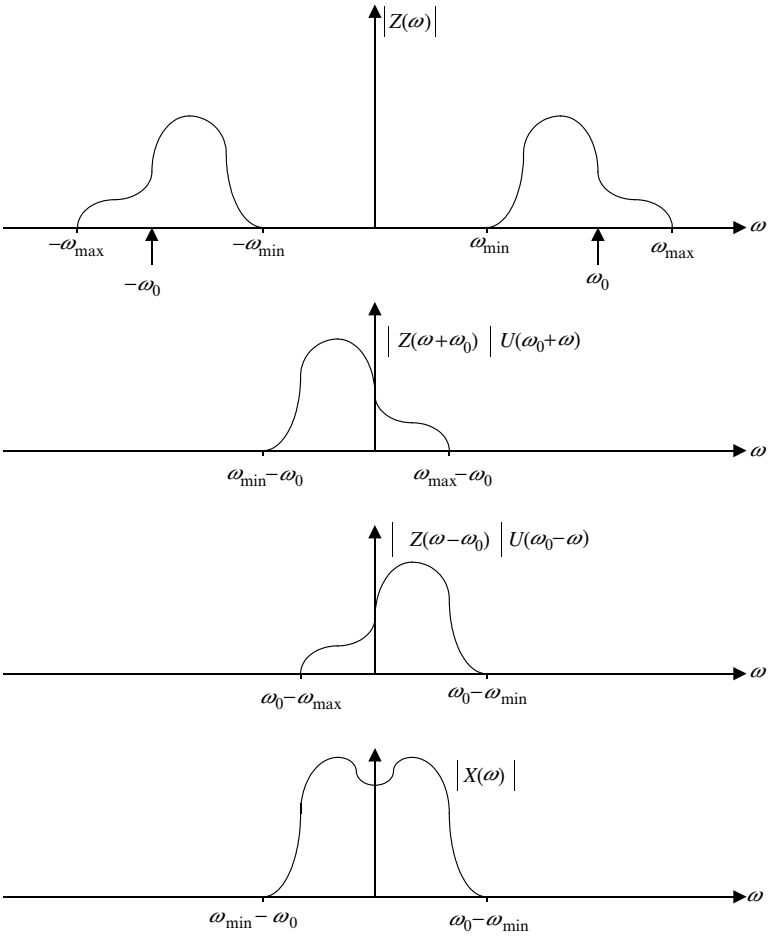

Figure 2.34: Bandpass and demodulated baseband spectra

In the case depicted $\omega_{\min} < \omega_0 < \omega_{\max}$ and $\omega_0 - \omega_{\min} > \omega_{\max} - \omega_0$. The synthesis of $X(\omega)$ from the two frequency-shifted sidebands follows from (2.225a) resulting in a total band occupancy of $2\ |\omega_0 - \omega_{\min}|$. It is easy to see from (2.225b) that $Y(\omega)$ must occupy the same bandwidth. Observe that shifting ω_0 closer to $\omega_{\min}$ until $\omega_{\max} - \omega_0 > \omega_0 - \omega_{\min}$ results in a

total band occupancy of $2\,|\omega_{\max} - \omega_0|$ and that the smallest possible baseband bandwidth is obtained by positioning ω_0 midway between $\omega_{\max}$ and $\omega_{\min}$.

The two real baseband signals $x\,(t)$ and $y(t)$ are referred to as the inphase and quadrature signal components. It is convenient to combine them into the single complex baseband signal

$$b(t) = x(t) + iy(t). \tag{2.227}$$

The analytic signal $w(t) = z(t) + i\hat{z}(t)$ follows from a substitution of (2.224a) and (2.224b)

$$\begin{aligned} w(t) &= x\,(t)\cos(\omega_0 t) - y(t)\sin(\omega_0 t) \\ &\quad + i[x\,(t)\sin(\omega_0 t) + y(t)\cos(\omega_0 t)] \\ &= [x(t) + iy(t)]\,e^{i\omega_0 t} = b\,(t)\,e^{i\omega_0 t}. \end{aligned} \tag{2.228}$$

The FT of (2.228) reads

$$W\,(\omega) = X\,(\omega - \omega_0) + iY\,(\omega - \omega_0) = B\,(\omega - \omega_0) \tag{2.229}$$

or, solving for $B\,(\omega)$,

$$B\,(\omega) = W\,(\omega + \omega_0) = 2U\,(\omega + \omega_0)\,Z(\omega + \omega_0) = X\,(\omega) + iY\,(\omega)\,. \tag{2.230}$$

In view of (2.224a) the real bandpass $z(t)$ signal is given by the real part of (2.228), i.e.,

$$z(t) = \Re e\left\{b\,(t)\,e^{i\omega_0 t}\right\}. \tag{2.228*}$$

Taking the FT we get

$$Z(\omega) = \frac{1}{2}\left[B\,(\omega - \omega_0) + B^*\,(-\omega - \omega_0)\right], \tag{2.228**}$$

which reconstructs the bandpass spectrum in terms of the baseband spectrum.

As the preceding formulation indicates, given a bandpass signal $z\,(t)$, the choice of ω_0 at the receiver effectively *defines* the inphase and quadrature components. Thus a different choice of (local oscillator) frequency, say ω_1, $\omega_1 \neq \omega_0$ leads to the representation

$$z\,(t) = x_1\,(t)\cos(\omega_1 t) - y_1\,(t)\sin(\omega_1 t)\,, \tag{2.229a}$$

$$\hat{z}\,(t) = x_1\,(t)\sin(\omega_1 t) + y_1\,(t)\cos(\omega_1 t)\,, \tag{2.229b}$$

wherein the $x_1\,(t)$ and $y_1\,(t)$ are the new inphase and quadrature components. The relationship between $x\,(t)$, $y\,(t)$ and $x_1\,(t)$ and $y_1\,(t)$ follows upon equating (2.229) to (2.224):

$$\begin{bmatrix} \cos(\omega_0 t) & -\sin(\omega_0 t) \\ \sin(\omega_0 t) & \cos(\omega_0 t) \end{bmatrix} \begin{bmatrix} x\,(t) \\ y\,(t) \end{bmatrix} = \begin{bmatrix} \cos(\omega_1 t) & -\sin(\omega_1 t) \\ \sin(\omega_1 t) & \cos(\omega_1 t) \end{bmatrix} \begin{bmatrix} x_1\,(t) \\ y_1\,(t) \end{bmatrix},$$

which yields

$$\begin{bmatrix} x\,(t) \\ y\,(t) \end{bmatrix} = \begin{bmatrix} \cos[(\omega_0 - \omega_1)\,t] & \sin[(\omega_0 - \omega_1)\,t] \\ -\sin[(\omega_0 - \omega_1)\,t] & \cos[(\omega_0 - \omega_1)\,t] \end{bmatrix} \begin{bmatrix} x_1\,(t) \\ y_1\,(t) \end{bmatrix}. \tag{2.230}$$

The linear transformations defined by the 2×2 matrices in (2.224), (2.229), and (2.230) are all orthogonal so that

$$z^2(t) + \hat{z}^2(t) = x^2(t) + y^2(t) = x_1^2(t) + y_1^2(t) = |b(t)|^2 = r^2(t). \quad (2.231)$$

This demonstrates directly that the analytic signal and the complex baseband signal have the same envelope $r(t)$ which is in fact independent of the frequency of the reference carrier. We shall henceforth refer to $r(t)$ as the signal envelope. Unlike the signal envelope, the phase of the complex baseband signal does depend on the carrier reference. Setting

$$\theta(t) = \tan^{-1}\frac{x(t)}{y(t)},\ \theta_1(t) = \tan^{-1}\frac{x_1(t)}{y_1(t)}, \quad (2.232)$$

we see that with a change in the reference carrier the analytic signal undergoes the transformation

$$\begin{aligned} w(t) &= r(t)\, e^{i\theta(t)} e^{i\omega_0 t} \\ &= r(t)\, e^{i\theta_1(t)} e^{i\omega_1 t} \end{aligned} \quad (2.233)$$

or, equivalently, that the two phase angles transform in accordance with

$$\theta(t) + \omega_0 t = \theta_1(t) + \omega_1 t. \quad (2.234)$$

It should be noted that in general the real and imaginary parts of a complex baseband signal need not be related by Hilbert transforms. In fact suppose $x(t)$ and $y(t)$ are two arbitrary real signals, bandlimited to $|\omega| < \omega_x$ and $|\omega| < \omega_y$, respectively. Then, as may be readily verified, for any ω_0 greater than $\omega_x/2$ and $\omega_y/2$ the Hilbert transform of the bandpass signal $z(t)$ defined by (2.224a) is given by (2.224b).

2.3.4 Bandpass Representation of Random Signals*

In the preceding discussion it was tacitly assumed that the signals are deterministic. The notion of an analytic signal is equally useful when dealing with stochastic signals. For example, if $z(t)$ is a real wide-sense stationary stochastic process, we can always append its Hilbert transform to form the complex stochastic process

$$w(t) = z(t) + i\hat{z}(t). \quad (2.235)$$

By analogy with (2.206) we shall refer to it as an analytic stochastic process. As we shall show in the sequel its power spectrum vanishes for negative frequencies. First we note that in accordance with (2.207) the magnitude of the transfer function that transforms $z(t)$ into $\hat{z}(t)$ is unity. Hence the power spectrum as well as the autocorrelation function of $\hat{z}(t)$ are the same as that of $z(t)$, i.e.,

$$\langle z(t+\tau)\, z(t)\rangle \equiv R_{zz}(\tau) = \langle \hat{z}(t+\tau)\, \hat{z}(t)\rangle = R_{\hat{z}\hat{z}}(\tau). \quad (2.236)$$

The cross-correlation between $z(t)$ and its Hilbert transform is then

$$\begin{aligned} R_{\hat{z}z}(\tau) &= \langle \hat{z}(t+\tau)\, z(t)\rangle = \frac{1}{\pi}\int_{-\infty}^{\infty} \frac{\langle z\left(\tau'\right) z(t)\rangle}{t+\tau-\tau'} d\tau' \\ &= \frac{1}{\pi}\int_{-\infty}^{\infty} \frac{R_{zz}\left(\tau'-t\right)}{t+\tau-\tau'} d\tau' = \frac{1}{\pi}\int_{-\infty}^{\infty} \frac{R_{zz}(\xi)}{\tau-\xi} d\xi. \end{aligned} \tag{2.237}$$

The last expression states that the cross-correlation between a stationary stochastic process and its Hilbert transform is the Hilbert transform of the autocorrelation function of the process. In symbols

$$R_{\hat{z}z}(\tau) = \hat{R}_{zz}(\tau). \tag{2.238}$$

Recall that the Hilbert transform of an even function is an odd function and conversely. Thus, since the autocorrelation function of a real stochastic process is always even, $R_{\hat{z}z}(\tau)$ is odd. Therefore we have

$$R_{z\hat{z}}(\tau) \equiv R_{\hat{z}z}(-\tau) = -R_{\hat{z}z}(\tau). \tag{2.239}$$

The autocorrelation function of $w(t)$ then becomes

$$\begin{aligned} R_{ww}(\tau) &= \langle w(t+\tau)\overset{*}{w}(t)\rangle = 2\left[R_{zz}(\tau) + iR_{\hat{z}z}(\tau)\right] \\ &= 2\left[R_{zz}(\tau) + i\hat{R}_{zz}(\tau)\right]. \end{aligned} \tag{2.240}$$

With

$$R_{zz}(\tau) \overset{\mathfrak{F}}{\Longleftrightarrow} S_{zz}(\omega) \tag{2.241}$$

we have in view of (2.238) and (2.207)

$$R_{\hat{z}z}(\tau) = \hat{R}_{zz}(\tau) \overset{\mathfrak{F}}{\Longleftrightarrow} -iS_{zz}(\omega)\, sign(\omega). \tag{2.242}$$

Denoting the spectral density of $w(t)$ by $S_{ww}(\omega)$, (2.240) together with (2.241) and (2.242) gives

$$S_{ww}(\omega) = \begin{cases} 4S_{zz}(\omega);\ \omega > 0, \\ 0;\ \omega < 0. \end{cases} \tag{2.243}$$

so that the spectral density of the analytic complex process has only positive frequency content. The correlation functions of the baseband (inphase) $x(t)$ and (quadrature) process $y(t)$ follow from (2.223). By direct calculation we get

$$\begin{aligned} R_{xx}(\tau) &= \langle\{z(t+\tau)\cos[\omega_0(t+\tau)] + \hat{z}(t+\tau)\sin[\omega_0(t+\tau)]\} \\ &\quad \{z(t)\cos(\omega_0 t) + \hat{z}(t)\sin(\omega_0 t)\}\rangle \\ &= R_{zz}(\tau)\cos(\omega_0\tau) + R_{\hat{z}z}(\tau)\sin(\omega_0\tau) \qquad (2.244a) \\ R_{yy}(\tau) &= \langle\{-z(t+\tau)\sin[\omega_0(t+\tau)] + \hat{z}(t+\tau)\cos[\omega_0(t+\tau)]\} \\ &\quad \{-z(t)\sin(\omega_0 t) + \hat{z}(t)\cos(\omega_0 t)\}\rangle \\ &= R_{zz}(\tau)\cos(\omega_0\tau) + R_{\hat{z}z}(\tau)\sin(\omega_0\tau) = R_{xx}(\tau) \qquad (2.244b) \end{aligned}$$

$$\begin{aligned} R_{xy}(\tau) &= \langle \{ z(t+\tau)\cos[\omega_0(t+\tau)] + \hat{z}(t+\tau)\sin[\omega_0(t+\tau)] \} \\ &\quad \{ -z(t)\sin(\omega_0 t) + \hat{z}(t)\cos(\omega_0 t) \} \rangle \\ &= -R_{\hat{z}z}(\tau)\cos(\omega_0\tau) + R_{zz}(\tau)\sin(\omega_0\tau) \\ &= -\hat{R}_{zz}(\tau)\cos(\omega_0\tau) + R_{zz}(\tau)\sin(\omega_0\tau). \end{aligned} \tag{2.244c}$$

Recall that for any two real stationary processes $R_{xy}(\tau) = R_{yx}(-\tau)$. Using this relation in (2.244c) we get

$$R_{yx}(\tau) = -R_{xy}(\tau). \tag{2.245}$$

Also according to (2.244a) and (2.244b) the autocorrelation functions of the in-phase and quadrature components of the stochastic baseband signal are identical and consequently so are the corresponding power spectra. These are

$$\begin{aligned} S_{xx}(\omega) &= S_{yy}(\omega) = \\ &\quad \frac{1}{2}[1 - sign(\omega - \omega_0)] S_{zz}(\omega - \omega_0) \\ &\quad + \frac{1}{2}[1 + sign(\omega + \omega_0)] S_{zz}(\omega + \omega_0). \end{aligned} \tag{2.246}$$

From (2.244c) we note that $R_{xy}(0) \equiv 0$ but that in general $R_{xy}(\tau) \neq 0$ when $\tau \neq 0$. The FT of this quantity, i.e., the cross-spectrum, is

$$\begin{aligned} S_{xy}(\omega) &= \frac{i}{2}[sign(\omega - \omega_0) - 1] S_{zz}(\omega - \omega_0) \\ &\quad + \frac{i}{2}[sign(\omega + \omega_0) + 1] S_{zz}(\omega + \omega_0). \end{aligned} \tag{2.247}$$

By constructing a mental picture of the relative spectral shifts dictated by (2.247) it is not hard to see that the cross spectrum vanishes identically (or, equivalently, $R_{xy}(\tau) \equiv 0$) when $S_{zz}(\omega)$, the spectrum of the band-pass process, is symmetric about ω_0.

Next we compute the autocorrelation function $R_{bb}(\tau)$of the complex stochastic baseband process $b(t) = x(t) + iy(t)$. Taking account of $R_{xx}(\tau) = R_{yy}(\tau)$ and (2.245) we get

$$R_{bb}(\tau) = \langle b(t+\tau)b^*(t) \rangle = 2[R_{xx}(\tau) + iR_{yx}(\tau)]. \tag{2.248}$$

In view of (2.240) and (2.228) the autocorrelation function of the analytic bandpass stochastic process is

$$R_{ww}(\tau) = 2\left[R_{zz}(\tau) + i\hat{R}_{zz}(\tau)\right] = R_{bb}(\tau)e^{i\omega_0\tau}. \tag{2.249}$$

The autocorrelation function of the real bandpass process can then be represented in terms of the autocorrelation function of the complex baseband process as follows:

$$R_{zz}(\tau) = \frac{1}{2}\Re e\left\{R_{bb}(\tau)e^{i\omega_0\tau}\right\}. \tag{2.250}$$

With the definition

$$R_{bb}(\tau) \overset{\mathfrak{F}}{\Longleftrightarrow} S_{bb}(\omega)$$

the FT of (2.250) reads

$$S_{zz}(\omega) = \frac{1}{4}\left[S_{bb}(\omega+\omega_0) + S_{bb}(-\omega-\omega_0)\right]. \tag{2.251}$$

Many sources of noise can be modeled (at least on a limited timescale) as stationary stochastic processes. The spectral distribution of such noise is usually of interest only in a relatively narrow pass band centered about some frequency, say ω_0. The measurement of the power spectrum within a predetermined pass band can be accomplished by using a synchronous detector that separates the inphase and quadrature channels, as shown in Fig. 2.35.

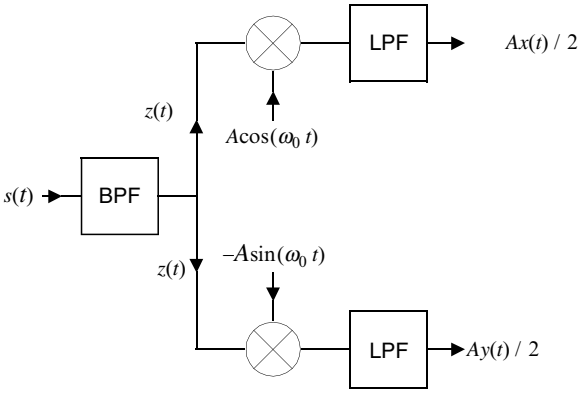

Figure 2.35: Synchronous detection

The signal $s(t)$ is first bandpass filtered to the bandwidth of interest and then split into two separate channels each of which is heterodyned with a local oscillator with a 90 degree relative phase shift. The inphase and quadrature components are obtained after lowpass filtering to remove the second harmonic contribution generated in each mixer. To determine the power spectral density of the bandpass signal requires measurement of the auto and cross spectra of $x(t)$ and $y(t)$. The power spectrum can then be computed with the aid of (2.246) and (2.247) which give

$$S_{zz}(\omega+\omega_0) = \frac{1}{2}\left[S_{xx}(\omega) - iS_{xy}(\omega)\right]. \tag{2.252}$$

This procedure assumes that the process $s(t)$ is stationary so that $S_{xx}(\omega) = S_{yy}(\omega)$. Unequal powers in the two channels would be an indication of nonstationarity on the measurement timescale. A rather common form of nonstationarity is the presence of an additive deterministic signal within the bandpass process.

A common model is a rectangular bandpass power spectral density. Assuming that ω_0 is chosen symmetrically disposed with respect to the bandpass power spectrum, the power spectra corresponding to the analytic and baseband stochastic processes are shown in Fig. 2.36. In this case the baseband autocorrelation function is purely real and equal to

$$R_{bb}(\tau) = N_0 \frac{\sin(2\pi B\tau)}{\pi\tau} = 2R_{xx}(\tau) = 2R_{yy}(\tau) \tag{2.253}$$

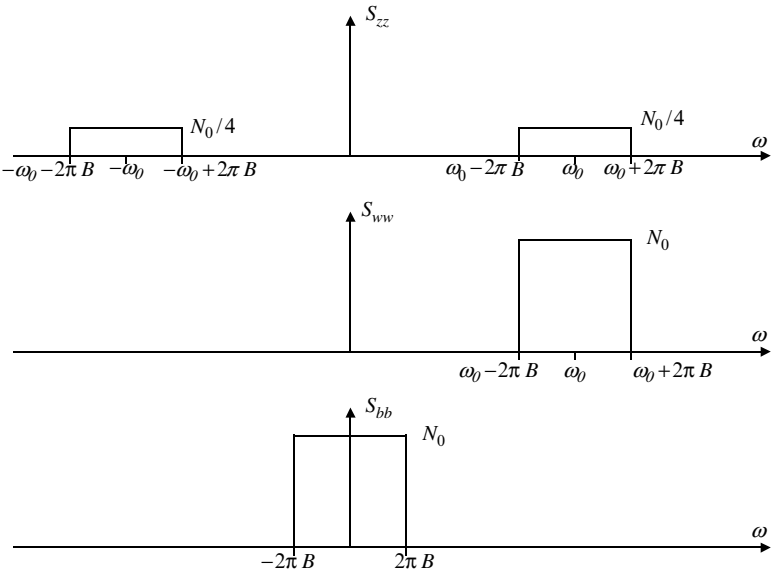

Figure 2.36: Bandpass-to-baseband transformation for a symmetric power spectrum

while $R_{xy}(\tau) \equiv 0$. What happens when the local oscillator frequency is set to $\omega = \omega_1 = \omega_0 - \Delta\omega$, i.e., off the passband center by $\Delta\omega$? In that case the baseband power spectral density will be displaced by $\Delta\omega$ and equal to

$$S_{bb}(\omega) = \begin{cases} N_0 \ ; & -2\pi B + \Delta\omega < \omega < 2\pi B + \Delta\omega, \\ 0 \ ; & otherwise. \end{cases} \tag{2.254}$$

The baseband autocorrelation function is now the complex quantity

$$R_{bb}(\tau) = e^{i\tau\Delta\omega} N_0 \frac{\sin(2\pi B\tau)}{\pi\tau}. \tag{2.255}$$

In view of (2.248) the auto and crosscorrelation functions of the inphase and quadrature components are

$$R_{xx}(\tau) = R_{yy}(\tau) = \cos(\tau\Delta\omega) N_0 \frac{\sin(2\pi B\tau)}{2\pi\tau}, \tag{2.256a}$$

$$R_{yx}(\tau) = \sin(\tau\Delta\omega) N_0 \frac{\sin(2\pi B\tau)}{2\pi\tau}. \tag{2.256b}$$

The corresponding spectrum $S_{xx}(\omega) = S_{yy}(\omega)$ occupies the band $|\omega| \leq 2\pi B + \Delta\omega$. Unlike in the symmetric case, the power spectrum is no longer flat but exhibits two steps caused by the spectral shifts engendered by $\cos(\tau\Delta\omega)$, as shown in Fig. 2.37.

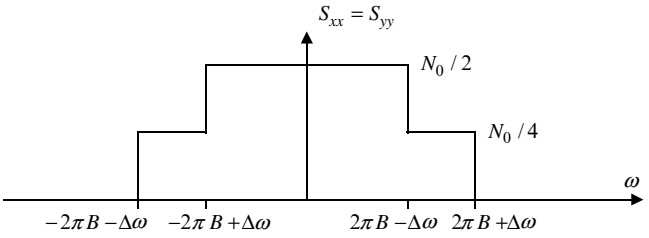

Figure 2.37: Baseband I&Q power spectra for assymmetric local oscillator frequency positioning

2.4 Fourier Transforms and Analytic Function Theory

2.4.1 Analyticity of the FT of Causal Signals

Even though both the direct and the inverse FT have been initially defined strictly for functions of a real variables one can always formally replace t and (or) ω by complex numbers and, as long as the resulting integrals converge, define the signal $f(t)$ and (or) the frequency spectrum $F(\omega)$ as functions of a complex variable. Those unfamiliar with complex variable theory should consult the Appendix, and in particular A.4.

Let us examine the analytic properties of the FT in the complex domain of a causal signal. To this end we replace ω by the complex variable $z = \omega + i\delta$ and write

$$F(z) = \int_0^\infty f(t)\, e^{-izt} dt, \tag{2.257}$$

wherein $F(\omega)$ is $F(z)$ evaluated on the axis of reals. Furthermore let us assume that

$$\int_0^\infty |f(t)|\, dt < \infty. \tag{2.258}$$

To put the last statement into the context of a physical requirement let us suppose that the signal $f(t)$ is the impulse response of a linear time-invariant system. In that case, as will be shown in 3.1.4, absolute integrability in the sense of (2.258) is a requirement for system stability. Using (2.257) we obtain in view of (2.258) for all $\operatorname{Im} z = \delta \leq 0$ the bound

$$\left| \int_0^\infty f(t)\, e^{-izt} dt \right| \leq \int_0^\infty |f(t)|\, e^{\delta t} dt < \infty. \tag{2.259}$$

From this follows (see Appendix) that $F(z)$ is an analytic function of the complex variable z in the closed lower half of the complex z plane, i.e., $\operatorname{Im} z \leq 0$. Moreover, for $\operatorname{Im} z \leq 0$,

$$\lim_{|z|\to\infty} F(z) \to 0 \tag{2.260}$$

as we see directly from (2.259) by letting δ approach $-\infty$. In other words, the FT of the impulse response of a causal linear time-invariant system is an analytic function of the complex frequency variable z in the closed lower half plane. This feature is of fundamental importance in the design and analysis of frequency selective devices (filters).

2.4.2 Hilbert Transforms and Analytic Functions

A direct consequence of the analyticity of $F(z)$ is that the real and imaginary parts of $F(\omega)$ may not be specified independently. In fact we have already established in 2.2.6 that for a causal signal they are linearly related through the Hilbert transform. The properties of analytic functions afford an alternative derivation. For this purpose consider the contour integral

$$I_R(\omega_0) = \oint_{\Gamma_R} \frac{F(z)}{z-\omega_0} dz, \tag{2.261}$$

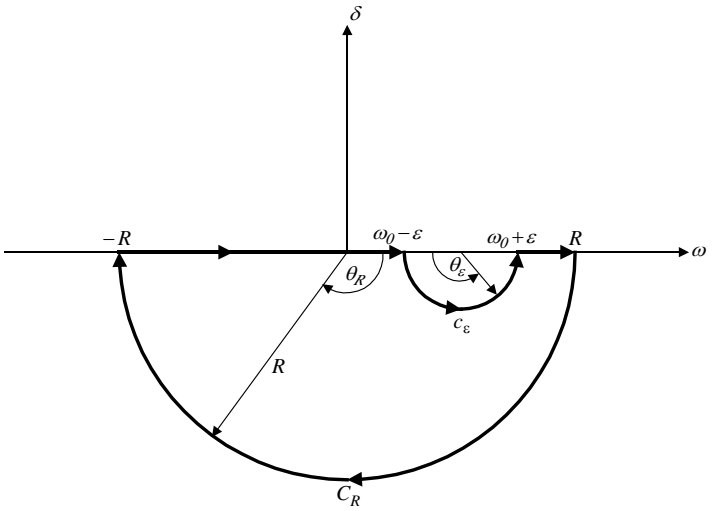

Figure 2.38: Integration contour Γ_R for the derivation of the Hilbert transforms

wherein ω_0 is real, taken in the clockwise direction along the closed path Γ_R as shown in Fig. 2.38. We note that Γ_R is comprised of the two linear segments $(-R, \omega_0 - \varepsilon)$, $(\omega_0 + \varepsilon, R)$ along the axis of reals, the semicircular contour $c_\varepsilon$of radius ε with the circle centered at $\omega = \omega_0$, and the semicircular contour C_R

of radius R in the lower half plane with the circle centered at $\omega = 0$. Since the integrand in (2.261) is analytic within Γ_R, we have $I_R(\omega_0) \equiv 0$, so that integrating along each of the path-segments indicated in Fig. 2.38 and adding the results in the limit as $\varepsilon \to 0$ and $R \to \infty$, we obtain

$$\begin{aligned} 0 &= \lim_{\varepsilon\to 0,\ R\to\infty} \left(\int_{-R}^{\omega_0-\varepsilon} \frac{F(\omega)}{\omega-\omega_0} d\omega + \int_{\omega_0+\varepsilon}^{R} \frac{F(\omega)}{\omega-\omega_0} d\omega \right) \\ &\quad + \lim_{\varepsilon\to 0} \int_{c_\varepsilon} \frac{F(z)}{z-\omega_0} dz + \lim_{R\to\infty} \int_{C_R} \frac{F(z)}{z-\omega_0} dz. \end{aligned} \tag{2.262}$$

On C_R we set $z = Re^{i\theta_R}$ so that $dz = iRe^{i\theta_R} d\theta_R$ and we have

$$\left| \int_{C_R} \frac{F(z)}{z-\omega_0} dz \right| = \left| \int_0^{-\pi} \frac{F\left(Re^{i\theta_R}\right)}{Re^{i\theta_R}-\omega_0} R d\theta_R \right|$$

so that in view of (2.260) in the limit of large R the last integral in (2.262) tends to zero. On c_ε we set $z - \omega_0 = \varepsilon e^{i\theta_\varepsilon}$ and substituting into the third integral in (2.262) evaluate it as follows:

$$\lim_{\varepsilon\to 0} \int_{c_\varepsilon} \frac{F(z)}{z-\omega_0} dz = \lim_{\varepsilon\to 0} \int_{-\pi}^{0} F\left(\omega_0 + \varepsilon e^{i\theta_\varepsilon}\right) i d\theta = i\pi F(\omega_0).$$

Now the limiting form of the first two integrals in (2.262) are recognized as the definition a CPV integral so that collecting our results we have

$$0 = P \int_{-\infty}^{\infty} \frac{F(\omega)}{\omega-\omega_0} d\omega + i\pi F(\omega_0). \tag{2.263}$$

By writing $F(\omega) = R(\omega) + iX(\omega)$ and similarly for $F(\omega_0)$, substituting in (2.263), and setting the real and the imaginary parts to zero we obtain

$$X(\omega_0) = \frac{1}{\pi} P \int_{-\infty}^{\infty} \frac{R(\omega)}{\omega-\omega_0} d\omega, \tag{2.264a}$$

$$R(\omega_0) = -\frac{1}{\pi} P \int_{-\infty}^{\infty} \frac{R(\omega)}{\omega-\omega_0} d\omega, \tag{2.264b}$$

which, apart from a different labeling of the variables, are the Hilbert Transforms in (2.173a) and (2.173b). Because the real and imaginary parts of the FT evaluated on the real frequency axis are not independent it should be possible to determine the analytic function $F(z)$ either from $R(\omega)$ of from $X(\omega)$. To obtain such formulas let z_0 be a point in the lower half plane (i.e., $\operatorname{Im} z_0 < 0$) and apply the Cauchy integral formula

$$F(z_0) = -\frac{1}{2\pi i} \oint_{\hat{\Gamma}_R} \frac{F(z)}{z-z_0} dz \tag{2.265}$$

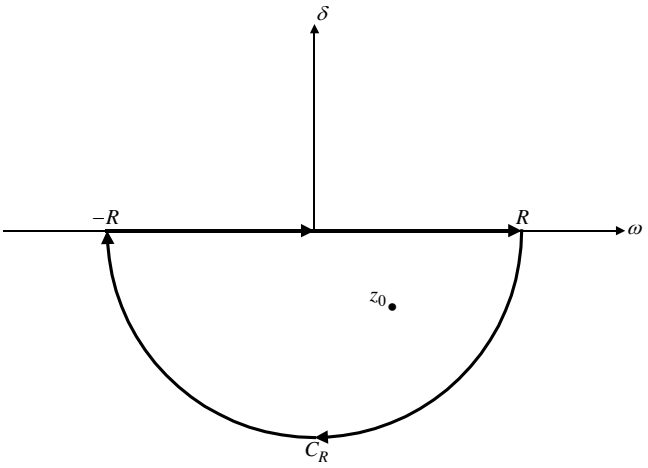

Figure 2.39: Integration contour for the evaluation of Eq. (2.265)

taken in the counterclockwise direction over the contour$\hat{\Gamma}_R$ as shown in Fig. 2.39 and comprised of the line segment $(-R, R)$ and the semicircular contour C_R of radius R. Again because of (2.260) the contribution over C_R vanishes as R is allowed to approach infinity so that (2.265) may be replaced by

$$\begin{aligned} F(z_0) &= -\frac{1}{2\pi i}\int_{-\infty}^{\infty}\frac{F(\omega)}{\omega - z_0}d\omega \\ &= -\frac{1}{2\pi i}\int_{-\infty}^{\infty}\frac{R(\omega)}{\omega - z_0}d\omega - \frac{1}{2\pi}\int_{-\infty}^{\infty}\frac{X(\omega)}{\omega - z_0}d\omega. \end{aligned} \tag{2.266}$$

In the last integral we now substitute for $X(\omega)$ its Hilbert Transform from (2.264a) to obtain

$$\begin{aligned} -\frac{1}{2\pi}\int_{-\infty}^{\infty}\frac{X(\omega)}{\omega - z_0}d\omega &= -\frac{1}{2\pi^2}\int_{-\infty}^{\infty}d\omega P\int_{-\infty}^{\infty}\frac{R(\eta)}{(\omega - z_0)(\eta - \omega)}d\eta \\ &= \frac{1}{2\pi^2}\int_{-\infty}^{\infty}R(\eta)\,d\eta P\int_{-\infty}^{\infty}\frac{d\omega}{(\omega - z_0)(\omega - \eta)}. \end{aligned} \tag{2.267}$$

The last CPV integral over ω is evaluated using the calculus of residues as follows:

$$P\int_{-\infty}^{\infty}\frac{d\omega}{(\omega - z_0)(\omega - \eta)} = \oint_{\Gamma_R}\frac{dz}{(z - z_0)(z - \eta)} - i\pi\frac{1}{\eta - z_0}, \tag{2.268}$$

where Γ_R is the closed contour in Fig. 2.38 and where the location of the simple pole at ω_0 is now designated by η. The contour integral in (2.268) is performed in the clockwise direction and the term $-i\pi/(\eta - z_0)$ is the negative of the contribution from the integration over the semicircular contour c_ε. The only

contribution to the contour integral arises from the simple pole at $z = z_0$ which equals $-i2\pi/(z_0 - \eta)$ resulting in a net contribution in (2.268) of $i\pi/(\eta - z_0)$. Substituting this into (2.267) and then into (2.266) gives the final result

$$F(z) = \frac{i}{\pi}\int_{-\infty}^{\infty} \frac{R(\eta)}{\eta - z} d\eta, \tag{2.269}$$

where we have replaced the dummy variable ω by η and z_0 by $z \equiv \omega + i\delta$. Unlike (2.257), the integral (2.269) defines the analytic function $F(z)$ only in the open lower half plane, i.e., for $\operatorname{Im} z < 0$. On the other hand, one would expect that in the limit as $\delta \to 0$, $F(z) \to F(\omega)$. Let us show that this limit is actually approached by the real part. Thus using (2.269) we get with $z = \omega + i\delta$

$$\operatorname{Re} F(z) = R(\omega, \delta) = \int_{-\infty}^{\infty} R(\eta) \frac{-\delta}{\pi\left[(\eta - \omega)^2 + \delta^2\right]} d\eta. \tag{2.270}$$

The factor multiplying $R(\eta)$ in integrand will be recognized as the delta function kernel in (1.250) so that $\lim R(\omega, \delta)$ as $-\delta \to 0$ is in fact $R(\omega)$.

2.4.3 Relationships Between Amplitude and Phase

We again suppose that $F(\omega)$ is the FT of a causal signal. Presently we write it in terms of its amplitude and phase

$$F(\omega) = A(\omega) e^{i\theta(\omega)} \tag{2.271}$$

and set

$$A(\omega) = e^{\alpha(\omega)}. \tag{2.272}$$

Taking logarithms we have

$$\ln F(\omega) = \alpha(\omega) + i\theta(\omega). \tag{2.273}$$

Based on the results of the preceding subsection it appears that if $\ln F(\omega)$ can be represented as an analytic function in the lower half plane one should be able to employ Hilbert Transforms to relate the phase to the log amplitude of the signal FT. From the nature of the logarithmic function we see that this is not possible for an arbitrary FT of a causal signal but only for signals whose FT, when continued analytically into the complex z-domain via formula (2.257) or (2.269), has no zeros in the lower half of the z-plane. Such transforms are said to be of the minimum-phaseshift type. If $f(t)$ is real so that $A(\omega)$ and $\theta(\omega)$ is, respectively, an even and an odd function of ω, we can express $\theta(\omega)$ in terms of $\alpha(\omega)$ using contour integration, provided the FT decays at infinity in accordance with

$$|F(\omega)| \underset{\omega\to\infty}{\sim} O\left(|\omega|^{-k}\right) \text{ for some } k > 0. \tag{2.274}$$

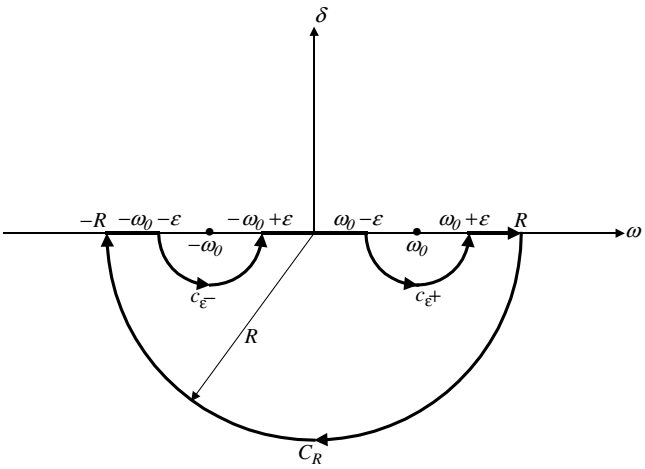

Figure 2.40: Integration contour for relating amplitude to phase

For this purpose we consider the integral

$$I_R = \oint_{\Gamma_R} \frac{\ln F(z)}{\omega_0^2 - z^2} dz \tag{2.275}$$

taken in the clockwise direction over the closed contour Γ_R comprised of the three linear segments $(-R, -\omega_0 - \varepsilon), (-\omega_0 + \varepsilon, \omega_0 - \varepsilon)$,$(\omega_0 + \varepsilon, R)$, the two semicircular arcs c_{ε^-} and c_{ε^+} each with radius ε, and the semicircular arc C_R with radius R, as shown in Fig. 2.40. By assumption $F(z)$ is free of zeros within the closed contour so that $I_R \equiv 0$. In the limit as $R \to \infty$ and $\varepsilon \to 0$ the integral over the line segments approaches a CPV integral while the integrals c_ε^- and c_ε^+ each approach $i\pi$ times the residue at the respective poles. The net result can then be written as follows:

$$\begin{aligned} 0 &= P\int_{-\infty}^{\infty} \frac{\ln F(\omega)}{\omega_0^2 - \omega^2} d\omega + i\pi \frac{\ln F(-\omega_0)}{2\omega_0} + i\pi \frac{\ln F(\omega_0)}{-2\omega_0} \\ &\quad + \lim_{R\to\infty} \oint_{C_R} \frac{\ln F(z)}{\omega_0^2 - z^2} dz. \end{aligned} \tag{2.276}$$

In view of (2.274) for sufficiently large R the last integral may be bounded as follows:

$$\left| \oint_{C_R} \frac{\ln F(z)}{\omega_0^2 - z^2} dz \right| \leq constant \times \int_0^{\pi} \frac{k \ln R}{|\omega_0^2 - R^2 e^{i2\theta}|} R d\theta. \tag{2.277}$$

Since $\ln R < R$ for $R > 1$, the last integral approaches zero as $R \to \infty$ so that the contribution from C_R in (2.276) vanishes. Substituting from (2.273) into

the first three terms on the right of (2.276) and taking account of the fact that $\alpha(\omega)$ is even while $\theta(\omega)$ is odd, one obtains

$$0 = P\int_{-\infty}^{\infty} \frac{\alpha(\omega) + i\theta(\omega)}{\omega_0^2 - \omega^2} d\omega + i\pi \frac{\alpha(\omega_0) - i\theta(\omega_0)}{2\omega_0} + i\pi \frac{\alpha(\omega_0) + i\theta(\omega_0)}{-2\omega_0}$$

Observe that the terms on the right involving $\alpha(\omega_0)$ cancel while the integration involving $\theta(\omega)$ vanishes identically. As a result we can solve for $\theta(\omega_0)$ with the result

$$\theta(\omega_0) = \frac{2\omega_0}{\pi} P\int_0^{\infty} \frac{\alpha(\omega)}{\omega^2 - \omega_0^2} d\omega. \tag{2.278}$$

Proceeding similarly with the aid of the contour integral

$$I_R = \oint_{\Gamma_R} \frac{\ln F(z)}{z(\omega_0^2 - z^2)} dz \tag{2.279}$$

one obtains the formula

$$\alpha(\omega_0) = \alpha(0) - \frac{2\omega_0^2}{\pi} P\int_0^{\infty} \frac{\theta(\omega)}{\omega(\omega^2 - \omega_0^2)} d\omega. \tag{2.280}$$

It is worth noting that the assumed rate of decay at infinity in (2.274) is crucial to the vanishing of the contribution over the semicircular contour C_R in Fig. 2.40 and hence the validity of (2.278). Indeed if the decay of the FT is too rapid the contribution from C_R will not vanish and can in fact diverge as, e.g., for $A(\omega) = \exp(-\omega^2)$. Note that in this case (2.278) also diverges. This means that for an arbitrary $A(\omega)$ one cannot find a $\theta(\omega)$ such that $A(\omega)\exp -i\theta(\omega)$ has a causal inverse, i.e., an $f(t)$ that vanishes for negative t. What properties must $A(\omega)$ possess for this to be possible? An answer can be given if $A(\omega)$ is square integrable over $(-\infty, \infty)$. In that case the necessary and sufficient condition for a $\theta(\omega)$ to exist is the convergence of the integral

$$\int_{-\infty}^{\infty} \frac{|\ln A(\omega)|}{1 + \omega^2} d\omega < \infty,$$

which is termed the Paley–Wiener condition [15]. Note that it precludes $A(\omega)$ from being identically zero over any finite segment of the frequency axis.

2.4.4 Evaluation of Inverse FT Using Complex Variable Theory

The theory of functions of a complex variable provides a convenient tool for the evaluation of inverse Fourier transforms. The evaluation is particularly straightforward when the FT is a rational function. For example, let us evaluate

$$f(t) = \frac{1}{2\pi} \int_{-\infty}^{\infty} \frac{e^{i\omega t} d\omega}{\omega^2 + i\omega + 2}. \tag{2.281}$$

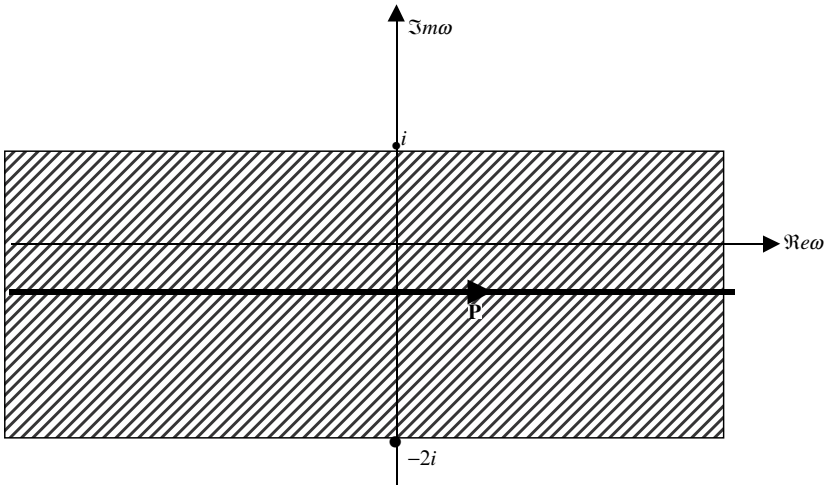

Figure 2.41: Deformation of integration path within the strip of analyticity

The only singularities of $F(\omega) = 1/(\omega^2 + i\omega + 2)$ in the complex ω plane are poles corresponding to the two simple zeros of $\omega^2 + i\omega + 2 = (\omega - i)(\omega + 2i) = 0$, namely $\omega_1 = i$ and $\omega_2 = -2i$. Therefore the integration path in (2.281) may be deformed away from the real axis into any path P lying within the strip of analyticity bounded by $-2 < \mathrm{Im}\,\omega < 1$, as depicted in Fig. 2.41. The exponential multiplying $F(\omega)$ decays for $t > 0$ in the upper half plane ($\mathrm{Im}\,\omega > 0$) and for $t < 0$ in the lower half plane ($\mathrm{Im}\,\omega < 0$). For $t > 0$ we form the contour integral

$$I_R = \oint e^{i\omega t} F(\omega) \frac{d\omega}{2\pi} \tag{2.282}$$

taken in the counterclockwise direction over the closed path formed by the linear segment $(-R, R)$ along P and the circular contour C_{R^+} lying in the upper half plane, as shown in Fig. 2.42. The residue evaluation at the simple pole at $\omega = i$ gives $I_R = e^{-t}/3$. As R is allowed to approach infinity the integral over the linear segment becomes just $f(t)$. Therefore

$$e^{-t}/3 = f(t) + \lim_{R\to\infty} \oint_{C_{R^+}} e^{i\omega t} F(\omega) \frac{d\omega}{2\pi}.$$

Since $F(\omega) \to 0$ as $\omega \to \infty$, and the exponential decays on C_{R^+} Jordan lemma (see Appendix A) applies so that in the limit the integral over C_{R^+} vanishes and we obtain $f(t) = e^{-t}/3$; $t > 0$. When $t < 0$ the contour integral (2.282) is evaluated in the clockwise direction over the closed path in Fig. 2.43 with a circular path C_{R^-} in the lower half plane. The residue evaluation at the simple pole at $\omega = -2i$ now gives $I_R = e^{2t}/3$ so that

$$e^{2t}/3 = f(t) + \lim_{R\to\infty} \oint_{C_{R^-}} e^{i\omega t} F(\omega) \frac{d\omega}{2\pi}.$$

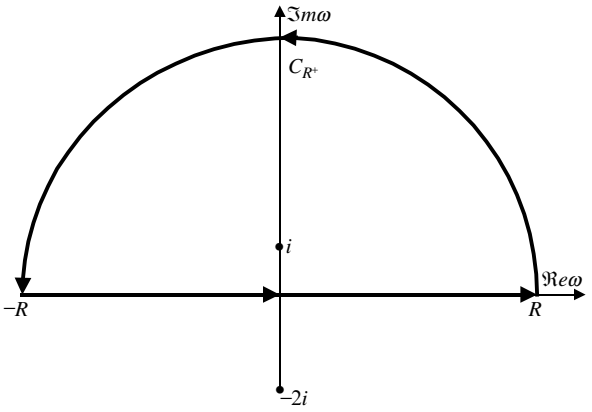

Figure 2.42: Integration contour for $t > 0$

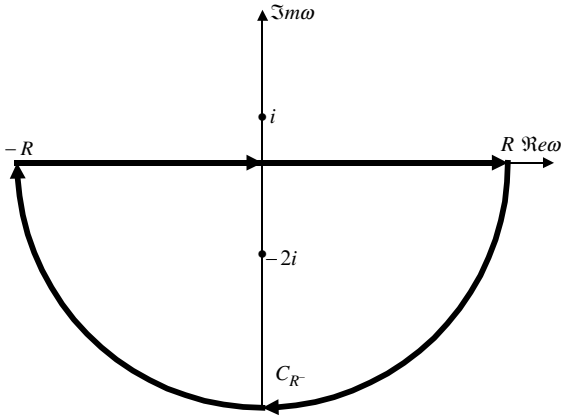

Figure 2.43: Integration contour for $t < 0$

Since now the exponential decays in the lower half plane, Jordan's lemma again guarantees that the limit of the integral over C_{R^-} vanishes. Thus the final result reads

$$f(t) = \begin{cases} e^{-t}/3 \ ; \ t \geq 0, \\ e^{2t}/3 \ ; \ t \leq 0. \end{cases} \tag{2.283}$$

This procedure is readily generalized to arbitrary rational functions. Thus suppose $F(\omega) = N(\omega)/D(\omega)$ with $N(\omega)$ and $D(\omega)$ polynomials in ω. We shall assume that[2] *degree* $N(\omega) <$ *degree* $D(\omega)$ so that $F(\omega)$ vanishes at infinity,

[2]If N and D are of the same degree, then the FT contains a delta function which can be identified by long division to obtain $N/D =$constant$+\hat{N}/D$, with degree $\hat{N} <$degree D. The inverse FT then equals constant$\times \delta(t) + \mathfrak{F}^{-1}\left(\hat{N}/D\right)$.

as required by the Jordan lemma. If $D(\omega)$ has no real zeros, then proceeding as in the preceding example we find that the inverse FT is given by the residue sums

$$f(t) = \begin{cases} i\sum_{k;\mathrm{Im}\,\omega_k>0} res\left[\frac{N(\omega)}{D(\omega)}e^{i\omega t}\right]_{\omega=\omega_k} & ;t \geq 0, \\ -i\sum_{k;\mathrm{Im}\,\omega_k<0} res\left[\frac{N(\omega)}{D(\omega)}e^{i\omega t}\right]_{\omega=\omega_k} & ;t \leq 0. \end{cases} \tag{2.284}$$

For example, suppose $F(\omega) = i/(\omega+2i)^2(\omega-i)$ which function has a double pole at $\omega = -2i$ and a simple pole at $\omega = i$. For $t \geq 0$ the contribution comes from the simple pole in the upper half plane and we get

$$f(t) = i\frac{ie^{-t}}{(i+2i)^2} = \frac{e^{-t}}{9} \; ; \; t \geq 0.$$

For $t \leq 0$ the double pole in the lower half plane contributes. Hence

$$\begin{aligned} f(t) &= -i\; i\frac{d}{d\omega}\frac{e^{i\omega t}}{(\omega-i)}\,|_{\omega=-2i} = \frac{(\omega-i)\,ite^{i\omega t} - e^{i\omega t}}{(\omega-i)^2}\,|_{\omega=-2i} \\ &= \frac{1-3t}{9}e^{-2t} \; ; \; t \leq 0. \end{aligned}$$

The case of $D(\omega)$ having real roots requires special consideration. First, if the order of any one of the zeros is greater than 1, the inverse FT does not exist.[3] On the other hand, as will be shown in the sequel, if the zeros are simple the inverse FT can computed by suitably modifying the residue formulas (2.284). Before discussing the general case we illustrate the procedure by a specific example. For this purpose consider the time function given by the inversion formula

$$f(t) = \frac{1}{2\pi}P\int_{-\infty}^{\infty}\frac{e^{i\omega t}}{(\omega^2-4)(\omega^2+1)}d\omega, \tag{2.285}$$

where $F(\omega) = 1/\,(\omega^2-4)(\omega^2+1)$ has two simple zeros at $\omega = \pm i$ and two at $\omega = \pm 2$ with the latter forcing a CPV interpretation of the integral. Before complementing (2.285) with a suitable contour integral it may be instructive to make the CPV form of (2.285) explicit. Thus

$$f(t) = \lim_{\varepsilon\to 0, R\to\infty} I_{R,\varepsilon} \tag{2.286}$$

with

$$I_{R,\varepsilon} = \frac{1}{2\pi}\left\{\int_{-R}^{-2-\varepsilon} + \int_{-2+\varepsilon}^{2-\varepsilon} + \int_{2+\varepsilon}^{R}\right\}\frac{e^{i\omega t}}{(\omega^2-4)(\omega^2+1)}d\omega. \tag{2.287}$$

[3]The corresponding time functions are unbounded at infinity and are best handled using Laplace transforms.

To evaluate (2.286) by residues we define a contour integral

$$\hat{I}_{R,\varepsilon} = \oint_{\Gamma} e^{i\omega t} F(\omega) \frac{d\omega}{2\pi} \tag{2.288}$$

over a closed path Γ that includes $I_{R,\varepsilon}$ as a partial contribution. For $t > 0$ the contour Γ is closed with the semicircle of radius R and includes the two semicircles c_{ε^+} and c_{ε^-} of radius ε centered, respectively, at $\omega = 2$ and $\omega = -2$, as shown in Fig. 2.44.

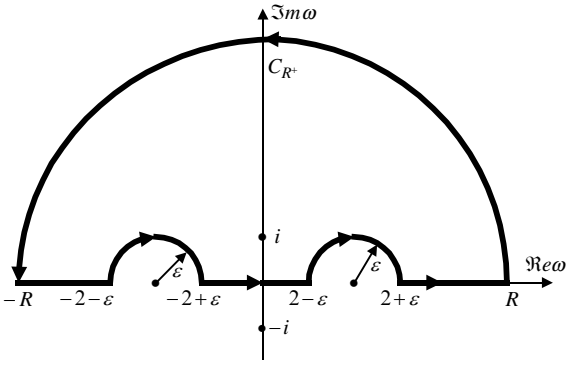

Figure 2.44: Integration contour for CPV integral

Writing (2.287) out in terms of its individual contributors we have

$$\hat{I}_{R,\varepsilon} = I_{R,\varepsilon} + \int_{c_{\varepsilon^-}} e^{i\omega t} F(\omega) \frac{d\omega}{2\pi} + \int_{c_{\varepsilon^+}} e^{i\omega t} F(\omega) \frac{d\omega}{2\pi} + \int_{C_{R^+}} e^{i\omega t} F(\omega) \frac{d\omega}{2\pi}. \tag{2.289}$$

Taking account of the residue contribution at $\omega = i$ we get for the integral over the closed path

$$\hat{I}_{R,\varepsilon} = i \frac{e^{i\omega t}}{(\omega^2 - 4)(2\omega)} \Big|_{\omega=i} = -\frac{e^{-t}}{10}.$$

As $\varepsilon \to 0$ the integrals over c_{ε^-} and c_{ε^-} each contribute $-2\pi i$ times one-half the residue at the respective simple pole (see Appendix A) and a $R \to \infty$ the integral over C_{R^+} vanishes by the Jordan lemma. Thus taking the limits and summing all the contributions in (2.289) we get

$$\begin{aligned} -\frac{e^{-t}}{10} &= f(t) - i \left[\frac{1}{2} \frac{e^{i\omega t}}{(2\omega)(\omega^2 + 1)} \Big|_{\omega=-2} + \frac{1}{2} \frac{e^{i\omega t}}{(2\omega)(\omega^2 + 1)} \Big|_{\omega=2} \right] \\ &= f(t) + \frac{1}{20} \sin(2t) \end{aligned}$$

and solving for $f(t)$,

$$f(t) = -\frac{1}{20} \sin(2t) - \frac{e^{-t}}{10} \quad ; \; t > 0. \tag{2.290}$$

For $t < 0$ we close the integration path $(-R, -2-\varepsilon) + c_{\varepsilon^-} + (-2+\varepsilon, 2-\varepsilon) + (2+\varepsilon, R)$ in Fig. 2.44 with a semicircular path in the lower half plane and carry out the integration in the clockwise direction. Now Γ encloses in addition to the pole at the pole at $\omega = -i$, the two poles at $\omega = \pm 2$. Hence

$$\begin{aligned}\hat{I}_{R,\varepsilon} &= -i\frac{e^{i\omega t}}{(\omega^2-4)(2\omega)}\,|_{\omega=-i} - i\left[\frac{e^{i\omega t}}{(2\omega)(\omega^2+1)}\,|_{\omega=-2} + \frac{e^{i\omega t}}{(2\omega)(\omega^2+1)}\,|_{\omega=2}\right] \\ &= -\frac{e^{-t}}{10} + \frac{1}{10}\sin(2t).\end{aligned}$$

Summing the contributions as in (2.289) and taking limits we get

$$-\frac{e^{t}}{10} + \frac{1}{10}\sin(2t) = f(t) - \frac{1}{10}\sin(2t).$$

Solving for $f(t)$ and combining with (2.290) we have for the final result

$$f(t) = -\frac{1}{20}\sin(2t)\ sign(t) - \frac{e^{-|t|}}{10}. \tag{2.291}$$

Note that we could also have used an integration contour with the semicircles c_{ε^-} and c_{ε^+} in the lower half plane. In that case we would have picked up the residue at $\omega = \pm 2$ for $t > 0$.

Based on the preceding example it is not hard to guess how to generalize (2.284) when $D(\omega)$ has simple zeros for real ω. Clearly for every real zero at $\omega = \omega_k$ we have to add the contribution $sign(t)\ (i/2)\, res\left[\frac{N(\omega)}{D(\omega)}e^{i\omega t}\right]|_{\omega=\omega_k}$. Hence we need to replace (2.284) by

$$\begin{aligned}f(t) &= (i/2)\ sign(t) \sum_{k;\mathrm{Im}\,\omega_k=0} res\left[\frac{N(\omega)}{D(\omega)}e^{i\omega t}\right]|_{\omega=\omega_k} \\ &+ \begin{cases} i\sum_{k;\mathrm{Im}\,\omega_k>0} res\left[\frac{N(\omega)}{D(\omega)}e^{i\omega t}\right]_{\omega=\omega_k} & ;t \geq 0, \\ -i\sum_{k;\mathrm{Im}\,\omega_k<0} res\left[\frac{N(\omega)}{D(\omega)}e^{i\omega t}\right]_{\omega=\omega_k} & ;t \leq 0. \end{cases}\end{aligned} \tag{2.292}$$

For example, for $F(\omega) = i\omega/(\omega_0^2 - \omega^2)$, the preceding formula yields $f(t) = \frac{1}{2}sign(t)\cos\omega_0 t$ and setting $\omega_0 = 0$ we find that the FT of $sign(t)$ is $2/i\omega$, in agreement with our previous result.

2.5 Time-Frequency Analysis

2.5.1 The Uncertainty Principle

A common feature shared by simple idealized signals such as rectangular, triangular, or Gaussian pulses is the inverse scaling relationship between signal duration and its bandwidth. Qualitatively a relationship of this sort actually holds for a large class of signals but its quantitative formulation ultimately

depends on the nature of the signal as well as on the definition of signal duration and bandwidth. A useful definition which also plays a prominent role not only in signal analysis but also in other areas where Fourier transforms are part of the basic theoretical framework is the so-called *rms* signal duration σ_t, defined by

$$\sigma_t^2 = \frac{1}{E}\int_{-\infty}^{\infty} (t - < t >)^2 \left| f(t) \right|^2 dt, \tag{2.293}$$

where

$$< t >= \frac{1}{E}\int_{-\infty}^{\infty} t \left| f(t) \right|^2 dt \tag{2.294}$$

and

$$E = \int_{-\infty}^{\infty} \left| f(t) \right|^2 dt \tag{2.295}$$

are the signal energies. We can accept this as a plausible measure of signal duration if we recall that σ_t^2 corresponds algebraically to the variance of a random variable with probability density $\left| f(t) \right|^2 / E$ wherein the statistical mean has been replaced by $< t >$. This quantity we may term "the average time of signal occurrence".[4] Although definition (2.295) holds formally for any signal (provided, of course, that the integral converges), it is most meaningful, just like the corresponding concept of statistical average in probability theory, when the magnitude of the signal is unimodal. For example, using these parameters a real Gaussian pulse takes the form

$$f(t) = \frac{\sqrt{E}}{\left(2\pi\sigma_t^2\right)^{1/4}} \exp - \frac{(t - < t >)^2}{4\sigma_t^2}. \tag{2.296}$$

To get an idea how the signal spectrum $F(\omega)$ affect the *rms* signal duration we first change the variables of integration in (2.293) from t to $t' = t - < t >$ and write it in the following alternative form:

$$\sigma_t^2 = \frac{1}{E}\int_{-\infty}^{\infty} t'^2 \left| f(t' + < t >) \right|^2 dt'. \tag{2.297}$$

Using the identities $\mathfrak{F}\{-itf(t)\} = dF(\omega)/d\omega$ and $\mathfrak{F}\{f(t + < t >)\} = F(\omega) \exp i\omega < t >$ we apply Parseval's theorem to (2.297) to obtain

$$\begin{aligned} \sigma_t^2 &= \frac{1}{2\pi E}\int_{-\infty}^{\infty} \left| \frac{d\left[F(\omega) \exp i\omega < t >\right]}{d\omega} \right|^2 d\omega \\ &= \frac{1}{2\pi E}\int_{-\infty}^{\infty} \left| \frac{dF(\omega)}{d\omega} + i < t > F(\omega) \right|^2 d\omega. \end{aligned} \tag{2.298}$$

This shows that the *rms* signal duration is a measure of the integrated fluctuations of the amplitude and phase of the signal spectrum. We can also express

[4] For a fuller discussion of this viewpoint see Chap. 3 in Leon Cohen, "Time-Frequency Analysis," Prentice Hall PTR, Englewood Cliffs, New Jersey (1995).

the average time of signal occurrence $< t >$ in terms of the signal spectrum by first rewriting the integrand in (2.294) as the product $tf(t)f(t)^*$ and using $\mathfrak{F}\{tf(t)\} = idF(\omega)/d\omega$ together with Parseval's theorem. This yields

$$< t >= \frac{1}{2\pi E}\int_{-\infty}^{\infty} i\frac{dF(\omega)}{d\omega}F^*(\omega)\,d\omega.$$

With $F(\omega) = A(\omega)\,e^{i\theta(\omega)}$ the preceding becomes

$$< t >= \frac{1}{2\pi E}\int_{-\infty}^{\infty}\left[-\theta'(\omega)\right]|F(\omega)|^2\,d\omega, \tag{2.299}$$

where $\theta'(\omega) = d\theta(\omega)/d\omega$. In 2.6.1 we shall identify the quantity $-\theta'(\omega)$ as the signal group delay. Equation then (2.299) states that the group delay, when averaged with the "density" function $|F(\omega)|^2/2\pi E$, is identical to the average time of signal occurrence.

We now apply the preceding definitions of spread and average location in the frequency domain. Thus the *rms* bandwidth σ_ω will be defined by

$$\sigma_\omega^2 = \frac{1}{2\pi E}\int_{-\infty}^{\infty}(\omega - < \omega >)^2\,|F(\omega)|^2\,d\omega, \tag{2.300}$$

where

$$< \omega >= \frac{1}{2\pi E}\int_{-\infty}^{\infty}\omega\,|F(\omega)|^2\,d\omega. \tag{2.301}$$

We can view $< \omega >$ as the center of mass of the amplitude of the frequency spectrum. Clearly for real signals $< \omega >\equiv 0$. By analogy with (2.297) we change the variable of integration in (2.300) to $\omega' = \omega - < \omega >$ and rewrite it as follows:

$$\sigma_\omega^2 = \frac{1}{2\pi E}\int_{-\infty}^{\infty}\omega'^2\,|F(\omega' + < \omega >)|^2\,d\omega \tag{2.302}$$

$\mathfrak{F}\{df(t)/dt\} = i\omega F(\omega)$ and Parseval's theorem obtain the dual to (2.295), viz.,

$$\begin{aligned}\sigma_\omega^2 &= \frac{1}{E}\int_{-\infty}^{\infty}\left|\frac{d\left[f(t)\exp -i < \omega > t\right]}{dt}\right|^2 dt \\ &= \frac{1}{E}\int_{-\infty}^{\infty}\left|\frac{df(t)}{dt} - i < \omega > f(t)\right|^2 dt.\end{aligned} \tag{2.303}$$

Thus the *rms* bandwidth increases in proportion to the norm of the rate of change of the signal. In other words, the more rapid the variation of the signal in a given time interval the greater the frequency band occupancy. This is certainly compatible with the intuitive notion of frequency as a measure of the number of zero crossings per unit time as exemplified, for instance, by signals of the form $\cos[\varphi(t)]$.

Again using $\mathfrak{F}\{df(t)/dt\} = i\omega F(\omega)$ and Parseval's theorem we transform (2.301) into

$$< \omega >= \frac{1}{E}\int_{-\infty}^{\infty} -i\frac{df(t)}{dt}f^*(t)\,dt.$$

If $f(t) = r(t) \exp i\psi(t)$ is an analytic signal, the preceding yields

$$< \omega >= \frac{1}{E} \int_{-\infty}^{\infty} \psi'(t) |f(t)|^2 dt, \tag{2.304}$$

where $\psi'(t) = d\psi(t)/dt$ is the instantaneous frequency. This equation provides another interpretation of $< \omega >$, viz., as the average instantaneous frequency with respect to the density $|f(t)|^2/E$, a result which may be considered a sort of dual to (2.299).

The *rms* signal duration and *rms* bandwidth obey a fundamental inequality, known as the uncertainty relationship, which we now proceed to derive. For this purpose let us apply the Schwarz inequality to the following two functions: $(t - < t >) f(t)$ and $df(t)/dt - i < \omega > f(t)$. Thus

$$\begin{aligned} & \int_{-\infty}^{\infty} (t - < t >)^2 |f(t)|^2 dt \int_{-\infty}^{\infty} \left| \frac{df(t)}{dt} - i < \omega > f(t) \right|^2 dt \\ \geq & \left| \int_{-\infty}^{\infty} (t - < t >) f^*(t) \left[\frac{df(t)}{dt} - i < \omega > f(t) \right] dt \right|^2. \end{aligned} \tag{2.305}$$

Substituting for the first two integrals in (2.305) the σ_t^2 and σ_ω^2 from (2.297) and (2.303), respectively, the preceding becomes

$$\begin{aligned} \sigma_t^2 \sigma_\omega^2 E^2 &\geq \left| \int_{-\infty}^{\infty} (t - < t >) f^*(t) \left[\frac{df(t)}{dt} - i < \omega > f(t) \right] dt \right|^2 \\ &= \left| \int_{-\infty}^{\infty} (t - < t >) f^*(t) \frac{df(t)}{dt} dt \right|^2, \end{aligned} \tag{2.306}$$

where in view of (2.294) we have set $\int_{-\infty}^{\infty} (t - < t >) |f(t)|^2 dt = 0$. We now integrate the last integral by parts as follows:

$$\begin{aligned} & \int_{-\infty}^{\infty} (t - < t >) f^*(t) \frac{df(t)}{dt} dt \\ = & (t - < t >) |f(t)|^2 \Big|_{-\infty}^{\infty} - \int_{-\infty}^{\infty} f(t) \frac{d[(t - < t >) f^*(t)]}{dt} dt \\ = & (t - < t >) |f(t)|^2 \Big|_{-\infty}^{\infty} - E - \int_{-\infty}^{\infty} (t - < t >) f(t) \frac{df^*(t)}{dt} dt. \end{aligned} \tag{2.307}$$

Because $f(t)$ has finite energy it must decay at infinity faster than $1/\sqrt{t}$ so that $(t - < t >) |f(t)|^2 \Big|_{-\infty}^{\infty} = 0$. Therefore after transposing the last term in (2.307) to the left of the equality sign we can rewrite (2.307) as follows:

$$\mathrm{Re} \left\{ \int_{-\infty}^{\infty} (t - < t >) f^*(t) \frac{df(t)}{dt} dt \right\} = -E/2. \tag{2.308}$$

Since the magnitude of a complex number is always grater or equal to the magnitude of its real part the right side of (2.306) equals at least $E^2/4$. Cancelling of E^2 and taking the square root of both sides result in

$$\sigma_t \sigma_\omega \geq \frac{1}{2}, \tag{2.309}$$

which is the promised uncertainty relation. Basically it states that simultaneous localization of a signal in time and frequency is not achievable to within arbitrary precision: the shorter the duration of the signal the greater its spectral occupancy and conversely. We note that except for a constant factor on the right (viz., Planck's constant), (2.309) is identical to the Heisenberg uncertainty principle in quantum mechanics where t and ω stand for any two canonically conjugate variables (e.g., particle position and particle momentum). When does (2.309) hold with equality? The answer comes from the Schwarz inequality (2.305) wherein equality can be achieved if and only if $(t- < t >) f(t)$ and $\frac{df(t)}{dt} - i < \omega > f(t)$ are proportional. Calling this proportionality constant $-\alpha$ results in the differential equation

$$\frac{df(t)}{dt} - i < \omega > f(t) + \alpha (t- < t >) f(t) = 0. \tag{2.310}$$

This is easily solved for $f(t)$ with the result

$$f(t) = A \exp\left\{ -\frac{\alpha}{2} (t- < t >)^2 + \frac{\alpha}{2} < t >^2 + i < \omega > t \right\}, \tag{2.311}$$

where A is a proportionality constant. Thus the optimum signal from the standpoint of simultaneous localization in time and frequency has the form of a Gaussian function. Taking account of the normalization (2.295) we obtain after a simple calculation

$$\alpha = 1/2\sigma_t^2, \; A = \sqrt{E/2\pi\sigma_t^2} \exp\left\{ - < t >^2 /2\sigma_t^2 \right\}. \tag{2.312}$$

2.5.2 The Short-Time Fourier Transform

Classical Fourier analysis draws a sharp distinction between the time and frequency domain representations of a signal. Recall that the FT of a signal of duration T can be computed only *after* the signal has been observed in its entirety. The computed spectrum furnishes the relative amplitude concentrations within the frequency band and the relative phases but information as to the times at which the particular frequency components have been added to the spectrum is not provided. Asking for such information is of course not always sensible particularly in cases of simple and essentially single scale signals such as isolated pulses. On the other hand for signals of long duration possessing complex structures such as speech, music, or time series of environmental parameters the association of particular spectral features with the times of their generation not only is meaningful but in fact also constitutes an essential step

in data analysis. A possible approach to the frequency/time localization problem is to multiply $f(t)$, the signal to be analyzed, by a sliding window function $g(t-\tau)$ and take the FT of the product. Thus

$$S(\omega,\tau)=\int_{-\infty}^{\infty} f(t)g(t-\tau)\,e^{-i\omega t}dt \tag{2.313}$$

whence in accordance with the FT inversion formula

$$f(t)g(t-\tau)=\frac{1}{2\pi}\int_{-\infty}^{\infty} S(\omega,\tau)\,e^{i\omega t}d\omega. \tag{2.314}$$

We can obtain an explicit formula for determining $f(t)$ from $S(\omega,\tau)$ by requiring that the window function satisfies

$$\int_{-\infty}^{\infty} |g(t-\tau)|^2\,d\tau=1 \tag{2.315}$$

for all t. For if we now multiply both sides of (2.314) by $g^*(t-\tau)$ and integrate with respect to τ we obtain

$$f(t)=\frac{1}{2\pi}\int_{-\infty}^{\infty}\int_{-\infty}^{\infty} S(\omega,\tau)\,g^*(t-\tau)\,e^{i\omega t}d\omega d\tau. \tag{2.316}$$

The two-dimensional function $S(\omega,\tau)$ is referred to as the short-time Fourier transform[5] (STFT) of $f(t)$ and (2.316) the corresponding inversion formula. The STFT can be represented graphically in various ways. The most common is the spectrogram, which is a two-dimensional plot of the magnitude of $S(\omega,\tau)$ in the $\tau\omega$ plane. Such representations are commonly used as an aid in the analysis of speech and other complex signals.

Clearly the characteristics of the STFT will depend not only on the signal but also on the choice of the window. In as much as the entire motivation for the construction of the STFT arises from a desire to provide simultaneous localization in frequency and time it is natural to choose for the window function the Gaussian function since, as shown in the preceding, it affords the optimum localization properties. This choice was originally made by Gabor [6] and the STFT with a Gaussian window is referred to as the Gabor transform. Here we adopt the following parameterization:

$$g(t)=\frac{2^{1/4}}{\sqrt{s}}e^{-\frac{\pi t^2}{s^2}}. \tag{2.317}$$

Reference to (2.311) and (2.312) shows that $\sigma_t=s/(2\sqrt{\pi})$. Using (2.142*) we have for the FT

$$G(\omega)=2^{1/4}\sqrt{s}e^{-s^2\omega^2/4\pi} \tag{2.318}$$

from which we obtain $\sigma_\omega=\sqrt{\pi}/s$ so that $\sigma_t\sigma_\omega=1/2$, as expected.

As an example, let us compute the Gabor transform of $\exp\left(\alpha t^2/2\right)$. We obtain

$$S(\omega,\tau)/\sqrt{s}=2^{1/4}\sqrt{\frac{\pi}{i\alpha s^2/2-\pi}}\exp-\frac{\left(\frac{2\pi\tau}{s}-i\omega s\right)^2}{4\left(i\alpha s^2/2-\pi\right)}-\frac{\pi\tau^2}{s^2}. \tag{2.319}$$

[5] Also referred to as the sliding-window Fourier transform

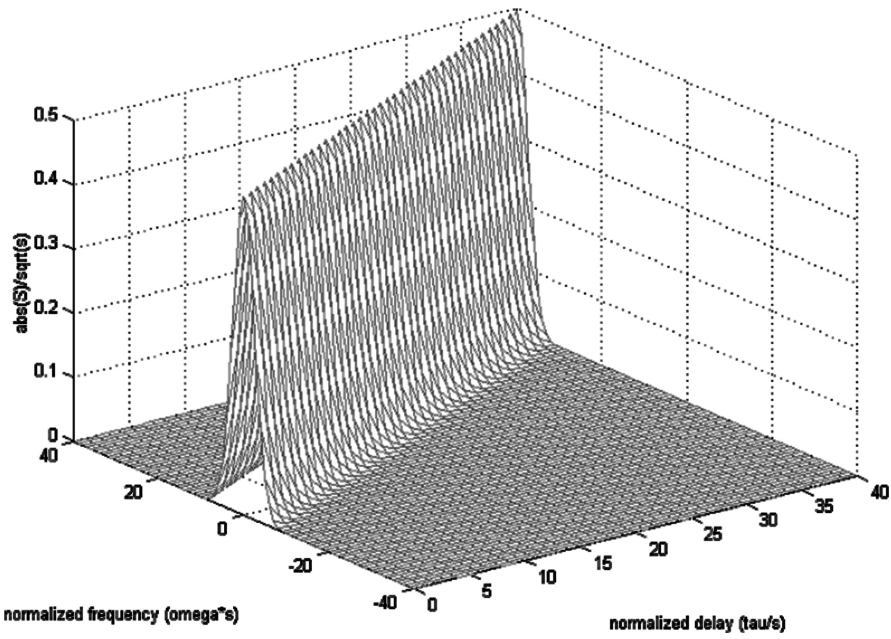

Figure 2.45: Magnitude of Gabor Transform of $\exp\left\{i\frac{1}{2}\alpha t^2\right\}$

A relief map of the magnitude of $S(\omega,\tau)/\sqrt{s}$ (spectrogram) as a function of the nondimensional variables τ/s (delay) and ωs (frequency) is shown in Fig. 2.45.

In this plot the dimensionless parameter $(1/2)\,\alpha s^2$ equals $1/2$. The map shows a single ridge corresponding to a straight line $\omega = \alpha\tau$ corresponding to the instantaneous frequency at time τ. As expected only positive frequency components are picked up by the transform. On the other hand, if instead we transform the real signal $\cos\left\{\frac{1}{2}\alpha t^2\right\}$, we get a plot as in Fig. 2.46. Since the cosine contains exponentials of both signs the relief map shows a second ridge running along the line $\omega = -\alpha\tau$ corresponding to negative instantaneous frequencies.

As a final example consider the signal plotted in Fig. 2.47. Even though this signal looks very much like a slightly corrupted sinusoid, it is actually comprised of a substantial band of frequencies with a rich spectral structure. This can be seen from Fig. 2.48 which shows a plot of the squared magnitude of the FT. From this spectral plot we can estimate the total signal energy and the relative contributions of the constitutive spectral components that make up the total signal but not their positions in the time domain. This information can be inferred from the Gabor spectrogram whose contour map is represented in Fig. 2.49. This spectrogram shows us that the spectral energy of the signal is in fact confined to a narrow sinuous band in the time-frequency plane. The width of this band is governed by the resolution properties of the sliding Gaussian window (5 sec. widths in this example) and its centroid traces out approximately the locus of the instantaneous frequency in the time-frequency plane.

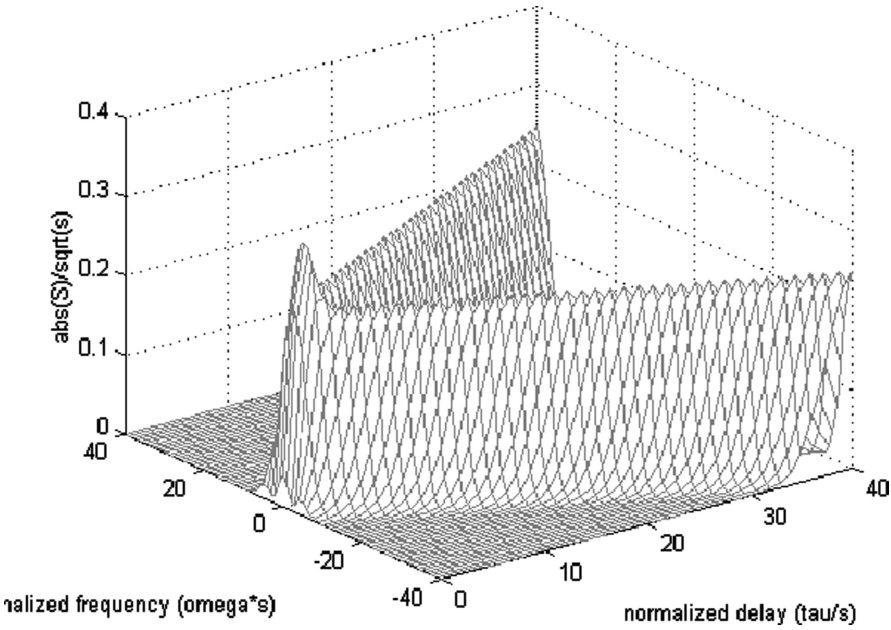

Figure 2.46: Magnitude of Gabor Transform of $\cos\left\{\frac{1}{2}\alpha t^2\right\}$

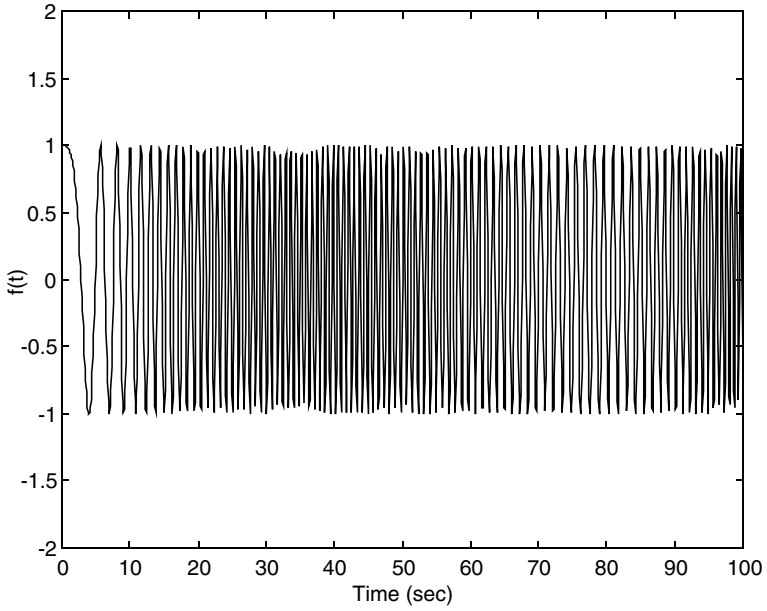

Figure 2.47: Constant amplitude signal comprising multiple frequencies

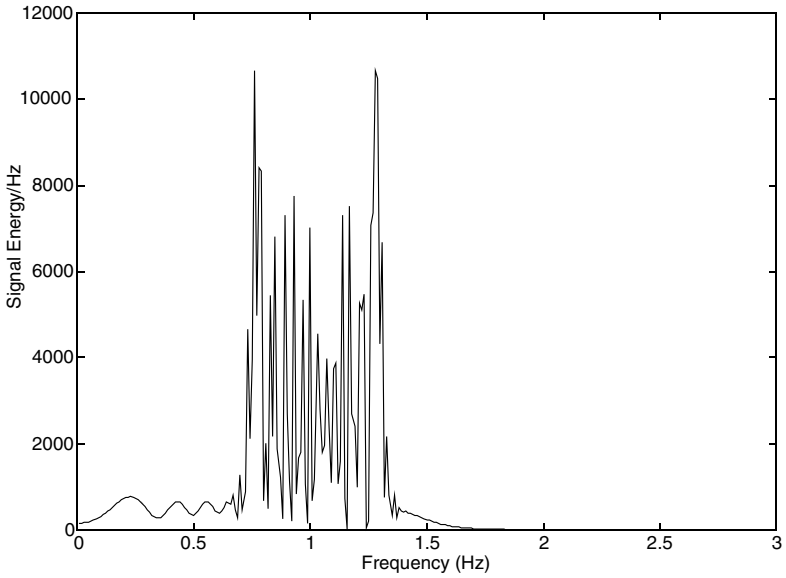

Figure 2.48: Squared magnitude of the FT of the signal in Fig. 2.47

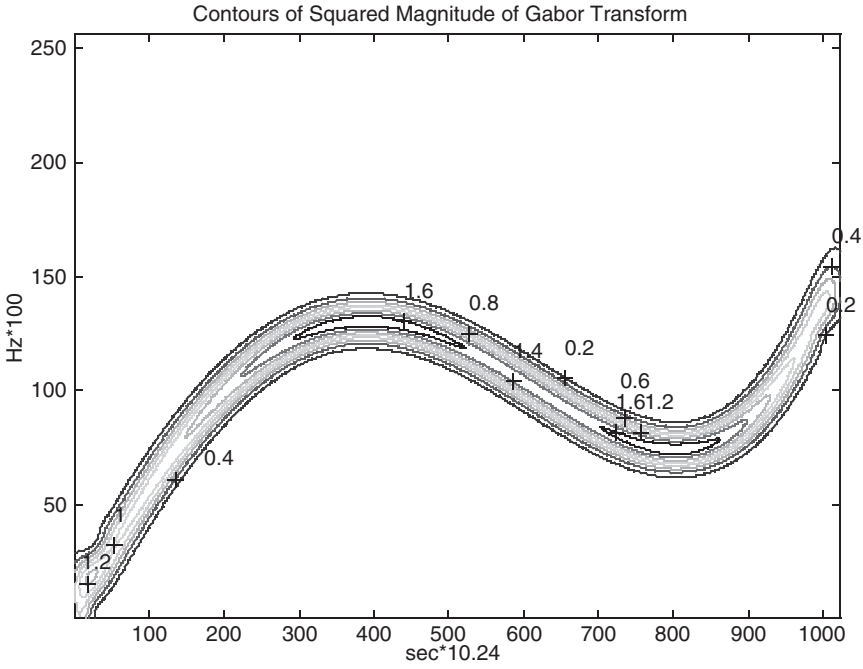

Figure 2.49: Contour map of the Gabor Transform of the signal in Fig. 2.48

2.6 Frequency Dispersion

2.6.1 Phase and Group Delay

In many physical transmission media the dominant effect on the transmitted signal is the distortion caused by unequal time delays experienced by different frequency components. In the frequency domain one can characterize such a transmission medium by the transfer function $e^{-i\psi(\omega)}$ where $\psi(\omega)$ is real. The FT $F(\omega)$ of the input signal $f(t)$ is then transformed into the FT $Y(\omega)$ of the output signal $y(t)$ in accordance with

$$Y(\omega) = e^{-i\psi(\omega)} F(\omega) . \tag{2.320}$$

The time domain representation of the output then reads

$$y(t) = \frac{1}{2\pi} \int_{-\infty}^{\infty} e^{i\omega t} e^{-i\psi(\omega)} F(\omega)\, d\omega \tag{2.321}$$

so that by Parseval's theorem the total energy of the output signal is identical to that of the input signal. However its spectral components are in general delayed by different amounts so that in the time domain the output appears as a distorted version of the input. The exceptional case arises whenever the transfer phase $\psi(\omega)$ is proportional to frequency for then with $\psi(\omega) = \omega T$ the output is merely a time delayed version of the input:

$$y(t) = f(t - T) . \tag{2.322}$$

Such distortionless transmission is attainable in certain special situations, the most notable of which is EM propagation through empty space. It may also be approached over limited frequency bands in certain transmission lines (coaxial cable, microstrip lines). In most practical transmission media however one has to count on some degree of phase nonlinearity with frequency, particularly as the signal bandwidth is increased. Clearly for any specific signal and transfer phase the quantitative evaluation of signal distortion can proceed directly via a numerical evaluation of (2.321). Nevertheless, guidance for such numerical investigations must be provided by a priori theoretical insights. For example, at the very minimum one should like to define and quantify measures of signal distortion. Fortunately this can usually be accomplished using simplified and analytically tractable models.

Let us first attempt to define the delay experienced by a typical signal. Because each spectral component of the signal will be affected by a different amount, it is sensible to first attempt to quantify the delay experienced by a typical narrow spectral constituent of the signal. For this purpose we conceptually subdivided the signal spectrum $F(\omega)$ into narrow bands, each of width $\Delta\omega$, as indicated in Fig. 2.50 (also shown is a representative plot of $\psi(\omega)$, usually referred to as the medium dispersion curve). The contribution to the output signal from such a typical band (shown shaded in the figure) is

$$y_n(t) = \Re e\{z_n(t)\} , \tag{2.323}$$

where

$$z_n(t) = \frac{1}{\pi} \int_{\omega_n - \Delta\omega/2}^{\omega_n + \Delta\omega/2} e^{i\omega t} e^{-i\psi(\omega)} F(\omega)\, d\omega \tag{2.324}$$

$z_n(t)$ is the corresponding analytic signal (assuming real $f(t)$ and $\psi(\omega) = -\psi(-\omega)$) and the integration is carried out over the shaded band in Fig. 2.50.

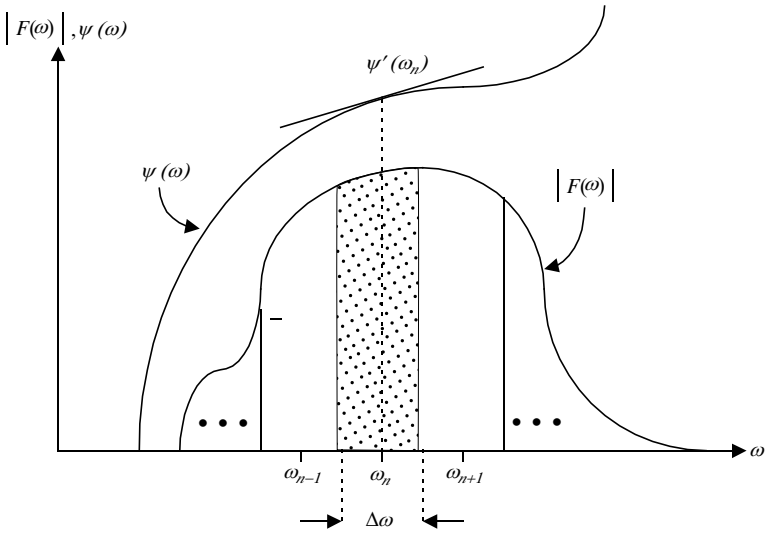

Figure 2.50: Group delay of signal component occupying a narrow frequency band

Clearly the complete signal $y(t)$ can be represented correctly by simply summing over the totality of such non-overlapping frequency bands, i.e.,

$$y(t) = \sum_n y_n(t). \tag{2.325}$$

For sufficiently small $\Delta\omega/\omega_n$ the phase function within each band may be approximated by

$$\psi(\omega) \sim \psi(\omega_n) + (\omega - \omega_n)\, \psi'(\omega_n), \tag{2.325*}$$

where $\psi'(\omega_n)$ is the slope of the dispersion curve at the center of the band in Fig. 2.50. If we also approximate the signal spectrum $F(\omega)$ by its value at the band center, (2.324) can be replaced by

$$z_n(t) \sim \frac{1}{\pi} F(\omega_n) \int_{\omega_n - \Delta\omega/2}^{\omega_n + \Delta\omega/2} e^{i\omega t} e^{-i\left[\psi(\omega_n) + (\omega - \omega_n)\psi'(\omega_n)\right]} d\omega.$$

After changing the integration variable to $\eta = \omega - \omega_n$ this becomes

$$z_n(t) \sim \frac{1}{\pi} F(\omega_n)\, e^{i(\omega_n t - \psi(\omega_n))} \int_{-\Delta\omega/2}^{\Delta\omega/2} e^{i\eta\left(t - \psi'(\omega_n)\right)} d\eta$$

$$= \quad 2iF(\omega_n)\, e^{i(\omega_n t - \psi(\omega_n))} \frac{\sin\left[\Delta\omega/2\left(t-\psi'(\omega_n)\right)\right]}{\pi\left(t-\psi'(\omega_n)\right)} \qquad (2.326)$$

and upon setting $F(\omega_n) = A(\omega_n)\, e^{i\theta(\omega_n)}$ the real signal (2.323) assumes the form

$$y_n(t) \sim A(\omega_n) \sin\left[\omega_n t + \theta(\omega_n) + \pi - \psi(\omega_n)\right] \frac{\sin\left[\Delta\omega/2\left(t-\psi'(\omega_n)\right)\right]}{\pi\left(t-\psi'(\omega_n)\right)} \qquad (2.327)$$

a representative plot of which is shown in Fig. 2.51. Equation (2.327) has the form of a sinusoidal carrier at frequency ω_n that has been phase shifted by

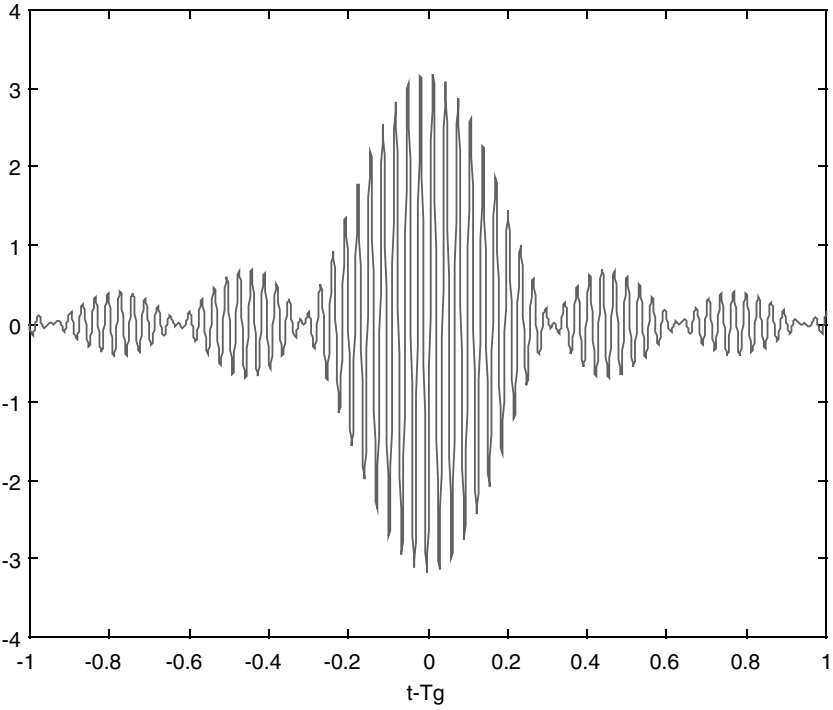

Figure 2.51: Plot of (2.327) for $\Delta\omega/2\theta'(\omega_n) = 10,\ \omega_n = 200rps$ and $A(\omega_n) = 1$

$\psi(\omega_n)$ radians. Note that the carrier is being modulated by an envelope in form of a sinc function delayed in time by $\psi'(\omega_n)$. Evidently this envelope is the time domain representation of the spectral components contained within the band $\Delta\omega$ all of which are undergoing the same time delay as a "group." Accordingly $\psi'(\omega_n)$ is referred to as the group delay (T_g) while the time (epoch) delay of the carrier $\theta(\omega_n)/\omega_n$ is referred to as the phase delay ($T\varphi$). One may employ these concepts to form a semi-quantitative picture of signal distortion by assigning to each narrow band signal constituent in the sum in (2.325) its own phase and group delay. Evidently if the dispersion curve changes significantly over the

signal bandwidth no single numerical measure of distortion is possible. Thus it is not surprising that the concept of group delay is primarily of value for signals having sufficiently narrow bandwidth. How narrow must $\Delta\omega$ be chosen for the representation (2.327) to hold? Clearly in addition to $\Delta\omega/\omega_n << 1$ the next term in the Taylor expansion in (2.325*) must be negligible by comparison with $(\omega - \omega_n)\,\psi'(\omega_n)$. Since $|\omega - \omega_n| \leq \Delta\omega/2$ this additional constraint translates into

$$\Delta\omega \ll \left| \frac{4\psi'(\omega_n)}{\psi''(\omega_n)} \right| \tag{2.328}$$

which evidently breaks down when $\psi'(\omega_n) = 0$.

2.6.2 Phase and Group Velocity

Phase and group delay are closely linked to phase and group velocities associated with wave motion. To establish the relationship we start with the definition of an the elementary wave

$$f(t, x) = f(t - x/v), \tag{2.329}$$

where t is time x, represents space, and v a constant. Considered as a function of

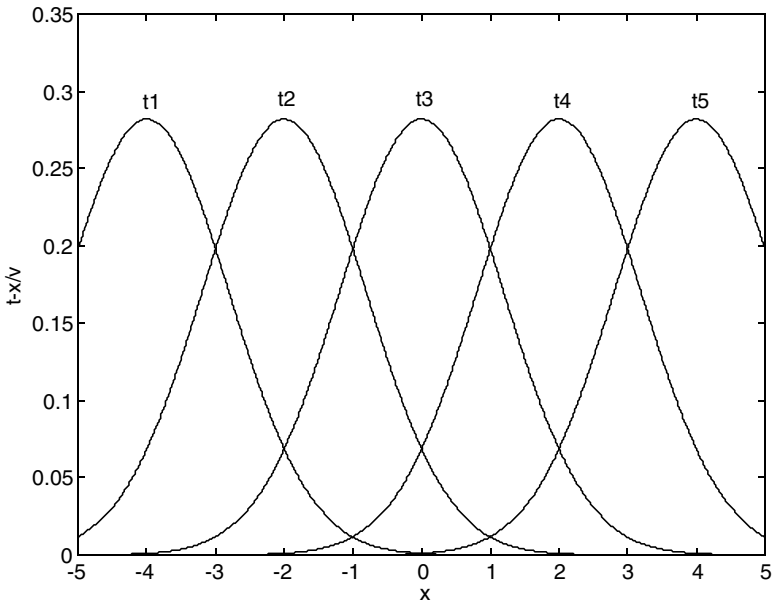

Figure 2.52: Self-preserving spatial pattern at successive instants of time ($t1 < t2 < t3 < t4 < t5$)

x which is sampled at discrete instances of time we can display it as in Fig. 2.52. Such a spatial display may be regarded as a sequence of snapshots of the function $f(\xi)$ which executes a continuous motion in the direction of the positive x-axis.

Clearly the speed of this translation may be defined unambiguously by the condition that the functional argument $t - x/v$ be maintained constant in time for a continuum of x. The derivative of the argument is then zero so that

$$\frac{dx}{dt} = v. \tag{2.330}$$

We take (2.330) as the *definition of* the velocity of the wave. Note that this definition is based entirely on the requirement that the functional form $f(\xi)$ be preserved exactly. This characterizes what is usually designated as dispersionless propagation. It is an idealization just as is distortionless transmission mentioned in the preceding subsection. Evidently as long as x is fixed the two concepts are identical as we see by setting $x/v = T$ in (2.322). In general the preservation of the waveform is approached only by narrow band signals. Hence we can again examine initially the propagation of a single sinusoid and appeal to Fourier synthesis to formulate the general case. For a time-harmonic signal the elementary wave function (2.329) reads

$$e^{i\omega(t-x/v(\omega))} = e^{i\omega t}e^{-i\beta(\omega)x}, \tag{2.331}$$

wherein we now allow the speed of propagation $v_\varphi(\omega)$ to depend on frequency. Note, however, that even though mathematically the functional forms (2.329) and (2.331) are identical, (2.331) represents an infinitely long periodic pattern so that we cannot really speak of the velocity of the translation of an identifiable space limited pattern (as, e.g., displayed in Fig. 2.52). Thus if we want to associate $v_\varphi(\omega)$ with the motion of some identifiable portion of the spatial pattern, we have only a phase reference at our disposal. Quite aptly then $v_\varphi(\omega)$ is referred to as the phase velocity. The quantity $\beta(\omega) = \omega/v(\omega)$ in (2.331) represents the propagation constant and may be taken as a fundamental characteristic of the propagation medium. The time domain representation of a general signal with spectrum $F(\omega)$ that has propagated through a distance x is obtained by multiplying (2.331) by $F(\omega)$ and taking the inverse FT. Thus

$$y(t,x) = \frac{1}{2\pi}\int_{-\infty}^{\infty} e^{i\omega t}e^{-i\beta(\omega)x}F(\omega)\,d\omega, \tag{2.332}$$

which is just (2.321) with the phase shift relabeled as $\beta(\omega)x$. Note that in the special case $\beta(\omega) = \omega/v$ and with v a constant (2.332) reduces to (2.329), i.e., the propagation is dispersionless. In the general case we proceed as in (2.326). After replacing $\psi(\omega)$ with $\beta(\omega)x$ in (2.327) we obtain

$$y_n(t,x) \sim A(\omega_n)\sin\left[\omega_n t + \theta(\omega_n) + \pi - \beta(\omega_n)x\right]\frac{\sin\left[\Delta\omega/2\left(t-\beta'(\omega_n)x\right)\right]}{\pi\left(t-\beta'(\omega_n)x\right)}. \tag{2.333}$$

Unlike (2.327), (2.333) depends on both space and time. It does not, however, have the same simple interpretation as the wavefunction defined in (2.329) because the speed of propagation of the carrier phase and the envelope differ. Thus while the carrier phase moves with the phase velocity

$$v_{\varphi n} = \omega_n/\beta(\omega_n) \tag{2.334}$$

the envelope[6] moves with velocity

$$v_{gn} = 1/\beta'(\omega_n) = \frac{d\omega}{d\beta}\Big|_{\beta=\beta(\omega_n).} \tag{2.335}$$

The latter is referred to as the group velocity and is the speed of propagation of the energy contained within the frequency band $\Delta\omega$ in Fig. 2.50. By contrast, the phase velocity has generally no connection with energy transport but represents merely the translation of a phase reference point.

2.6.3 Effects of Frequency Dispersion on Pulse Shape

Thus far we have not explicitly addressed quantitative measures of signal distortion. For this purpose consider a pulse with a (baseband) spectrum $P(\omega)$ most of whose energy is confined to the nominal frequency band $(-\Omega, \Omega)$. The pulse, after having been modulated by a carrier of frequency ω_0, propagates through a medium of length L characterized by the propagation constant $\beta(\omega)$. The output signal occupies the frequency band $\omega_0 - \Omega < \omega < \omega_0 + \Omega$ with and has the time domain representation

$$\begin{aligned} y(t,\omega_0) &= \Re e\left\{2\int_{\omega_0-\Omega}^{\omega_0+\Omega}(1/2)P(\omega-\omega_0)\,e^{-i\beta(\omega)L}e^{i\omega t}\frac{d\omega}{2\pi}\right\} \\ &= \Re e\left\{e^{i\omega_0 t}\int_{-\Omega}^{\Omega}P(\eta)\,e^{-i\beta(\eta+\omega_0)L}e^{i\eta t}\frac{d\eta}{2\pi}\right\}, \end{aligned} \tag{2.336}$$

where we have assumed that the pulse is a real function. From the last expression we identify the complex baseband output signal as

$$s(t) = \int_{-\Omega}^{\Omega}P(\eta)\,e^{-i\beta(\eta+\omega_0)L}e^{i\eta t}\frac{d\eta}{2\pi}. \tag{2.337}$$

Irrespective of the nature of the pulse spectrum the frequencies at the band center $\omega = \omega_0$ will be delayed by the group delay $\beta'(\omega_0)L$. In order to focus on pulse distortion (e.g., pulse broadening) it will be convenient to subtract this delay. We do this by initially adding and subtracting $\eta\beta'(\omega_0)L$ from the phase of the integrand in (2.337) as follows:

$$s(t) = \int_{-\Omega}^{\Omega}P(\eta)\,e^{-i\left[\beta(\eta+\omega_0)-\beta'(\omega_0)\eta\right]L}e^{i\eta\left[t-\beta'(\omega_0)L\right]}\frac{d\eta}{2\pi}. \tag{2.338}$$

Observe that this integral defines the time delayed version of $\hat{s}(t)$ defined by

$$s(t) = \hat{s}\left[t - \beta'(\omega_0)L\right] \tag{2.339}$$

[6] When the emphasis is on wave propagation rather than signal analysis, it is customary to represent the wavefunction (2.332) as a superposition of propagation constants β, in terms of the so-called wavenumber spectrum. In that case the envelope in (2.333) (usually referred to as a wavepacket) assumes the form

$$\frac{\sin\left[\Delta\beta/2\left(v_{gn}t-x\right)\right]}{v_{gn}\pi\left(v_{gn}t-x\right)},$$

where $\Delta\beta$ is the range of propagation constants corresponding to the frequency band $\Delta\omega$.

or, explicitly, by

$$\hat{s}(t) = \int_{-\Omega}^{\Omega} P(\eta)\, e^{-i\left[\beta(\eta+\omega_0)-\beta'(\omega_0)\eta\right]L} e^{i\eta t} \frac{d\eta}{2\pi}. \tag{2.340}$$

We shall obtain an approximation to this integral under the following two assumptions:

$$\omega_0 \gg \Omega, \tag{2.341a}$$

$$\Omega^2 \beta''(\omega_0) L \gg 1. \tag{2.341b}$$

The first of these is the conventional narrow band approximation while the second implies a long propagation path.[7] Thus in view of (2.341a) we may approximate $\beta(\eta+\omega_0)$ by

$$\beta(\eta+\omega_0) \sim \beta(\omega_0) + \beta'(\omega_0)\eta + \frac{1}{2}\beta''(\omega_0)\eta^2. \tag{2.342}$$

Substituting this into (2.340) leads to the following series of algebraic steps:

$$\begin{aligned}
\hat{s}(t) &\sim e^{-i\beta(\omega_0)L} \int_{-\Omega}^{\Omega} P(\eta)\, e^{-i\frac{L}{2}\beta''(\omega_0)\eta^2} e^{i\eta t} \frac{d\eta}{2\pi} \\
&= e^{-i\beta(\omega_0)L} \int_{-\Omega}^{\Omega} P(\eta)\, e^{-i\frac{L}{2}\beta''(\omega_0)\Omega^2\left[\left(\frac{\eta}{\Omega}\right)^2 - 2\left(\frac{\eta}{\Omega}\right)\left(\frac{t}{\Omega\beta''(\omega_0)L}\right)\right]} \frac{d\eta}{2\pi} \\
&= \Omega e^{-i\beta(\omega_0)L} \int_{-1}^{1} P(\nu\Omega)\, e^{-i\frac{L}{2}\beta''(\omega_0)\Omega^2\left[\nu^2 - 2\nu\left(\frac{t}{\Omega\beta''(\omega_0)L}\right)\right]} \frac{d\nu}{2\pi} \\
&= \Omega e^{-i\beta(\omega_0)L} e^{-i\frac{t^2}{2L\beta''(\omega_0)}} \int_{-1}^{1} P(\nu\Omega)\, e^{-i\frac{L}{2}\beta''(\omega_0)\Omega^2\left[\nu - \frac{t}{\Omega\beta''(\omega_0)L}\right]^2} \frac{d\nu}{2\pi} \\
&= \Omega e^{-i\beta(\omega_0)L} e^{-i\frac{t^2}{2L\beta''(\omega_0)}} \\
&\qquad \int_{-1-t/\Omega\beta''(\omega_0)L}^{1-t/\Omega\beta''(\omega_0)L} P\left[x\Omega + t/\beta''(\omega_0)L\right] e^{-i\frac{L}{2}\beta''(\omega_0)\Omega^2 x^2} \frac{dx}{2\pi}.
\end{aligned} \tag{2.343}$$

Since we are interested primarily in assessing pulse distortion the range of the time variable of interest is on the order of $t \sim 1/\Omega$ we have in view of (2.341b)

$$t/\Omega\beta''(\omega_0)L \ll 1\ . \tag{2.344}$$

Consequently the limits in the last integral in (2.343) may be replaced by $-1, 1$. Again in view of (2.341b) we may evaluate this integral by appealing to the principle of stationary phase. Evidently the point of stationary phase is at $x = 0$ which leads to the asymptotic result

$$\hat{s}(t) \sim \frac{1}{\sqrt{2\pi\left|\beta''(\omega_0)\right|L}} e^{-i\pi/4 sign\left[\beta''(\omega_0)\right]} e^{-i\beta(\omega_0)L} e^{-i\frac{t^2}{2L\beta''(\omega_0)}} P\left(\frac{t}{\beta''(\omega_0)L}\right). \tag{2.345}$$

[7] Note (2.341b) necessarily excludes the special case $\beta''(\omega_0) = 0$.

In many applications (e.g., intensity modulation in fiber optic communication systems) only the pulse envelope is of interest. In that case (2.345) assumes the compact form

$$|\hat{s}(t)|^2 \sim \frac{1}{2\pi \left|\beta''(\omega_0)\right| L} \left| P\left(\frac{t}{\beta''(\omega_0) L}\right)\right|^2 \tag{2.346}$$

Parseval's theorem tells us that the energies of the input and output signals must be identical. Is this still the case for the approximation (2.346)? Indeed it is as we verify by a direct calculation:

$$\begin{aligned}\int_{-\infty}^{\infty} |\hat{s}(t)|^2 dt &= (1/2\pi \left|\beta''(\omega_0)\right| L) \int_{-\infty}^{\infty} \left|P\left(t/\beta''(\omega_0) L\right)\right|^2 dt \\ &= \frac{1}{2\pi} \int_{-\infty}^{\infty} |P(\omega)|^2 d\omega \equiv \frac{1}{2\pi} \int_{-\Omega}^{\Omega} |P(\omega)|^2 d\omega.\end{aligned}$$

Equation (2.346) states that the envelope of a pulse propagating over a sufficiently long path assumes the shape of its Fourier transform wherein the timescale is determined only by the path length and the second derivative of the propagation constant at the band center. For example, for a pulse of unit amplitude and duration T we obtain

$$|\hat{s}(t)|^2 \sim 4 \frac{\sin^2\left(\frac{tT}{2\beta''(\omega_0)L}\right)}{\left(\frac{t}{\beta''(\omega_0)L}\right)^2}$$

giving a peak-to-first null pulsewidth of

$$T_L = \left|\frac{2\pi\beta''(\omega_0) L}{T}\right|. \tag{2.347}$$

In optical communications pulse broadening is usually described by the group index $N(\omega)$ defined as the ratio of the speed of light in free space to the group velocity in the medium:

$$N(\omega) = \frac{c}{v_g(\omega)} = c\beta'(\omega). \tag{2.348}$$

Expressed in terms of the group index the pulse width in (2.347) reads

$$T_L = \left|\frac{2\pi L}{cT} \frac{d}{d\omega} N(\omega)\,|_{\omega=\omega_0}\right|. \tag{2.349}$$

In view of (2.341b) these results break down whenever $\beta''(\omega_0) = 0$, i.e., at the inflection points (if they exist) of the dispersion curve. To include the case of inflection points requires the retention of the third derivative in Taylor expansion (2.342), i.e.,

$$\beta(\eta + \omega_0) \sim \beta(\omega_0) + \beta'(\omega_0)\eta + \frac{1}{2}\beta''(\omega_0)\eta^2 + \frac{1}{6}\beta'''(\omega_0)\eta^3 \tag{2.350}$$

so that

$$\hat{s}(t) \sim e^{-i\beta(\omega_0)L} \int_{-\Omega}^{\Omega} P(\eta)\, e^{-i\frac{L}{2}\beta''(\omega_0)\eta^2 - i\frac{L}{6}\beta'''(\omega_0)\eta^3} e^{i\eta t} \frac{d\eta}{2\pi}. \tag{2.351}$$

We shall not evaluate (2.351) for general pulse shapes but confine our attention to a Gaussian pulse. In that case we may replace the limits in (2.351) by $\pm\infty$ and require only that (2.341a) hold but not necessarily (2.341b). Using the parameterization in (2.296) we have

$$p(t) = \frac{2^{1/4}}{\sqrt{T}} e^{-\frac{\pi t^2}{T^2}}, \tag{2.352}$$

where we have relabeled the nominal pulse width s by T. The corresponding FT then reads

$$P(\omega) = 2^{1/4}\sqrt{T} e^{-T^2\omega^2/4\pi} \tag{2.353}$$

so that (2.351) assumes the form

$$\begin{aligned} \hat{s}(t) &\sim 2^{1/4}\sqrt{T} e^{-i\beta(\omega_0)L} \int_{-\infty}^{\infty} e^{-T^2\eta^2/4\pi} e^{-i\frac{L}{2}\beta''(\omega_0)\eta^2 - i\frac{L}{6}\beta'''(\omega_0)\eta^3} e^{i\eta t} \frac{d\eta}{2\pi} \\ &= 2^{1/4}\sqrt{T} e^{-i\beta(\omega_0)L} \int_{-\infty}^{\infty} e^{-i\frac{L\beta'''(\omega_0)}{6}\left[\eta^3 + B\eta^2 - C\eta\right]} \frac{d\eta}{2\pi}, \end{aligned} \tag{2.354}$$

where

$$B = \frac{3\beta''(\omega_0)}{\beta'''(\omega_0)} - i\frac{3T^2}{2\pi L\beta'''(\omega_0)}, \tag{2.355a}$$

$$C = \frac{6t}{L\beta'''(\omega_0)}. \tag{2.355b}$$

Changing the variable of integration to z via $\eta = z - B/3$ eliminates the quadratic term in the polynomial in the exponential (2.354) resulting in

$$\eta^3 + B\eta^2 - C\eta = z^3 - z\left(B^2/3 + C\right) + (2/27)B^3 + BC/3.$$

Because of the analyticity of the integrand the integration limits in (2.354) may kept at $\pm\infty$. A subsequent change of the integration from z to $w = \left[L\beta'''(\omega_0)/2\right]^{1/3} z$ transforms (2.354) into

$$\begin{aligned} \hat{s}(t) \sim\ & 2^{1/4}\sqrt{T} e^{-i\beta(\omega_0)L} e^{-i\frac{\beta'''(\omega_0)L}{6}\left[(2/27)B^3 + BC/3\right]} \\ & \left\{\frac{\beta'''(\omega_0)L}{2}\right\}^{-1/3} Ai\left\{-\left[\frac{\beta'''(\omega_0)L}{2}\right]^{2/.3}\left(B^2/9 + C/3\right)\right\}, \end{aligned} \tag{2.356}$$

where $Ai(x)$ is the Airy function defined by the integral

$$Ai(x) = \frac{1}{2\pi}\int_{-\infty}^{\infty} e^{-i\left(w^3/3 + xw\right)} dw. \tag{2.357}$$

The interpretation of (2.356) will be facilitated if we introduce the following dimensionless parameters:

$$q = \frac{\beta''(\omega_0)\,T}{\beta'''(\omega_0)}, \tag{2.358a}$$

$$p = \frac{\beta'''(\omega_0)\,L}{T^3}, \tag{2.358b}$$

$$\chi = 2qp = \frac{2\beta''(\omega_0)\,L}{T^2}. \tag{2.358c}$$

Introducing these into (2.357) we obtain

$$\begin{aligned}\hat{s}(t) \sim\ & 2^{1/4}(1/\sqrt{T})e^{-i\beta(\omega_0)L}e^{-i\left\{\frac{\chi q^2}{6}\left(1-\frac{i}{\pi\chi}\right)\left[\left(1-\frac{i}{\pi\chi}\right)^2+\frac{6}{\chi q}\left(\frac{t}{T}\right)\right]\right\}} \\ & (p/2)^{-1/3}\,Ai\left\{-q^2\left(\frac{p}{2}\right)^{2/3}\left[\left(1-\frac{i}{\pi\chi}\right)^2+4\frac{t}{q\chi T}\right]\right\}. \end{aligned} \tag{2.359}$$

Let us first examine this expression for the case in which the third derivative term in (2.350) can be neglected. Clearly this is tantamount to dropping the cubic term in (2.351). The integral then represents the FT of a Gaussian function and can be evaluated exactly. On the other hand, from the definition of q in (2.358a) we note that $\beta'''(\omega_0) \to 0$ and $\beta''(\omega_0) \neq 0$ correspond to $q \to \infty$. Hence we should be able to obtain the same result by evaluating (2.359) in the limit as $q \to \infty$. We do this with the aid of the first-order asymptotic form of the Airy function for large argument the necessary formula for which is given in [1]. It reads

$$Ai(-z) \sim \pi^{-1/2}z^{-1/4}\sin(\zeta+\frac{\pi}{4}), \tag{2.360}$$

where

$$\zeta = \frac{2}{3}z^{3/2} \quad ; \quad |\arg(z)| < \pi. \tag{2.361}$$

Thus we obtain for[8] $|q| \sim \infty$

$$\begin{aligned} & (p/2)^{-1/3}\,Ai\left\{-q^2\left(\frac{p}{2}\right)^{2/.3}\left[\left(1-\frac{i}{\pi\chi}\right)^2+4\frac{t}{q\chi T}\right]\right\} \\ \sim\ & -i\left[\pi\chi(1-\frac{i}{\pi\chi})\right]^{-1/2} \\ & \left(\begin{array}{c} \exp\left\{i\,(p/3)\,q^3\left[\left(1-\frac{i}{\pi\chi}\right)^2+4\frac{t}{q\chi T}\right]^{3/2}+i\frac{\pi}{4}\right\} \\ -\exp\left\{-i\,(p/3)\,q^3\left[\left(1-\frac{i}{\pi\chi}\right)^2+4\frac{t}{q\chi T}\right]^{3/2}-i\frac{\pi}{4}\right\} \end{array}\right), \end{aligned} \tag{2.362}$$

[8] q is real but may be of either sign.

where in the algebraic term corresponding to $z^{-1/4}$ in (2.360) we have dropped the term $o(1/q)$. Next we expand the argument of the first exponentials term in (2.362) as follows:

$$\begin{aligned}
& i\left(\chi q^2/6\right)\left[\left(1-\frac{i}{\pi\chi}\right)^2+4\frac{t}{q\chi T}\right]^{3/2} \\
= \; & i\left(\chi q^2/6\right)\left(1-\frac{i}{\pi\chi}\right)^3\left[1+4\frac{t}{q\chi T\left(1-\frac{i}{\pi\chi}\right)^2}\right]^{3/2} \\
= \; & i\left(\chi q^2/6\right)\left(1-\frac{i}{\pi\chi}\right)^3 \\
& \left[1+6\frac{t}{q\chi T\left(1-\frac{i}{\pi\chi}\right)^2}+6\frac{t^2}{(q\chi T)^2\left(1-\frac{i}{\pi\chi}\right)^4}+o(1/q^3)\right] \\
= \; & i\left(\chi q^2/6\right)\left(1-\frac{i}{\pi\chi}\right)^3+iq\frac{t}{T}\left(1-\frac{i}{\pi\chi}\right) \\
& +i\frac{t^2}{\chi T^2}\left(1-\frac{i}{\pi\chi}\right)^{-1}+o(1/q). \qquad (2.363)
\end{aligned}$$

In identical fashion we can expand the argument of the second exponential which would differ from (2.363) only by a minus sign. It is not hard to show that for sufficiently large $|q|$ is real part will be negative provided

$$\chi^2 > \frac{1}{3\pi^2}. \qquad (2.364)$$

In that case the second exponential in (2.362) asymptotes to zero and may be ignored. Neglecting the terms $o(1/q)$ in (2.363) we now substitute (2.362) into (2.359) and note that the first two terms in the last line of (2.363) cancel against the exponential in (2.359). The final result then reads

$$\begin{aligned}
\hat{s}\,(t) \; & \sim \; 2^{1/4}(1/\sqrt{T})e^{-i\beta(\omega_0)L} \\
& \left\{-i\left[\pi\chi(1-\frac{i}{\pi\chi})\right]^{-1/2}\right\}\exp\left\{i\frac{t^2}{\chi T^2}\left(1-\frac{i}{\pi\chi}\right)^{-1}+i\frac{\pi}{4}\right\} \\
& = \; 2^{1/4}(1/\sqrt{T})e^{-i\beta(\omega_0)L}\left(1+i\pi\chi\right)^{-1/2}\exp-\frac{\pi t^2}{T^2}\left(1+i\pi\chi\right)^{-1}. \qquad (2.365)
\end{aligned}$$

For the squared magnitude of the pulse envelope we get

$$|\hat{s}\,(t)|^2 \sim \frac{\sqrt{2}}{T}\left(1+\pi^2\chi^2\right)^{-1/2}\exp-\frac{\pi t^2}{(T^2/2)\left(1+\pi^2\chi^2\right)}. \qquad (2.366)$$

The nominal duration of this Gaussian signal may be defined by $(T/2\sqrt{\pi})$ $\sqrt{1+\pi^2\chi^2}$ so that χ plays the role of a pulse-stretching parameter. When $\chi \gg 1$ (2.366) reduces to

$$|\hat{s}(t)|^2 \sim \frac{\sqrt{2}}{\pi\chi T}\exp -\frac{2t^2}{\pi T^2\chi^2} = \frac{T}{\pi\sqrt{2}\beta''(\omega_0)L}\exp -\frac{T^2t^2}{2\pi\beta''(\omega_0)L}. \quad (2.367)$$

The same result also follows more directly from the asymptotic form (2.346) as is readily verified by the substitution of the FT of the Gaussian pulse (2.353) into (2.346). Note that with $\chi = 0$ in (2.366) we recover the squared magnitude of the original (input) Gaussian pulse (2.352). Clearly this substitution violates our original assumption $|q| \sim \infty$ under which (2.366) was derived for in accordance with (2.358) $\chi = 0$ implies $q = 0$. On the other hand if $\beta'''(\omega_0)$ is taken to be *identically zero* (2.366) is a valid representation of the pulse envelope for *all values of* χ. This turns out to be the usual assumption in the analysis of pulse dispersion effects in optical fibers. In that case formula (2.366) can be obtained directly from (2.351) by simply completing the square in the exponential and integrating the resulting Gaussian function. When $\beta'''(\omega_0) \neq 0$ with q arbitrary numerical calculations of the output pulse can be carried out using (2.359). For this purpose it is more convenient to eliminate χ in favor of the parameters p and q. This alternative form reads

$$\begin{aligned}\hat{s}(t) \quad &\sim \quad 2^{1/4}(1/\sqrt{T})e^{-i\beta(\omega_0)L}e^{-i\left\{\frac{p}{3}\left(q-\frac{i}{2\pi p}\right)\left[\left(q-\frac{i}{2\pi p}\right)^2+\frac{3}{p}\left(\frac{t}{T}\right)\right]\right\}} \\ &\quad (|p|/2)^{-1/3}\,Ai\left\{-\left(\frac{|p|}{2}\right)^{2/3}\left[\left(q-\frac{i}{2\pi p}\right)^2+2\frac{t}{pT}\right]\right\}. \quad (2.368)\end{aligned}$$

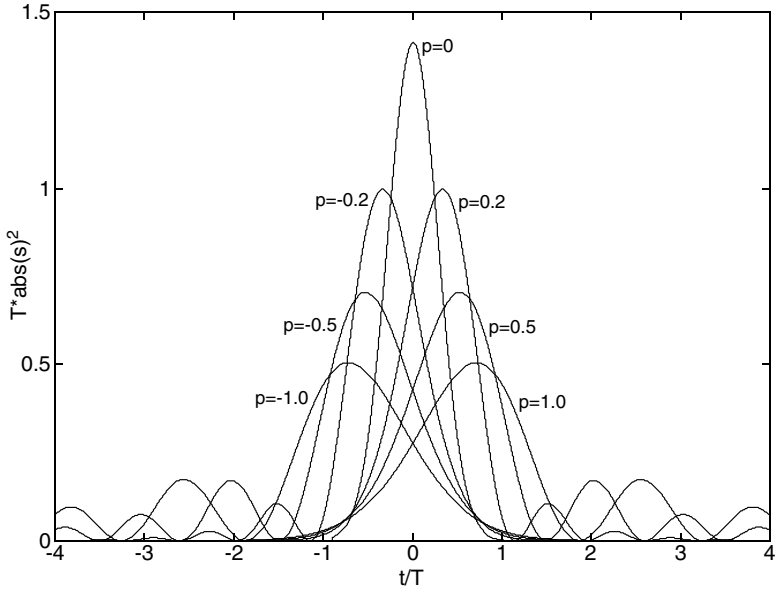

Figure 2.53: Distortion of Gaussian pulse envelope by cubic phase nonlinearities in the propagation constant

To assess the influence of the third derivative of the phase on the pulse envelope we set $q = 0$ and obtain the series of plots for several values of p as shown in Fig. 2.53. The center pulse labeled $p = 0$ corresponds to the undistorted Gaussian pulse ($\chi = 0$ in (2.366)). As p increases away from zero the pulse envelope broadens with a progressive increase in time delay. For sufficiently large p the envelope will tend toward multimodal quasi-oscillatory behavior the onset of which is already noticeable for p as low as 0.2. For negative p the pulse shapes are seen to be a mirror images with respect to $t = 0$ of those for positive p so that pulse broadening is accompanied by a time advance.

2.6.4 Another Look at the Propagation of a Gaussian Pulse When $\beta'''(\omega_0) = 0$

As was pointed out above in the absence of cubic (and higher order) nonlinearities (2.366) is an exact representation of the pulse envelope. In fact we can also get the complete waveform in the time domain with the aid of (2.336), (2.339), and (2.365). Thus

$$y(t,\omega_0) = 2^{1/4}/\sqrt{T}\Re e\left\{\begin{array}{c} e^{i\omega_0\left[\widetilde{t}-\frac{\pi^2\chi\widetilde{t}^2}{(T^2)(1+\pi^2\chi^2)}\right]}e^{-i\left[\beta(\omega_0)L+(1/2)\tan^{-1}(\pi\chi)\right]} \\ \left(1+\pi^2\chi^2\right)^{-1/4}\exp-\frac{\pi t^2}{(T^2)(1+\pi^2\chi^2)} \end{array}\right\}, \tag{2.369}$$

where

$$\widetilde{t} = t - \beta'(\omega_0)L. \tag{2.370}$$

Note that the instantaneous frequency of this complex waveform varies linearly with time, i.e.,

$$\omega(t) = \omega_0 - \frac{2\pi^2\chi\left(t-\beta'(\omega_0)L\right)}{(T^2)(1+\pi^2\chi^2)}. \tag{2.371}$$

In fiber optics such a pulse is referred to as a chirped pulse. This "chirping," (or linear FM modulation) is just a manifestation of the fact that the pulse distortion is due entirely to the quadratic nonlinearity in the phase rather than in the amplitude of the effective transfer function. On the other hand, chirping can occur also due to intrinsic characteristics of the transmitter generating the input pulse. We can capture this effect using the analytic form

$$p(t) = Ae^{-\frac{t^2}{2T_0^2}(1+i\kappa)}, \tag{2.372}$$

where A is a constant, κ the so-called chirp factor, and $2T_0$ the nominal pulse width.[9] Evidently when this pulse gets upconverted to the carrier frequency ω_0 its instantaneous frequency becomes

[9]Note that $T_0 = \left(1/\sqrt{2\pi}\right)T$ where T represents the definition of pulse width in (2.352). Also $A = 2^{1/4}/\sqrt{T}$.

$$\omega(t) = \omega_0 \left[1 - \frac{\kappa}{\omega_0 T_0}\left(\frac{t}{T_0}\right)\right] \tag{2.373}$$

so that over the nominal pulse interval $-T_0 \le t \le T_0$ the fractional change in the instantaneous frequency is $2\kappa/\omega_0 T_0$. Presently we view this chirping as the intrinsic drift in the carrier frequency during the formation of the pulse. How does this intrinsic chirp affect pulse shape when this pulse has propagated over a transmission medium with transfer function $exp - \beta(\omega) L$? If we neglect the effects of the third and higher order derivatives of the propagation constant the answer is straightforward. We first compute the FT of (2.372) as follows:

$$\begin{aligned} P(\omega) &= A\int_{-\infty}^{\infty} e^{-\frac{t^2}{2T_0^2}(1+i\kappa)} e^{-i\omega t} dt = A\int_{-\infty}^{\infty} e^{-\frac{(1+i\kappa)}{2T_0^2}\left[\left(t-\frac{i\omega T_0^2}{1+i\kappa}\right)^2 + \frac{\omega^2 T_0^4}{(1+i\kappa)^2}\right]} dt \\ &= Ae^{-\frac{\omega^2 T_0^2}{2(1+i\kappa)}} \int_{-\infty}^{\infty} e^{-\frac{(1+i\kappa)}{2T_0^2}\left(t-\frac{i\omega T_0^2}{1+i\kappa}\right)^2} dt \\ &= AT_0\sqrt{\frac{2\pi}{1+i\kappa}} e^{-\frac{\omega^2 T_0^2}{2(1+i\kappa)}}, \end{aligned} \tag{2.374}$$

where the last result follows from the formula for the Gaussian error function with (complex) variance parameter $T_0^2/\sqrt{1+i\kappa}$. Next we substitute (2.374) in (2.340) with $\Omega = \infty$ together with the approximation (2.342) to obtain

$$\hat{s}(t) = e^{-i\beta(\omega_0)L} \int_{-\infty}^{\infty} P(\eta)\, e^{-i\frac{1}{2}\beta''(\omega_0)\eta^2 L} e^{i\eta t} \frac{d\eta}{2\pi} \tag{2.375}$$

Simplifying,

$$s(t) = AT_0\sqrt{\frac{2\pi}{1+i\kappa}} e^{-i\beta(\omega_0)L} \int_{-\infty}^{\infty} e^{-\left[\frac{T_0^2}{2(1+i\kappa)} + i\frac{L\beta''(\omega_0)}{2}\right]\eta^2} e^{i\eta t} \frac{d\eta}{2\pi}. \tag{2.376}$$

Setting $Q = T_0^2/[2(1+i\kappa)] + iL\beta''(\omega_0)/2$ we complete the square in the exponential as follows:

$$e^{-Q\eta^2 + i\eta t} = e^{-Q\left[\left(\eta - \frac{it}{2Q}\right)^2 + \frac{t^2}{4Q^2}\right]} = e^{-\frac{t^2}{4Q}} e^{-Q\left(\eta - \frac{it}{2Q}\right)^2}. \tag{2.377}$$

From this we note that the complex variance parameter is $1/(2Q)$ so that (2.376) integrates to

$$\begin{aligned} \hat{s}(t) &= \frac{AT_0}{2\pi}\sqrt{\frac{2\pi}{1+i\kappa}} e^{-i\beta(\omega_0)L} e^{-\frac{t^2}{4Q}} \sqrt{\frac{\pi}{Q}} \\ &= \frac{A}{\sqrt{1+i\kappa}} e^{-i\beta(\omega_0)L} \\ &\quad \frac{T_0}{\sqrt{T_0^2 + i\beta''(\omega_0) L(1+i\kappa)}} \exp - \frac{t^2(1+i\kappa)}{2\left[T_0^2 + i\beta''(\omega_0) L(1+i\kappa)\right]}. \end{aligned} \tag{2.378}$$

Expression for the pulse width and chirp is obtained by separating the argument of the last exponential into real and imaginary parts as follows:

$$\begin{aligned} & \exp -\frac{t^2\left(1+i\kappa\right)}{2\left[T_0^2+i\beta''\left(\omega_0\right)L\left(1+i\kappa\right)\right]} \\ = \quad & \exp -\frac{T_0^2t^2}{2\left\{\left[T_0^2-\beta''\left(\omega_0\right)L\kappa\right]^2+\left[\beta''\left(\omega_0\right)L\right]^2\right\}}\exp -i\psi, \end{aligned} \tag{2.379}$$

where

$$\psi=\frac{\kappa t^2\left[T_0^2-\beta''\left(\omega_0\right)L(1+\kappa)\right]}{2\left\{\left[T_0^2-\beta''\left(\omega_0\right)L\kappa\right]^2+\left[\beta''\left(\omega_0\right)L\right]^2\right\}}. \tag{2.380}$$

Defining the magnitude of (2.379) as $\exp -t^2/\left(2T_L^2\right)$ we get for the pulse length T_L

$$T_L=T_0\sqrt{\left(1-\frac{\beta''\left(\omega_0\right)L\kappa}{T_0^2}\right)^2+\left(\frac{\beta''\left(\omega_0\right)L}{T_0^2}\right)^2}. \tag{2.381}$$

When the input pulse is unchirped $\kappa=0$, and we get

$$T_L=\sqrt{T_0^2+\left(\frac{\beta''\left(\omega_0\right)L}{T_0}\right)^2}. \tag{2.382}$$

We see from (2.381) that when $\kappa\neq 0$, T_L may be smaller or larger than the right side of (2.382) depending on the sign of κ. and the magnitude of L. Note, however, that for sufficiently large L, (2.381) is always larger than (2.382) regardless of the sign of κ. The quantity

$$L_D=T_0^2/\beta''(\omega_0) \tag{2.383}$$

is known as the dispersion length. Using this in (2.381) we have

$$T_L=T_0\sqrt{\left(1-\frac{L}{L_D}\kappa\right)^2+\left(\frac{L}{L_D}\right)^2}. \tag{2.384}$$

The significance of L_D is that with $\kappa=0$ for $L\ll L_D$ the effect of dispersion may be neglected.

2.6.5 Effects of Finite Transmitter Spectral Line Width*

In the preceding it was assumed that the carrier modulating the pulse is monochromatic, i.e., an ideal single frequency sinusoid with constant phase. In practice this will not be the case. Instead the carrier will have a fluctuating amplitude and phase which we may represent as

$$\widetilde{a(t)}\cos(\omega_0t+\widetilde{\phi(t)}), \tag{2.385}$$

where $\widetilde{a(t)}$ and $\widetilde{\phi(t)}$ are random functions of time and ω_0 is the nominal carrier frequency which itself has to be quantified as a statistical average. In the following we assume that only the phase is fluctuating and that the carrier amplitude is fixed. Reverting to complex notation we then assume that the pulse $p(t)$ upon modulation is of the form

$$p(t)e^{i\omega_0 t}e^{i\widetilde{\phi(t)}}. \tag{2.386}$$

If we denote the FT of $e^{i\widetilde{\phi(t)}}$ by the random function $\widetilde{X(\omega)}$, we get for the FT of (2.386)

$$\int_{-\infty}^{\infty} p(t)e^{i\omega_0 t}e^{i\widetilde{\phi(t)}}e^{-i\omega t}dt = \frac{1}{2\pi}\int_{-\infty}^{\infty} P\left(\omega-\xi-\omega_0\right)\widetilde{X(\xi)}d\xi. \tag{2.387}$$

To get the response that results after this random waveform has propagated over a transmission medium with transfer function $\exp -i\beta(\omega)L$ we have to replace $P\left(\omega-\omega_0\right)$ in (2.336) by the right side of (2.387). Thus we obtain

$$\begin{aligned} y(t) &= \Re e\left\{2\int_{\omega_0-\Omega}^{\omega_0+\Omega}(1/2)\left\{\frac{1}{2\pi}\int_{-\infty}^{\infty}P\left(\omega-\xi-\omega_0\right)\widetilde{X(\xi)}d\xi\right\}e^{-i\beta(\omega)L}e^{i\omega t}\frac{d\omega}{2\pi}\right\} \\ &= \Re e\left\{e^{i\omega_0 t}\int_{-\Omega}^{\Omega}\left\{\frac{1}{2\pi}\int_{-\infty}^{\infty}P\left(\eta-\xi\right)\widetilde{X(\xi)}d\xi\right\}e^{-i\beta(\eta+\omega_0)L}e^{i\eta t}\frac{d\eta}{2\pi}\right\} \\ &= \Re e\left\{e^{i\omega_0 t}\widetilde{s}(t-\beta^{'}(\omega_0)L\right\}, \end{aligned}$$

where

$$\widetilde{s}(t)=\int_{-\Omega}^{\Omega}\left\{\frac{1}{2\pi}\int_{-\infty}^{\infty}P\left(\eta-\xi\right)\widetilde{X(\xi)}d\xi\right\}e^{-i\left[\beta(\eta+\omega_0)-\beta^{'}(\omega_0)\eta\right]L}e^{i\eta t}\frac{d\eta}{2\pi} \tag{2.388}$$

is the complex random envelope of the pulse. It is reasonable to characterize this envelope by its statistical average which we denote by

$$|ENV|^2 \equiv \langle|s\left(t\right)|^2\rangle. \tag{2.389}$$

In evaluating (2.389) we shall assume that $e^{i\widetilde{\phi(t)}}$ is a WSS process so that its spectral components are uncorrelated, i.e.,

$$\langle\widetilde{X}(\xi)\widetilde{X}^*(\xi')\rangle = 2\pi F\left(\xi\right)\delta\left(\xi-\xi'\right), \tag{2.390}$$

where $F\left(\xi\right)$ is the spectral power density of $e^{i\widetilde{\phi(t)}}$. If we approximate the propagation constant in (2.388) by the quadratic form (2.342), and substitute (2.388) into (2.389) we obtain with the aid of (2.390)

$$|ENV|^2 = \int_{-\infty}^{\infty}F\left(\xi\right)d\xi\frac{1}{(2\pi)^3}\left|\int_{-\Omega}^{\Omega}P(\eta-\xi)e^{-i\beta''(\omega_0)\eta^2L/2}e^{i\eta t}d\eta\right|^2. \tag{2.391}$$

Assuming a Gaussian pulse with the FT as in (2.374) the inner integral in (2.391) can be expressed in the following form:

$$\frac{1}{(2\pi)^3}\left|\int_{-\Omega}^{\Omega} P(\eta-\xi)e^{-i\beta''(\omega_0)\eta^2 L/2}e^{i\eta t}d\eta\right|^2 = \frac{A^2T_0^2\pi}{(2\pi)^2\sqrt{1+\kappa^2}\,|Q|}f(\xi), \quad (2.392)$$

where $Q = T_0^2/\left[2\left(1+i\kappa\right)\right] + iL\beta''\left(\omega_0\right)/2$,

$$f(\xi) = e^{2\Re e\left\{Qb^2\right\}}e^{-\frac{\xi^2T_0^2}{2}\left[\frac{1}{1+i\kappa}+\frac{1}{1-i\kappa}\right]} \quad (2.393)$$

and

$$b = \frac{\xi T_0^2}{2Q(1+i\kappa)} + \frac{it}{2Q}. \quad (2.394)$$

To complete the calculation of the average pulse envelope we need the functional form of the power spectral density of the phase fluctuations. The form depends on the physical process responsible for these fluctuations. For example for high quality solid state laser sources the spectral line width is Lorenzian, i.e., of the form

$$F(\omega-\omega_0) = \frac{2/W}{1+\left(\frac{\omega-\omega_0}{W}\right)^2}. \quad (2.395)$$

Unfortunately for this functional form the integration in (2.391) has to be carried out numerically. On the other hand, an analytical expression is obtainable if we assume the Gaussian form

$$F(\omega-\omega_0) = \frac{1}{\sqrt{2\pi W^2}}\exp-\left(\omega-\omega_0\right)/2W^2. \quad (2.396)$$

After some algebra we get

$$\begin{aligned}|ENV|^2 &= \frac{A^2T_0^2\pi}{(2\pi)^2\sqrt{1+\kappa^2}\,|Q|}\frac{\sqrt{\left(T_0^2-\beta''\left(\omega_0\right)L\kappa\right)^2+\left(\beta''\left(\omega_0\right)L\right)^2}}{\left[\left(T_0^2-\beta''\left(\omega_0\right)L\kappa\right)^2+(1+2W^2T_0^2)\left(\beta''(\omega_0)\,L\right)^2\right]}\\ &\exp-\frac{t^2T_0^2}{\left(T_0^2-\beta''\left(\omega_0\right)L\kappa\right)^2+\left(1+2W^2T_0^2\right)\left(\beta''\left(\omega_0\right)L\right)^2}. \quad (2.397)\end{aligned}$$

Note that the preceding is the squared envelope so that to get the effective pulse length of the envelope itself an additional factor of 2 needs to be inserted (see (2.381)). We then get

$$T_L = T_0\sqrt{\left(1-\frac{\beta''\left(\omega_0\right)L\kappa}{T_0^2}\right)^2+\left(1+2W^2T_0^2\right)\left(\frac{\beta''\left(\omega_0\right)L}{T_0^2}\right)^2}. \quad (2.398)$$

It should be noted that this expression is not valid when $\beta''\left(\omega_0\right)=0$ as then the cubic phase term dominates. In that case the pulse is no longer Gaussian. The pulse width can then be defined as an r.m.s. duration. The result reads

$$T_L = T_0\sqrt{\left(1-\frac{\beta''\left(\omega_0\right)L\kappa}{T_0^2}\right)^2+\left(1+2W^2T_0^2\right)\left(\frac{\beta''\left(\omega_0\right)L}{T_0^2}\right)^2+C}, \quad (2.399)$$

where

$$C = (1/4)\,(1 + \kappa^2 + 2W^2T_0^2)\left(\frac{\beta'''(\omega_0)\,L}{T_0^3}\right)^2. \tag{2.400}$$

2.7 Fourier Cosine and Sine Transforms

In Chap. 2.2 we took as the starting point in our development of the FT theory the LMS approximation of a function defined in $(-T/2, T/2)$ in terms of sinusoids with frequencies spanning the interval $(-\Omega, \Omega)$. The formal solution can then be phrased in terms of the integral equation (2.106) for the unknown coefficients (functions). For arbitrary finite intervals no simple analytical solutions of the normal equation appears possible. On the other hand, when both the expansion interval in the time domain and the range of admissible frequencies are allowed to approach infinity the normal equations admit a simple solution which we have identified with FT. As we shall see in the following a suitable set of normal equations can also be solved analytically when the expansion intervals in the time domain and in the frequency domain are chosen as semi-infinite.

We suppose that $f(t)$ is defined over $(0, T)$ and seek its LMS approximation in terms of $\cos(\omega t)$ with ω in the interval $(0, \Omega)$:

$$f(t) \sim \int_0^{\Omega} \cos(\omega t)\hat{f}_c\,(\omega)\,d\omega = f_c^{\Omega}(t), \tag{2.401}$$

where $\hat{f}_c\,(\omega)$ if the expansion (coefficient) function. In accordance with (1.100) the normal equation reads

$$\int_0^T \cos(\omega t) f\,(t)\,dt = \int_0^{\Omega} \hat{f}_c\,(\omega')\,d\omega' \int_0^T \cos(\omega t)\cos(\omega' t)dt. \tag{2.402}$$

Using the identity $\cos(\omega t)\cos(\omega' t) = (1/2)\{\cos[t(\omega - \omega')] + \cos[t(\omega + \omega')]\}$ we carry out the integration with respect to t to obtain

$$\int_0^T \cos(\omega t) f\,(t)\,dt = \frac{\pi}{2}\int_0^{\Omega} \hat{f}_c\,(\omega')\,d\omega'\{\frac{\sin[(\omega - \omega')T]}{\pi(\omega - \omega')} + \frac{\sin[(\omega + \omega')T]}{\pi(\omega + \omega')}\}. \tag{2.403}$$

For arbitrary T this integral equation does not admit of simple analytical solutions. An exceptional case obtains when T is allowed to approach infinity for then the two Fourier Integral kernels approach delta functions. Because $\Omega > 0$ only the first of these contributes. Assuming that $\hat{f}_c\,(\omega')$ is a smooth function and we obtain in the limit

$$F_c(\omega) = \int_0^{\infty} \cos(\omega t) f\,(t)\,dt, \tag{2.404}$$

where we have defined

$$F_c(\omega) = \frac{\pi}{2}\hat{f}_c\,(\omega)\,. \tag{2.405}$$

Inserting (2.404) into (2.401) the LMS approximation to $f(t)$ reads

$$\begin{aligned} f_c^{\Omega}(t) &= \frac{2}{\pi}\int_0^{\Omega}\cos(\omega t)\int_0^{\infty}\cos(\omega t')f\left(t'\right)dt'd\omega \\ &= \int_0^{\infty} f\left(t'\right)dt'\frac{2}{\pi}\int_0^{\Omega}\cos(\omega t)\cos(\omega t')d\omega \\ &= \int_0^{\infty} f\left(t'\right)dt'(1/\pi)\int_0^{\Omega}\{\cos[\omega(t-t')]+\cos[\omega(t+t')]\}d\omega \\ &= \int_0^{\infty} f\left(t'\right)dt'\left\{\frac{\sin[(t-t')\Omega]}{\pi(t-t')}+\frac{\sin[(t+t')\Omega]}{\pi(t+t')}\right\}. \end{aligned} \tag{2.406}$$

Using the orthogonality principle the corresponding LMS error $\varepsilon_{\Omega\,\min}$ is

$$\varepsilon_{\Omega\,\min}=\int_0^{\infty}\left|f\left(t\right)\right|^2dt-\int_0^{\infty}f^*\left(t\right)f_c^{\Omega}(t)dt$$

and using (2.401) and (2.404)

$$\begin{aligned} \varepsilon_{\Omega\,\min} &= \int_0^{\infty}\left|f\left(t\right)\right|^2dt-\int_0^{\infty}f^*\left(t\right)\int_0^{\Omega}\cos(\omega t)\hat{f}_c\left(\omega\right)d\omega dt \\ &= \int_0^{\infty}\left|f\left(t\right)\right|^2dt-\frac{2}{\pi}\int_0^{\Omega}\left|F_c(\omega)\right|^2d\omega\geq 0. \end{aligned} \tag{2.407}$$

As $\Omega\to\infty$ the two Fourier kernels yield the limiting form

$$\lim_{\Omega\to\infty}f_c^{\Omega}(t)=\frac{f\left(t^+\right)+f(t^-)}{2}. \tag{2.408}$$

We may then write in lieu of (2.401)

$$\frac{f\left(t^+\right)+f(t^-)}{2}=\frac{2}{\pi}\int_0^{\infty}\cos(\omega t)F_c(\omega)d\omega. \tag{2.409}$$

At the same time $\lim\limits_{\Omega\to\infty}\varepsilon_{\Omega\,\min}=0$ so that (2.407) gives the identity

$$\int_0^{\infty}\left|f\left(t\right)\right|^2dt=\frac{2}{\pi}\int_0^{\infty}\left|F_c(\omega)\right|^2d\omega. \tag{2.410}$$

When $f(t)$ is a smooth function (2.409) may be replaced by

$$f(t)=\frac{2}{\pi}\int_0^{\infty}\cos(\omega t)F_c(\omega)d\omega. \tag{2.411}$$

The quantity $F_c(\omega)$ defined by (2.404) is the Fourier Cosine Transform (FCT) and (2.411) the corresponding inversion formula. Evidently (2.410) is the corresponding Parseval formula. As in the case of the FT we can use the compact notation

$$f\left(t\right)\overset{\mathcal{F}_c}{\Longleftrightarrow}F_c\left(\omega\right). \tag{2.412}$$

Replacing $F_c(\omega)$ in (2.411) by (2.404) yields the identity

$$\delta(t-t') = \int_0^\infty \sqrt{\frac{2}{\pi}}\cos(\omega t)\sqrt{\frac{2}{\pi}}\cos(\omega t')d\omega, \tag{2.413}$$

which may be taken as the completeness relationship for the FCT.

Note that the derivative of $f_c^\Omega(t)$ at $t=0$ vanishes identically. This means that pointwise convergence for the FCT is only possible for functions that possess a zero derivative at $t=0$. This is, of course, also implied by the fact that the completeness relationship (2.413) is comprised entirely of cosine functions.

What is the relationship between the FT and the FCT? Since the FCT involves the cosine kernel one would expect that the FCT can be expressed in terms of the FT of an even function. This is actually the case. Thus suppose $f(t)$ is even then

$$F(\omega) = \int_0^\infty 2f(t)\cos(\omega t)dt \tag{2.414}$$

so that $F(\omega)$ is also even. Therefore the inversion formula becomes

$$f(t) = \frac{1}{\pi}\int_0^\infty F(\omega)\cos(\omega t)d\omega. \tag{2.415}$$

Evidently with $F_c(\omega) = F(\omega)/2$ (2.414) and (2.415) correspond to (2.404) and (2.411), respectively.

In a similar manner, using the sine kernel, one can define the Fourier Sine Transform (FST):

$$F_s(\omega) = \int_0^\infty \sin(\omega t)f(t)\,dt. \tag{2.416}$$

The corresponding inversion formula (which can be established either formally in terms of the normal equation as above or derived directly from the FT representation of an odd function) reads

$$f(t) = \frac{2}{\pi}\int_0^\infty F_s(\omega)\sin(\omega t)d\omega. \tag{2.417}$$

Upon combining (2.416) and (2.417) we get the corresponding completeness relationship

$$\delta(t-t') = \int_0^\infty \sqrt{\frac{2}{\pi}}\sin(\omega t)\sqrt{\frac{2}{\pi}}\sin(\omega t')d\omega. \tag{2.418}$$

Note that (2.417) and (2.418) require that $f(0)=0$ so that only for such functions a pointwise convergent FST representation is possible.

Problems

1. Using (2.37) compute the limit as $M\to\infty$, thereby verifying (2.39).
2. Prove (2.48).

3. Derive the second-order Fejer sum (2.42).

4. For the periodic function shown in the following sketch:

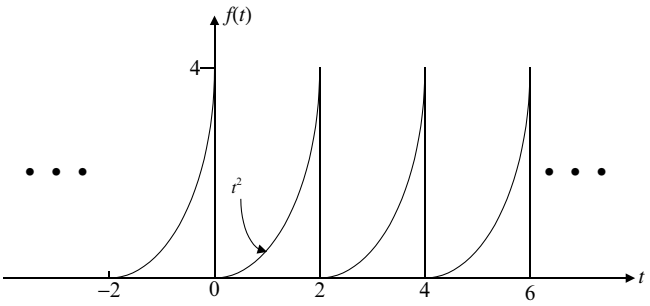

Figure P4: Periodic function with step discontinuities

   (a) Compute the FS coefficients $\hat{f}_n$.
   (b) Compute and plot the partial sum $f^N(t)$ for $N = 5$ and $N = 20$. Also compute the corresponding LMS errors.
   (c) Repeat (b) for the first-order Fejer sum.
   (d) Repeat (c) for the second-order Fejer sum.

5. Derive the interpolation formula (2.82)

6. Derive the interpolation formula (2.88)

7. Approximate the signal $f(t) = te^{-t}$ in the interval $(0, 4)$ by the first five terms of a Fourier sine series and an anharmonic Fourier series with expansion functions as in (2.101) assuming (a) $\beta = -1/3$ and (b) $\beta = -1$. Plot $f^5(t)$ for the three cases together with $f(t)$ on the same set of axes. Account for the different values attained by the three approximating sums at $t = 4$.

8. The integral
$$I = P\int_{-2}^{2} \frac{tdt}{(t-1)(t^2+1)\sin t}$$
is defined in the CPV sense. Evaluate it numerically.

9. Derive formulas (2.137)(2.137*)(2.141) and (2.142).

10. The differential equation
$$x''(t) + x'(t) + 3x(t) = 0$$
is to be solved for $t \geq -2$ using the FT. Assuming initial conditions $x(-2) = 3$ and $x'(-2) = 1$ write down the general solution in terms of the FT inversion formula.

11. Derive formula (2.73).

12. Prove that $K_{\Omega}^{(1)}(t)$ in (2.200) is a delta function kernel.

13. Prove the asymptotic form (2.201).

14. Compute the Fourier transform of the following signals:

$$a)\ \left(e^{-3t}\cos 4t\right)U(t) \quad b)e^{-4|t|}\sin 7t$$

$$c)\ \left(te^{-5t}\sin 4t\right)U(t) \quad d)\ \sum_{n=0}^{\infty} 4^{-n}\delta(t-nT)$$

$$e)\ \left(\frac{\sin at}{at}\right)\left(\frac{\sin 2a\,(t-1)}{a\,(t-1)}\right) \quad f)\ \sum_{n=-\infty}^{\infty} e^{-|t-4n|}$$

15. Compute the Fourier transform of the following signals:

(a) $f(t) = \frac{\sin at}{\pi t}U(t)$

(b) $f(t) = \int_{-\infty}^{\infty} g(t+x)g^*(x)dx$ with $g(t) = e^{-at}U(t-2)$

(c) $f(t) = w(t)$ with $w(t)$ defined in the following sketch.

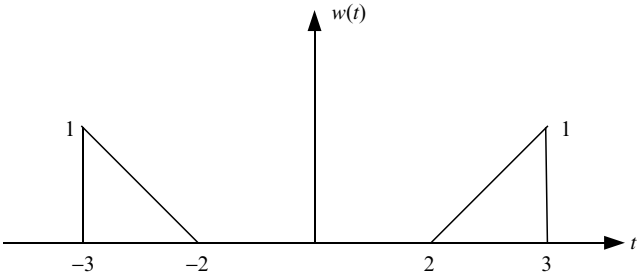

16. With the aid of Parseval's theorem evaluate $\int_{-\infty}^{\infty} \frac{\sin^4 x}{x^4}dx$.

17. With $F(\omega) = R(\omega) + iX(\omega)$ the FT of a causal signal find $X(\omega)$ when a) $R(\omega) = 1/(1+\omega^2)$ b) $R(\omega) = \frac{\sin^2 2\omega}{\omega^2}$.

18. Given the real signal $1/\left(1+t^2\right)$ construct the corresponding analytic signal and its FT.

19. Derive (2.217).

20. For the signal $z(t) = \frac{\cos 5t}{1+t^2}$ compute and plot the spectra of the inphase and quadrature components $x(t)$ and $y(t)$ for $\omega_0 = 5, 10, 20$. Interpret your results in view of the constraint (2.226).

21. The amplitude of a minimum phase FT is given by $|F(\omega)| = \frac{1}{1+\omega^{2n}}$, $n > 1$. Compute the phase.

http://www.springer.com/978-1-4614-3286-9

Signals and Transforms in Linear Systems Analysis

Wasylkiwskyj, W.

2013, XIV, 375 p., Hardcover
ISBN: 978-1-4614-3286-9